PROCESS NMR ASSOCIATES, LLC

Technical White Paper Series

Quantitative Nuclear Magnetic Resonance Analysis of Beer

Composition, Process Chemistry, Residual Dextrins, and the Spectral Foundation for Chemometrics and Machine Learning

John C. Edwards, Ph.D.

Process NMR Associates, LLC

84 Patrick Lane, Suite 115, Poughkeepsie, NY 12603

www.process-nmr.com

Version 2.1 | August 27, 2026

Document Details

Field	Entry
Filename	PNA_White_Paper_qNMR_Analysis_of_Beer_v2.1.docx
Version	2.1 - expanded non-fractionated beer and dextrin-character integration
Author	John C. Edwards, Ph.D., Process NMR Associates, LLC
Generation date	August 27, 2026
Drafting system	OpenAI Codex, GPT-5 family (ChatGPT Work mode); extended analytical effort
Primary author sources	World Brewing Congress 2016 poster; Bell's Brewery presentation, October 12, 2018; UC Davis Master Brewers Certificate Program presentation, April 28, 2022
Literature basis	Author-supplied beer, carbohydrate, starch, aging, metabolomics, non-alcoholic beer, and qNMR papers, supplemented only where a claim required a primary source
Reference validation	Bibliographic metadata and DOI destinations were checked online against Crossref and/or publisher records on August 20, 2026; the Petersen et al. non-fractionated beer record (Ref. 63) and related primary-paper metadata were rechecked on August 27, 2026. Unverifiable candidate references were excluded or explicitly flagged.
Status	Technical white paper for author review. Version 2.1 expands the interpretation of non-fractionated beer carbohydrate NMR, defines a multidimensional dextrin-character panel, and states the transfer limits for routine 300 MHz implementation. Additional residual-dextrin experiments and subsequent chemometric/ML results remain planned.

The experimental figures reproduced in this paper are drawn from presentations and a poster supplied by the author and are treated as Process NMR Associates work. Peer-reviewed publications are used for context, validation, and comparison. Proposed experiments, commercial architectures, and future model-development recommendations are identified as proposals rather than completed validation.

Abstract

Beer is a chemically dense, dynamic fermentation matrix in which water and ethanol coexist with residual starch-derived carbohydrates, organic acids, amino acids, nucleosides, higher alcohols, esters, aldehydes, hop-derived bitter compounds, cereal polysaccharides, proteins, minerals, and specialty-ingredient markers. Conventional brewery laboratories divide this composition across many methods. Quantitative nuclear magnetic resonance spectroscopy (qNMR) provides a different analytical architecture: a single spectrum observes a broad cross-section of the soluble proton-bearing chemistry, and integrated signal area is intrinsically proportional to molar amount when pulse sequence, relaxation, referencing, and spectral overlap are controlled.

This white paper develops that architecture from the author's 300 MHz beer studies and a validated primary literature base. It covers direct and lyophilized sample workflows; internal-standard, PULCON, and electronic-reference quantitation; water and ethanol suppression; a region-by-region ^{1}H spectral atlas; direct measurement of alcohol, sugars, organic acids, amino acids, nucleosides, glycerol, higher alcohols, selected esters and aldehydes; hop and aging chemistry; low- and non-alcoholic beer; specialty ingredients; ^{13}C, ^{2}H, ^{23}Na, ^{31}P, HSQC, DOSY, and relaxation methods; and the validation and uncertainty controls required for label-facing or troubleshooting work.

Residual dextrin chemistry is treated as a central development opportunity. The paper relates malt starch structure and mash enzymology to the α-(1→4) backbone, α-(1→6) branch, reducing-end, and diffusion behavior observed in wort and finished beer, and it sets out a staged program to validate degree-of-polymerization and branching descriptors

against defined standards, enzymatic treatments, and chromatographic size methods. Figures from the 2016 World Brewing Congress poster and the 2018/2022 presentations illustrate whole-spectrum assignments, commercial-beer diversity, wort-to-beer conversion, sour-mash chemistry, mash-dependent maltodextrin distributions, nutritional calculations, low-alcohol verification, amino-acid patterns, and hop raw-material analysis.

The final sections translate the spectrum into a future analytical intelligence system. Targeted concentration tables and full-resolution spectral fingerprints are retained as linked data products; process samples are modeled as trajectories rather than isolated points; metadata and QC are treated as measurements; and unsupervised chemometrics, supervised learning, and anomaly detection are assigned validation strategies that hold out entire lots, breweries, or production periods. The result is a broad technical foundation for a PNA beer-NMR database and the next phase of residual-dextrin, chemometric, and machine-learning development.

Revision 2.1 integrates the six-beer non-fractionated study of Petersen et al. That work expands dextrin character from a bulk dextrin result into a composition-structure-mobility profile: more than 50 local carbohydrate moieties, more than 20 small carbohydrates represented by more than 38 isomeric forms, starch-, β-glucan-, and arabinoxylan-cleavage motifs, and diffusion-resolved polymer behavior. These findings strengthen the structural basis of the proposed PNA dextrin panel but do not make every reporter quantitatively portable to 300 MHz; species-specific concentration, motif-equivalent response, integrated envelope, and diffusion class remain distinct evidence levels. 63

Table of Contents

1. Introduction

2. The Beer Matrix as an NMR Sample

3. Sample Preparation and Experimental Methodology

  3.1 Sample Preparation

  3.2 Solvent and Ethanol Suppression

  3.3 Quantitation Strategies

  3.4 Two-Dimensional and Diffusion Methods

  3.5 The metrological qNMR equation

  3.6 Direct beer and lyophilized beer answer different questions

  3.7 Acquisition design for quantitative beer spectra

  3.8 Suppression is part of the measurement model

  3.9 What beer NMR does not measure well

4. Assignment of the ^{1}H Spectrum of Beer

  4.1 High-Field Aliphatic Region (δ 0.8–1.6)

  4.2 Mid-Field Region (δ 1.6–3.1)

  4.3 Carbohydrate Bulk Region (δ 3.1–4.4)

  4.4 Anomeric Region (δ 4.4–5.5)

  4.5 Olefinic, Aromatic, and Aldehydic Region (δ 5.5–9.7)

5. Residual Dextrins, Starch Fragments, and Glucans: A Deep NMR View

  5.1 The carbohydrate system carried from grain to beer

  5.2 Anomeric configuration and linkage-specific NMR reporters

  5.3 Degree of polymerization, branching, and what can be quantified

  5.4 Process information encoded in residual dextrins

5.5 What each NMR experiment can and cannot deliver
5.6 Practical Applications and Capability Boundaries
6. Quantitative ^{1}H NMR of Beer Constituents
6.1 Alcohol content and the volatile fermentation profile
6.2 Organic acids as a map of yeast, bacteria, raw materials, and storage
6.3 Amino acids, nitrogen metabolism, and the boundary of “FAN by NMR”
6.4 Nucleosides, purines, and hopping-dependent yeast metabolism
6.5 Carbohydrate mass balance, calories, and label-facing calculations
6.6 Non-alcoholic beer and dealcoholization diagnostics
6.7 Adjuncts, specialty ingredients, and formulation markers
6.8 Hops, lipids, proteins, and colloids: observable, but method-dependent
6.9 An analyte-to-process interpretation matrix
7. Hop-Derived Bitter Acids and Beer Aging Chemistry
8. Multivariate Analysis and NMR Metabolomics of Beer
9. Multinuclear and Advanced NMR Dimensions
9.1 ^{13}C and ^{1}H-^{13}C correlation spectroscopy
9.2 ^{2}H NMR and site-specific isotope fractionation
9.3 ^{23}Na, ^{31}P, and other nuclei
9.4 DOSY, diffusion editing, and relaxation
10. From a Spectrum to Pattern Recognition and Process Understanding
10.1 Two linked data products: targeted chemistry and the full fingerprint
10.2 Process trajectories rather than static product clusters
10.3 Preprocessing must be subordinate to chemistry
10.4 Validation strategy for chemometric and machine-learning models
10.5 Metadata is an analytical measurement
11. High-Field, Benchtop, and Process NMR Deployment
11.1 The two-tier architecture
11.2 At-line fermentation monitoring
11.3 Method transfer and lifecycle control
12. Validation Framework for a Brewery qNMR Method
12.1 Intended use comes first
12.2 Core validation characteristics
12.3 System suitability and ongoing QC
12.4 Reporting language
13. Process NMR Associates Beer Studies: Evidence Already Demonstrated
13.1 The 23-commercial-beer World Brewing Congress panel
13.2 Wort-to-beer and mash-extract comparisons

13.3 Sour-mash temperature series
13.4 Near-beer label check
13.5 Hop raw-material profiling
14. Research Program for Residual Dextrins and Beer Chemical Space
14.1 Dextrins are the priority development axis
14.2 Proposed staged experimental design
14.3 Chemometric deliverables for the next phase
14.4 The forward-looking analytical product
15. Conclusions
Summary

1. Introduction

Beer is among the most compositionally complex beverages subjected to routine analytical control. A finished lager contains water, ethanol, and a residual solute load of some 20–40 g/L that is distributed across carbohydrates, organic acids, amino acids, higher alcohols, esters, nucleosides, polyphenols, hop-derived bitter acids, and cereal polysaccharides, with individual constituent concentrations spanning more than five orders of magnitude. Conventional brewery quality control addresses this complexity by fragmentation: density measurement for alcohol and real extract, ion or liquid chromatography for individual sugars, enzymatic kits for organic acids, gas chromatography for volatiles, and dedicated HPLC or spectrophotometric methods for bitterness. Each method answers a narrow question, and the aggregate picture is assembled from many separate determinations performed on many separate aliquots.

Nuclear magnetic resonance spectroscopy offers a fundamentally different proposition. A single ^{1}H spectrum, acquired in minutes on an untreated, degassed sample, encodes the identity and concentration of essentially every soluble hydrogen-bearing constituent above the detection limit, and the inherent proportionality between integrated signal area and molar concentration makes that spectrum quantitative without compound-specific calibration.1–4 The application of high-resolution NMR to beer was placed on a systematic footing in the early 2000s through the work of Gil and co-workers, who combined 500 MHz ^{1}H spectroscopy with multivariate analysis to characterize ale and lager production,5 and the intervening two decades have produced validated quantitative methods, automated profiling platforms covering more than eighty beer metabolites, and an extensive style-discrimination and authentication literature.6,7

The present white paper serves two purposes. The first is to provide a working spectral atlas of beer: tabulated ^{1}H chemical shifts, multiplicities, and coupling constants for the constituents that are reliably observed at 300–600 MHz, organized by spectral region, together with the sample-handling and suppression methodology required to obtain quantitative data from a matrix dominated by water and ethanol. The second purpose is a detailed treatment of the residual dextrin fraction — the branched α-glucan material that survives mashing and fermentation, constitutes the majority of the non-volatile carbohydrate in finished beer, and is essentially invisible to the sugar-by-sugar chromatographic methods used in most breweries. The structural information available from the dextrin anomeric region, including number-average degree of polymerization and α-(1→6) branch content, is developed quantitatively, because it is precisely here that NMR provides analytical access that no other routine technique matches. Throughout, the document has been prepared as an AI-drafted framework into which experimental spectra, client data, and interpretive conclusions generated at Process NMR Associates are to be incorporated by the author.

In this revision, dextrin character is deliberately defined as a vector rather than a scalar. It combines the amount of NMR-visible starch-derived carbohydrate with the balance of α-(1→4) and α-(1→6) linkages, reducing-end abundance, lower- versus higher-DP reporter patterns, local branch-neighborhood signals, and hydrodynamic mobility. Mixed-linkage β-glucan and arabinoxylan signals are not relabeled as dextrins; they are measured or flagged separately because they can overlap the same residual-carbohydrate envelope and can influence viscosity, filtration, and apparent size distributions. 54,56,63

2. The Beer Matrix as an NMR Sample

The analytical difficulty of beer resides not in any individual assignment but in dynamic range. Water is present at roughly 50 M in proton equivalents, ethanol at 0.7–1.1 M, the carbohydrate pool at tens of millimolar in glucose-residue equivalents, and the analytically interesting minor constituents — bitter acids, staling aldehydes, trace amino acids — at micromolar levels. Useful quantitation of a 10 µM aldehyde in the presence of 100 M of water protons demands suppression performance and receiver linearity that were not routinely available before the pulsed-field-gradient era, which is one reason the beer NMR literature is almost entirely a post-2000 phenomenon.1,5

The matrix imposes three further constraints. Beer is carbonated at roughly 5 g/L dissolved CO_2, and outgassing in the NMR tube degrades shimming and lineshape unless the sample is degassed beforehand. Beer is acidic, with typical pH

values of 3.9–4.6 for conventional styles and 3.2–3.6 for sour styles, which places the sample near the pK_a values of the major organic acids and renders many chemical shifts strongly composition-dependent, a point developed in Section 3. Finally, beer contains dissolved macromolecules — proteins, β-glucans, arabinoxylans, and the higher dextrins — whose shorter transverse relaxation times produce broad baseline components beneath the sharp small-molecule signals. Table 1 summarizes the principal constituent classes, their typical levels in a conventional lager, and the spectral windows in which they are observed. Comprehensive small-molecule coverage is illustrated by the automated MagMet-B profiling platform, whose beer library comprises 81 quantifiable metabolites,21 while the classical Aveiro and Carlsberg studies established the assignment framework on which subsequent work has been built.5–7

Table 1. Principal constituent classes of a conventional lager and their ^{1}H NMR observability.

Class	Representative constituents	Typical level	Principal ^{1}H window (δ, ppm)	Analytical remarks
Water	H_2O / HDO	900–950 g/L	4.7–4.9	Suppressed; residual line sets the local dynamic range
Ethanol	ethanol	30–50 g/L	1.18; 3.65	^{13}C satellites interfere near δ 1.28–1.33; suppression or ^{13}C decoupling advisable
Residual carbohydrate	dextrins, maltotriose, maltose, glucose	15–35 g/L	3.1–4.0; 4.4–5.5	Dominated by non-fermentable dextrins (Section 5)
Glycerol	glycerol	1.2–2.5 g/L	3.55–3.80	Fermentation by-product; overlaps carbohydrate bulk region
Organic acids	lactic, acetic, succinic, citric, malic, pyruvic, formic	0.3–1.5 g/L (total)	1.3–3.0; 8.3–8.5	Shifts strongly pH-dependent at beer pH
Amino acids	proline, alanine, GABA, branched-chain and aromatic amino acids	0.3–1.5 g/L (total)	0.9–4.2; 6.8–8.7	Proline dominant in fermented beer
Higher alcohols and esters	1-propanol, isobutanol, isoamyl alcohol, 2-phenylethanol, tyrosol, ethyl acetate	50–250 mg/L (total)	0.85–1.3; 2.7–4.2; 7.1–7.4	Fermentation flavor volatiles; sharp resolved multiplets
Hop bitter acids	cis- and trans-iso-α-acids	10–100 mg/L	1.0–1.1; 2.4–3.1; 5.0–6.1	Micromolar; 2D or extract-assisted characterization (Section 7)
Nucleosides and purines	uridine, adenosine, inosine	10–60 mg/L	5.9–6.1; 7.8–8.4	Clean low-field markers; hopping-regime sensitive
Carbonyl and staling markers	acetaldehyde, 5-HMF, 2-furaldehyde	1–20 mg/L	9.4–9.7	Aldehyde region essentially background-free
Polysaccharide interferents	(1→3,1→4)-β-glucan, arabinoxylan	0.1–4 g/L	3.2–4.0; 4.4–4.8; 5.2–5.4	Broad; diffusion-distinct from dextrins (Section 5.7)
Dissolved gases and buffers	CO_2/bicarbonate, phosphate	≈5 g/L CO_2	indirect	Degassing required; phosphate contributes pH buffering

Levels are indicative for a conventional all-malt or adjunct lager and vary substantially with style; sour, wheat, non-alcoholic, and high-gravity products depart from several entries. Compiled from the quantitative beer NMR literature.5–7,20,21

3. Sample Preparation and Experimental Methodology

3.1 Sample Preparation

Preparation for high-resolution work is deliberately minimal so that the quantitative integrity of the sample is preserved. Decarbonation is accomplished by brief sonication, by gentle agitation, or by filtration, with ten to fifteen

minutes of sonication generally sufficient to prevent bubble evolution in the tube; a small upward drift in pH accompanies CO_2 loss and should be accepted as part of the defined sample state rather than corrected inconsistently. A typical composition places 450–540 µL of degassed beer with 50–60 µL of D_2O for the field-frequency lock and an internal chemical-shift reference, most commonly 3-(trimethylsilyl)propionic acid-d_4 sodium salt (TSP-d_4) at 0.1–1 mM defining δ 0.00.5–7 Buffered variants, in which phosphate or oxalate buffer fixes the pH of all samples at a common value, trade a small dilution for greatly improved shift reproducibility and are preferred when spectra are destined for multivariate modeling across large sample sets.6,30 Because TSP is known to associate weakly with proteins and polyphenols, its use as a quantitation reference in beer carries a small negative bias risk, and the electronic and external referencing schemes discussed in Section 3.3 remove this dependence entirely.12,13

3.2 Solvent and Ethanol Suppression

Two abundant species must be managed rather than one. Water suppression in modern beer work is performed almost universally with the one-dimensional NOESY-presaturation experiment, whose behavior and artifacts have been analyzed in detail by McKay,9 or with pulsed-field-gradient schemes — WET10 and excitation sculpting11 — that achieve comparable suppression with shorter recycle overhead. Ethanol presents the subtler problem. Its methyl triplet at δ 1.18 and methylene quartet at δ 3.65 can be handled by multiple-frequency presaturation, but the ^{13}C satellites of the methyl resonance, displaced by half of $^1J(^{13}C–^1H) \approx 125$ Hz on either side of the parent line, remain at roughly 0.55% of the parent intensity each — comparable to or larger than many analyte signals. The high-frequency satellite falls at δ ≈ 1.28–1.33 depending on field strength, directly beneath the threonine and acetaldehyde-hydrate doublets, and the low-frequency satellite encroaches on the branched-chain amino acid region. Application of ^{13}C decoupling during acquisition, an option built into the WET scheme,10 collapses the satellites into the suppressed parent and is strongly recommended for quantitative beer work; where decoupling hardware is not used, the satellites must be modeled explicitly in any fitting procedure.21

3.3 Quantitation Strategies

Quantitative ^1H NMR of beer follows the general discipline of qNMR:14 a calibrated 90° (or defined small-angle) excitation, a recycle delay long relative to the longest relevant T_1 or an explicit T_1-based correction, sufficient digital resolution, and integration or lineshape fitting against a reference of known concentration. Internal referencing against TSP-d_4 is the simplest scheme but inherits the binding bias noted above. The PULCON principle, in which the reciprocity relation transfers a calibration measured on an external standard to the analytical sample through the 360° pulse length, removes the internal standard entirely and has been validated specifically for beer and beer-based mixed beverages in a fully automated implementation covering ingredients and additives at legal-compliance level.12,15 The ERETIC method, which injects a synthesized pseudo-signal of defined amplitude, accomplishes the same end electronically.13 Validation data for beer are favorable across all three schemes: the Carlsberg laboratory demonstrated quantification of organic and amino acids in beer with precision competitive with enzymatic and chromatographic reference methods,7 organic acid quantification by both integration and multivariate regression has been critically compared,20 and automated lineshape-fitting platforms report median absolute errors below ten percent against expert manual profiling.21 Because beer pH sits on the steep portion of several acid titration curves, peak position itself carries analytical information, and it has been demonstrated that concentration can be inferred from chemical shift rather than integral for suitable acid systems — an elegant inversion of the usual view of pH-dependent shifts as a nuisance.16 Where shift variability is treated as a nuisance, spectral alignment by interval correlation-optimized shifting (icoshift) is the standard preprocessing remedy ahead of multivariate analysis.17

3.4 Two-Dimensional and Diffusion Methods

Assignment support in the congested mid-field region is provided by the conventional homonuclear and heteronuclear repertoire. Two-dimensional J-resolved spectroscopy projects the crowded one-dimensional spectrum onto a proton-decoupled chemical-shift axis and was applied early to beer differentiation, where its simplified projections proved well suited to multivariate treatment.19 COSY, TOCSY, and ^1H-^{13}C HSQC underpin the definitive carbohydrate assignments, and the coupling of chromatographic separation to NMR detection - LC-NMR and LC-NMR/MS - resolved the beer oligosaccharide series directly, providing the firmest experimental basis for the dextrin assignments

presented in Section 5.18 Diffusion-ordered spectroscopy adds a hydrodynamic dimension because small sugars, oligosaccharides, and larger polymeric material exhibit different translational mobilities. Port wine supplied an early liquid-food precedent,28 and the Petersen study demonstrated the principle directly in six non-fractionated beers, where DOSY supported polysaccharide-fragment assignments and indicated especially high-molecular-weight arabinoxylan material. A measured diffusion coefficient is quantitative as mobility, but it is not an exact molecular weight without temperature, viscosity, conformation, association, and matrix-matched calibration controls. 63

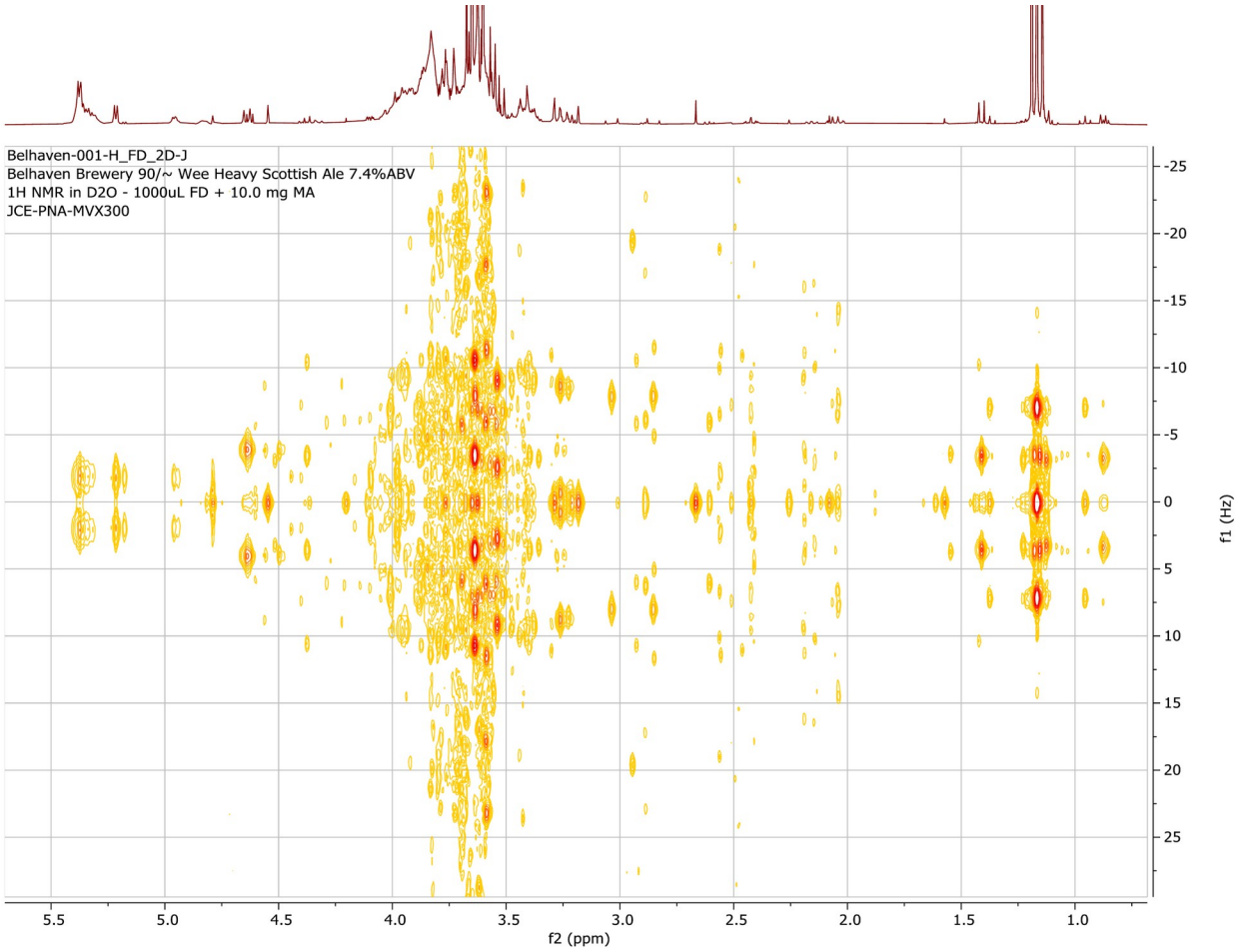

Figure 1. Two-dimensional J-resolved-style spectrum of a lyophilized beer, illustrating separation of chemical-shift and coupling information in an overlapped matrix. The source slide does not specify the complete pulse sequence or vertical-axis convention; the panel is therefore presented as an assignment-support example, not a quantitative result. Source: Process NMR Associates, author-supplied 2022 presentation (Ref. 68, p. 33).

3.5 The metrological qNMR equation

The practical value of qNMR rests on a physical property that chromatography does not share: after excitation and complete relaxation, integrated signal area is proportional to the number of contributing nuclei. A detector response factor does not have to be determined independently for ethanol, lactate, acetate, maltose, or any other proton-bearing analyte. For an internal standard, the mass concentration of component *x* is calculated from

where *P*IS is the certified mass fraction of the internal standard, *m*IS is the mass of standard in milligrams, *I* is integrated area, *N* is the number of nuclei represented by the integral, *M* is molar mass, and *V*s is the volume of original beverage represented in the tube in microliters. The equation is simple; obtaining defensible values for every term is not. Purity and water content of the standard, gravimetric delivery, pulse calibration, longitudinal relaxation, baseline behavior, spectral overlap, receiver linearity, and the uncertainty in the original sample volume all contribute to the result. qNMR is therefore calibration-light, not metrology-free.12-15

Process NMR Associates has used maleic acid as the internal calibrant in the author-supplied beer studies because its two equivalent olefinic protons give a sharp, isolated singlet near δ 6.4-6.5, outside the dense aliphatic and carbohydrate regions. The 2016 World Brewing Congress poster and the 2018 and 2022 presentations describe a direct-beer preparation containing 175 µL of degassed beer, a maleic-acid solution containing 10 mg of standard, and sufficient D_2O to furnish the lock and final tube volume. For lyophilized analysis, the residue from 1.000 mL of beer was redissolved in D_2O with the same mass of maleic acid. The stated equations normalize the maleic-acid integral to 100, so $I_{IS}/N_{IS} = 50$. These are useful historical operating conditions and are reproduced here as the provenance of the experimental examples; a released routine method should define all additions gravimetrically, specify the certified standard value and its uncertainty, and verify analyte-specific relaxation under the exact pulse sequence used.

3.6 Direct beer and lyophilized beer answer different questions

Direct analysis preserves ethanol, methanol, ethyl acetate, acetaldehyde, 1-propanol, isobutanol, 2-methyl-1-butanol, 3-methyl-1-butanol, and other volatile or semivolatile products. Lyophilization increases the amount of nonvolatile material presented to the probe and removes most water and ethanol, greatly improving observation of carbohydrates, amino acids, organic acids, nucleosides, and broad polymer signals. It also deliberately destroys quantitative information for volatile compounds and can alter pH, ionic strength, aggregation, and chemical-shift positions after reconstitution. Neither preparation is the universal answer. A two-aliquot protocol is the analytically correct architecture when both volatile fermentation products and the residual carbohydrate matrix matter.

Workflow	Material represented	Best analytical targets	Principal limitations
Direct, degassed beer	175-500 µL typical	Ethanol/ABV, methanol, higher alcohols, esters, aldehydes, acids, glycerol, selected sugars	Water and ethanol dynamic range; carbonation; overlap; lower mass loading for nonvolatile trace compounds
Buffered direct beer	Same, with defined dilution	Comparative profiling, stable peak positions, chemometric databases, routine quantitation	Dilution; buffer may move equilibria and no longer represents native beer pH
Lyophilized and reconstituted beer	Commonly 1.000 mL or more	Dextrins, maltose/maltotriose, amino acids, nucleotides, organic acids, minor nonvolatile components	Volatile loss; reconstitution bias; possible incomplete recovery; altered aggregation
Raw material or wort extract	Defined mass or volume	Malt and adjunct carbohydrates, enzyme conversion products, hop constituents	Extraction selectivity must be validated; result is method-defined rather than absolute composition
Time-series process sample	Fixed volume at each stage	Trajectories in sugar consumption, ethanol, acids, glycerol, amino acids and dextrin remodeling	Sampling time, quenching, temperature and biological activity must be controlled

The choice also affects chemometrics. Models should not be trained on a mixture of direct and lyophilized spectra unless preparation is explicitly encoded and the scientific question requires that heterogeneity. Otherwise, the preparation difference will dominate principal components and can be mistaken for product chemistry.

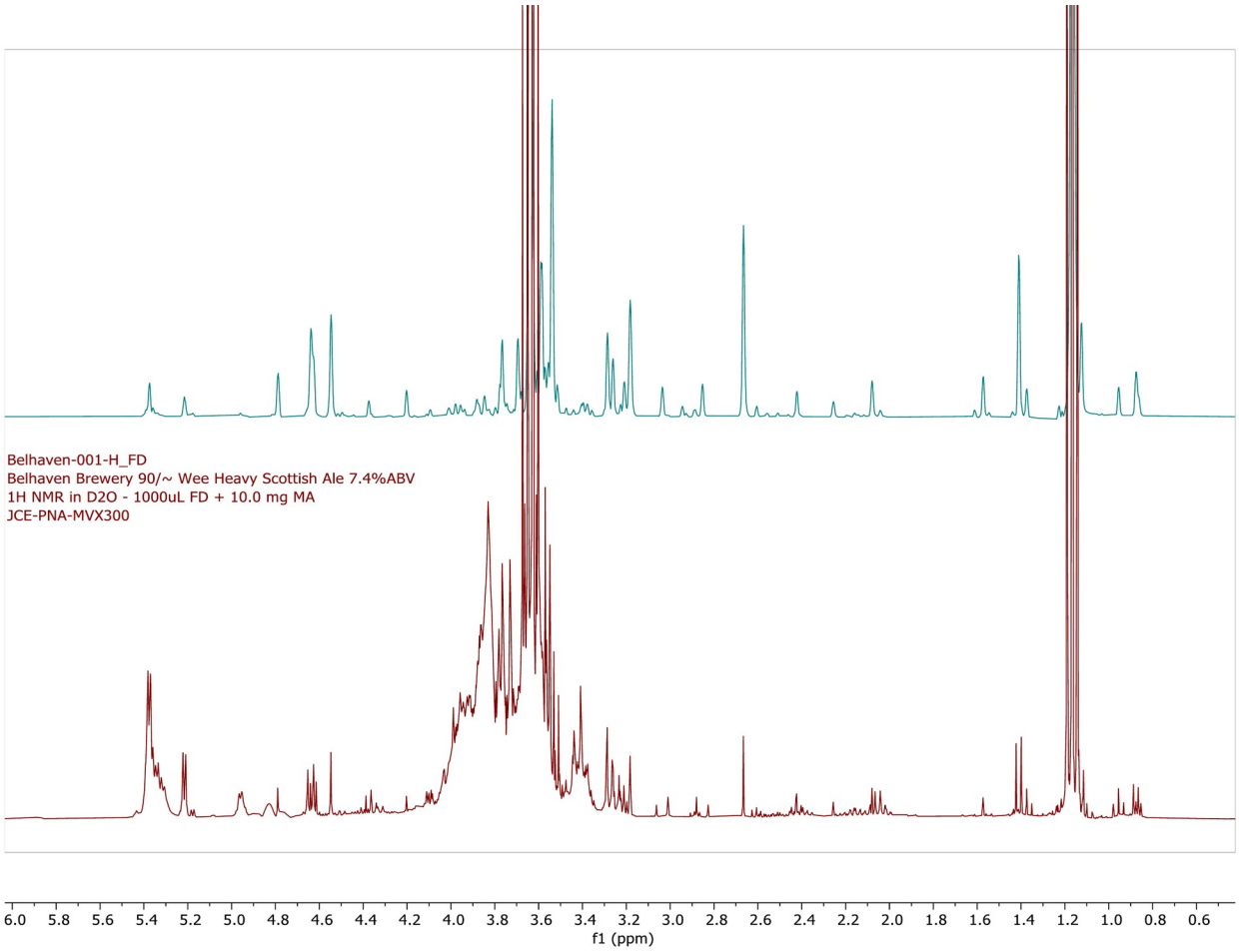

Figure 2. Paired direct and lyophilized/reconstituted spectra of the same beer. The direct spectrum retains volatile chemistry; the lyophilized aliquot concentrates nonvolatile carbohydrate, acid, amino-acid, and nucleoside signals. Visual intensity ratios should not be interpreted as recovery without normalization. Source: Process NMR Associates, author-supplied 2022 presentation (Ref. 68, p. 35).

3.7 Acquisition design for quantitative beer spectra

The World Brewing Congress work used a Varian Mercury MVX 300 MHz system with a 5 mm probe, an approximately 60° pulse, an 8 kHz spectral width, 64k acquired points, an 8 s acquisition time, a 7 s relaxation delay, and 64 transients. That combination produced a spectrum in approximately fifteen minutes and demonstrated that useful beer qNMR does not require the highest available magnetic field. The method nevertheless must be regarded as analyte- and purpose-specific. A 60° pulse with a 7 s delay may be quantitative for many small beer metabolites but not automatically for every slowly relaxing isolated resonance. A validation study should measure representative T_1 values and demonstrate acceptable bias, or increase the repetition time until residual saturation is negligible for the reporting panel.

Digital resolution matters because beer quantitation often depends on narrow integration windows beside much larger peaks. Long acquisition, adequate zero filling, conservative apodization, careful phasing, and a stable baseline are more valuable than cosmetic line broadening. Temperature should be controlled, normally at 298 K unless the method specifies otherwise, because viscosity, chemical exchange, acid-base equilibria, and water position all move with temperature. Spectra intended for a long-lived database should include a system-suitability sample and retain the raw free-induction decay, pulse program, probe tuning, temperature, receiver gain, shim metrics, linewidth, signal-to-noise, and complete processing history.

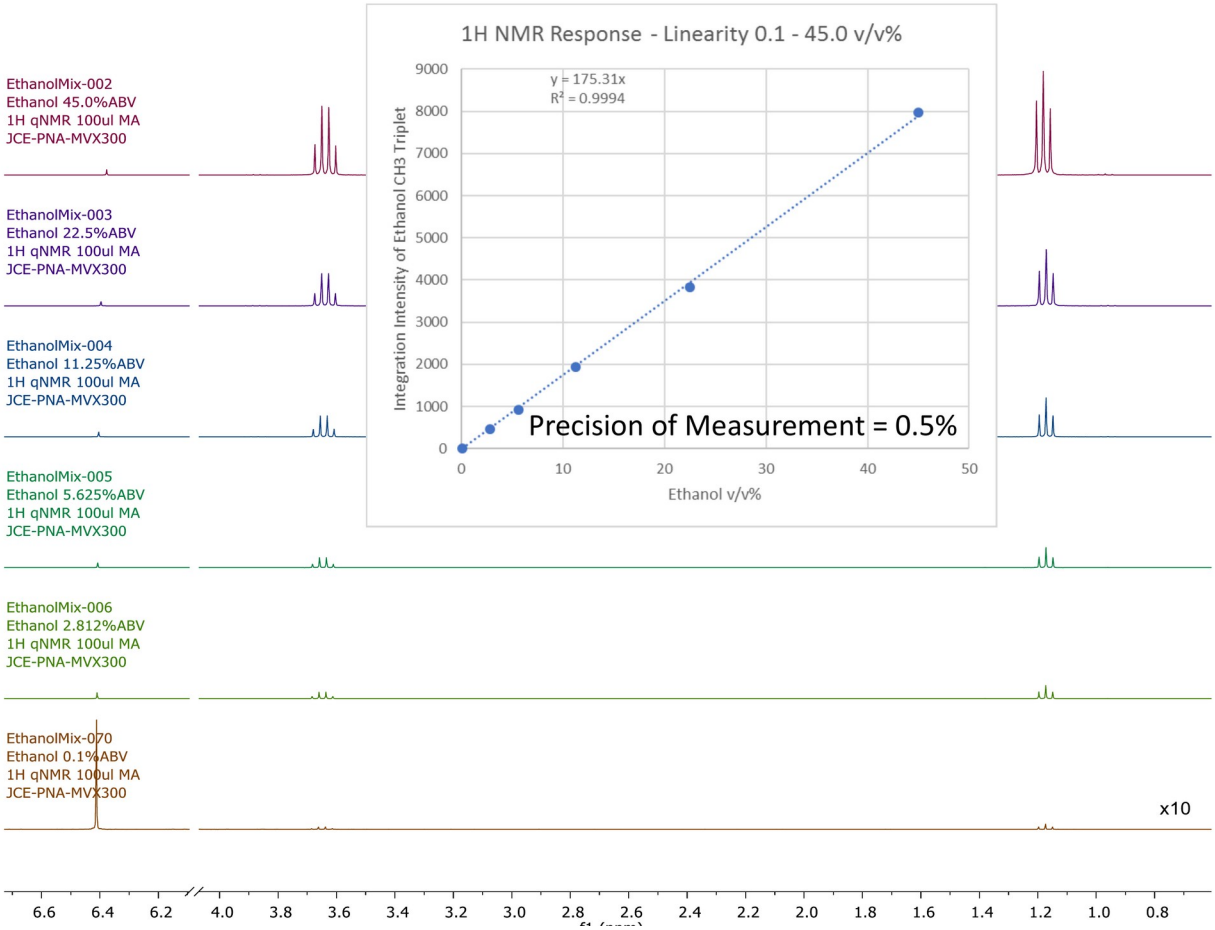

Figure 3. Integral response for ethanol standards spanning approximately 0.1-45% v/v. The strong linear response demonstrates the dynamic range available to qNMR; the slide's stated 0.5% precision is not treated as a universal method-performance claim because the underlying replicate design and uncertainty basis were not supplied. Source: Process NMR Associates, author-supplied 2018 presentation (Ref. 67, p. 11).

3.8 Suppression is part of the measurement model

Water and ethanol suppression cannot be treated as a purely cosmetic preprocessing step. Presaturation can attenuate nearby exchangeable or exchanging resonances and can transfer saturation by chemical exchange or nuclear Overhauser pathways. Multisite suppression may distort ethanol-adjacent signals. Ethanol ^{13}C satellites, each approximately 0.55% of the parent signal at natural abundance, can be comparable in amplitude to legitimate minor beer constituents. At 300 MHz their offsets in ppm differ from those at 600 MHz even though the offsets in hertz are controlled by the one-bond coupling. Any library or fitting routine must therefore model the field-dependent satellite positions or remove them by validated ^{13}C decoupling.

For targeted qNMR, the preferred approach is to select an analyte resonance outside the suppression bandwidth and demonstrate recovery with a spiked matrix. For untargeted fingerprints, a no-suppression or minimally suppressed companion spectrum can be invaluable even if it is not directly quantifiable across the full dynamic range. The companion exposes suppression artifacts and preserves the native relationship among the dominant water, ethanol, and carbohydrate signals.

3.9 What beer NMR does not measure well

A broad-scope platform is credible only if its boundaries are explicit. Routine ^{1}H NMR is insensitive relative to mass spectrometry and fluorescence detection. Many potent aroma compounds occur at microgram-per-liter concentrations and remain below the direct detection limit even though they dominate sensory character. Sulfur compounds, vicinal diketones such as diacetyl, geosmin, and many hop odorants are better addressed by headspace GC-MS or selective methods. Inorganic anions and metal ions lack directly observed protons; they require other nuclei, indirect

correlations, ion chromatography, ICP-MS, or electrode methods. Macromolecular and colloidal material often gives broad, relaxation-weighted signals rather than clean stoichiometric integrals. NMR also does not measure flavor, freshness, or quality in the human sense. It measures molecular composition and physical behavior; sensory or quality conclusions require an independently validated relationship between those measurements and the claimed outcome.

These limits do not weaken the business case. They define the correct division of labor: NMR supplies the integrated compositional map and discovers which changes matter; specialized orthogonal methods then resolve analytes that are below the NMR detection floor or lack an accessible nucleus.

4. Assignment of the ^{1}H Spectrum of Beer

The assignments collected in Tables 2–5 are organized by spectral region and are referenced to TSP-d_4 at δ 0.00 in beer containing approximately 10% D_2O at native pH (4.0–4.6) unless otherwise noted. Entries marked as pH-sensitive move appreciably across the beer pH range and across styles; ranges rather than single values are quoted for these. The assignment corpus rests principally on the systematic studies of the Aveiro group,5,6,18 the quantitative Carlsberg work,7 dedicated organic acid studies,20 and the curated 81-compound library underlying automated beer profiling.21

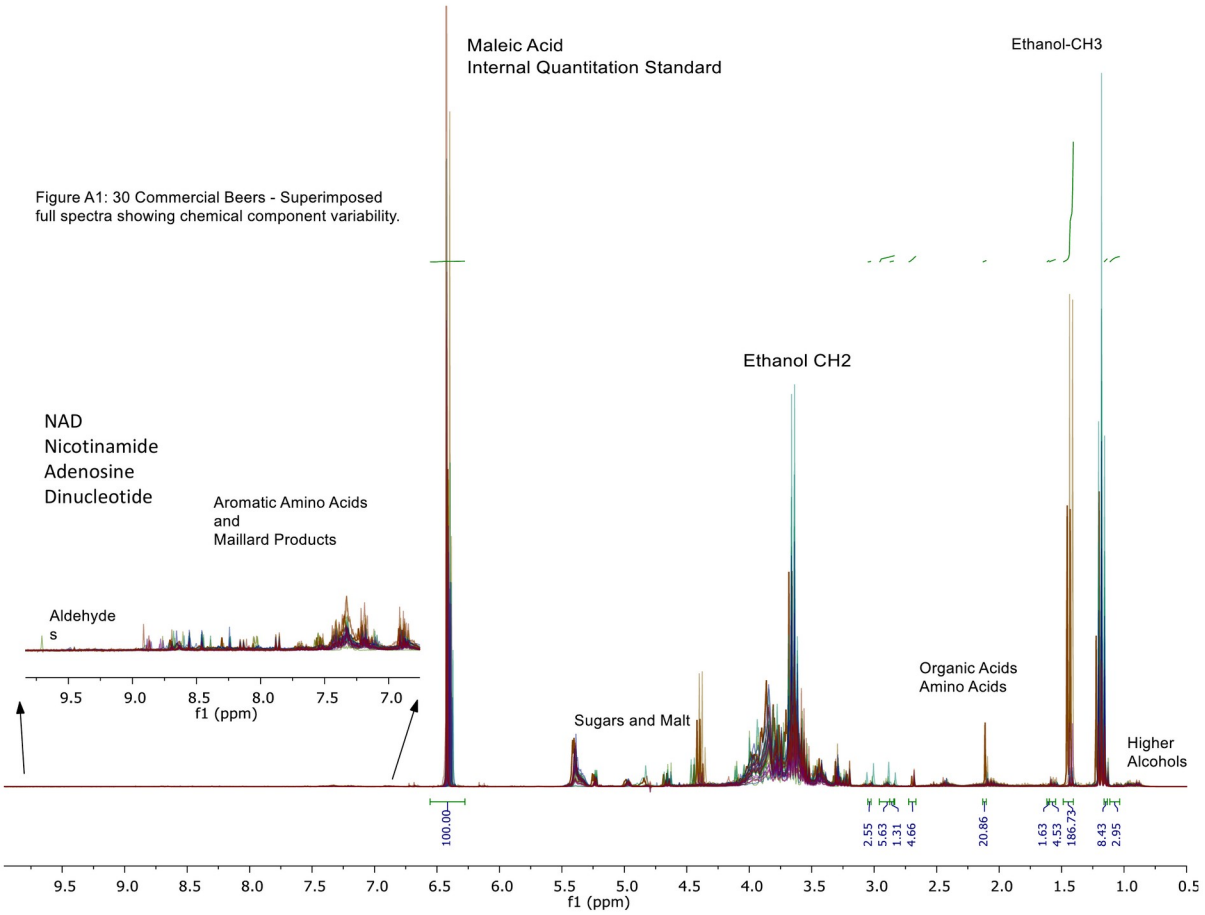

Figure 4. Whole-spectrum superposition from 30 commercial beer spectra, showing the information-rich regions used for targeted qNMR and untargeted fingerprinting. The source deck separately presents a 23-beer quantitative survey; the two cohort counts should not be conflated. Source: Process NMR Associates, author-supplied 2022 presentation (Ref. 68, p. 23).

4.1 High-Field Aliphatic Region (δ 0.8–1.6)

The region opens with the overlapped methyl resonances of the fusel alcohols and branched-chain amino acids between δ 0.85 and 1.05, proceeds through the diagnostic doublets of 2,3-butanediol, the ethanol methyl triplet with its flanking satellites, threonine, acetaldehyde hydrate, and lactate, and closes with the alanine doublet at δ 1.48.

Resolution of the fusel methyls from valine, leucine, and isoleucine at 400 MHz requires either J-resolved projection or lineshape fitting; at 600 MHz the separations are workable directly.7,19,21

4.2 Mid-Field Region (δ 1.6–3.1)

Between δ 1.6 and 3.1 lie the methylene manifolds of proline and GABA, the acetate and pyruvate singlets, the succinate singlet, the citrate and malate AB and ABX systems, the acetyl singlet of ethyl acetate, and the benzylic triplets of tyrosol and 2-phenylethanol. This is the region in which pH sensitivity is most acute: citrate, succinate, and malate each traverse several hundredths to tenths of a ppm across the beer pH range, and it is here that alignment or pH standardization earns its keep.6,16,17,20

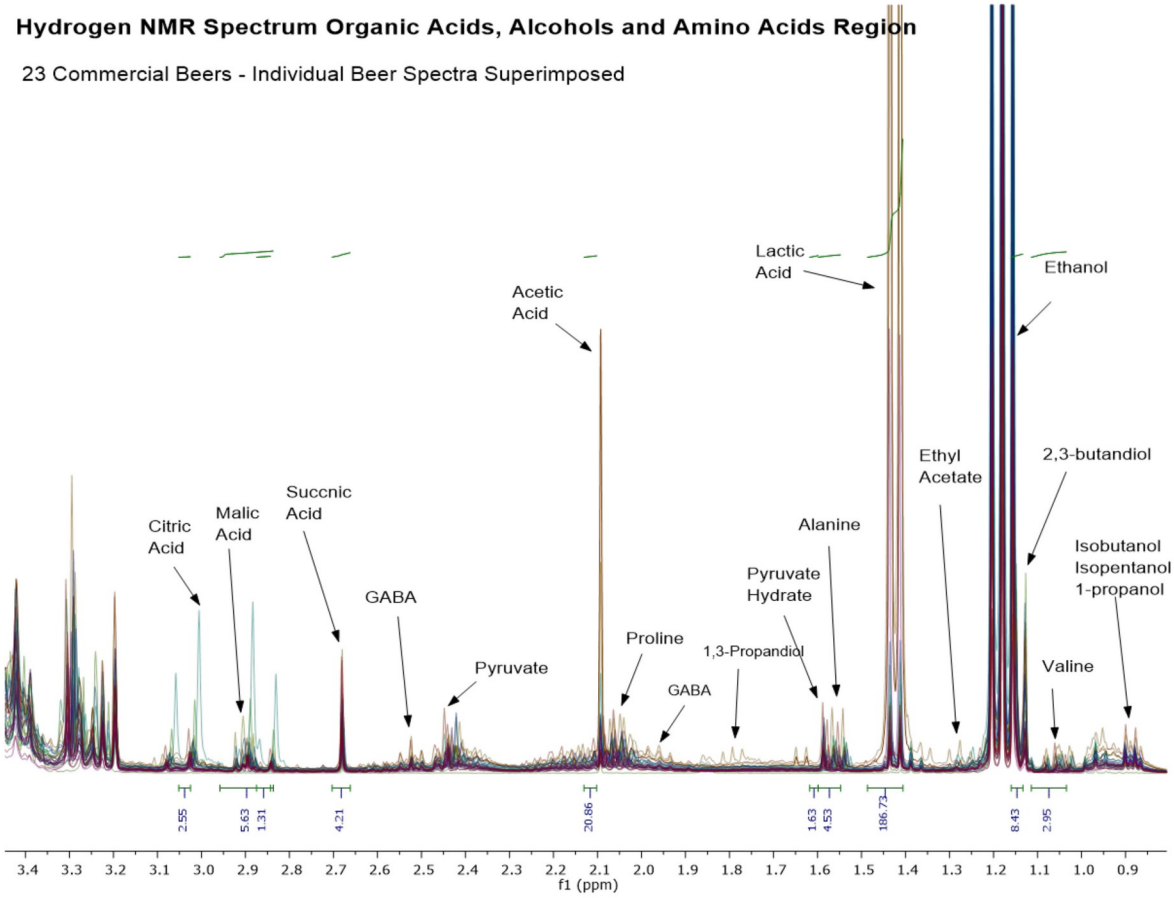

Figure 5. Superimposed aliphatic region from commercial beers, with source assignments for organic acids, amino-acid signals, ethanol, esters, diols, and fusel alcohols. Crowded assignments require matrix-specific confirmation and validated fitting. Source: Process NMR Associates, author-supplied 2018 presentation (Ref. 67, p. 17).

4.3 Carbohydrate Bulk Region (δ 3.1–4.4)

The massif between δ 3.1 and 4.4 contains the ring protons H2–H6 of every glucose residue in the sample — free, oligomeric, and polymeric — together with glycerol, the ethanol methylene quartet, the choline and betaine trimethylammonium singlets, and the hydroxymethylene resonances of the higher alcohols. Little compound-specific quantitation is attempted here in one dimension; the region serves instead as the mass-balance anchor for total carbohydrate and as the HSQC hunting ground for structural work.18,21

4.4 Anomeric Region (δ 4.4–5.5)

The anomeric window is treated in full in Section 5, since its information content is dominated by the dextrin fraction. In brief, it contains the β-anomeric doublets of free and reducing-end glucose near δ 4.65, the β-glucan anomeric pair,

the α-anomeric doublets of free and reducing-end glucose at δ 5.23, the α-(1→6) branch signal at δ 4.96–5.01, and the internal α-(1→4) envelope at δ 5.34–5.44.18,23–25

4.5 Olefinic, Aromatic, and Aldehydic Region (δ 5.5–9.7)

Downfield of the suppressed water line the spectrum thins dramatically, and correspondingly minor species become tractable. Uridine contributes a characteristic pair of doublets near δ 5.90–5.92 with its H6 partner at δ 7.87; the purine nucleosides resonate between δ 8.2 and 8.4; tyrosine, tyrosol, phenylalanine, and 2-phenylethanol populate δ 6.8–7.45; the histidine imidazolium singlets appear near δ 7.3 and 8.6 with pronounced pH dependence; formate provides a clean singlet at δ 8.30–8.46; and the aldehyde window above δ 9.4 carries acetaldehyde, 5-hydroxymethylfurfural, and 2-furaldehyde as essentially background-free staling and heat-load markers.6,7,35,38 The olefinic resonances of the hop-derived iso-α-acids are distributed between δ 5.0 and 6.1 at micromolar concentrations and are discussed in Section 7. In wheat beers, 4-vinylguaiacol produced by yeast decarboxylation of ferulic acid is observed through its vinyl dd near δ 6.67 and terminal methylene doublets at δ 5.63 and 5.10.41

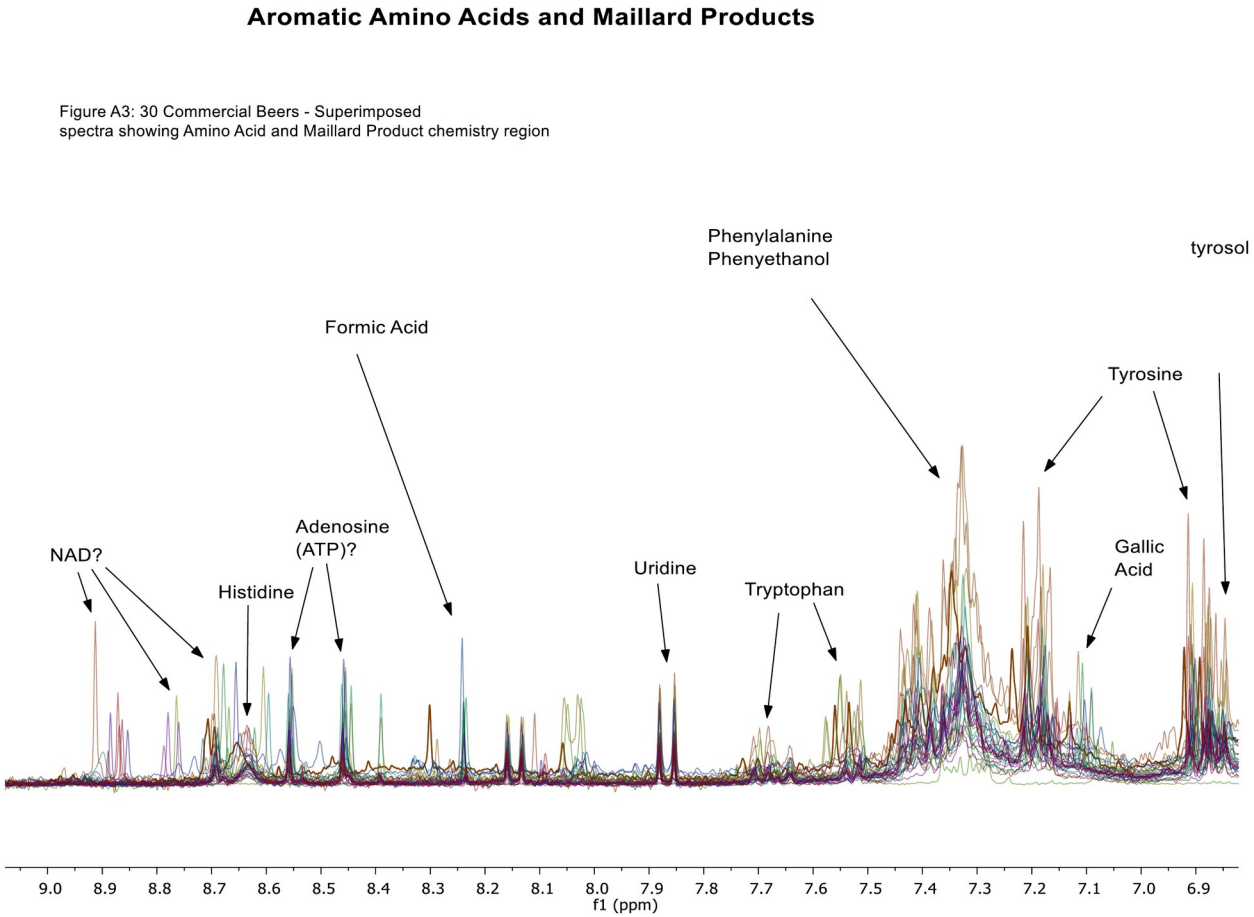

Figure 6. Aromatic and downfield beer region containing nucleotide, amino-acid, phenolic, aromatic-alcohol, formate, and Maillard/aging-related information. Several crowded labels are best regarded as putative until confirmed by 2D NMR or standard addition. Source: Process NMR Associates, author-supplied 2022 presentation (Ref. 68, p. 25).

Table 2. ^{1}H assignments: alcohols, polyols, esters, and carbonyl compounds in beer (δ vs TSP-d_4; s, singlet; d, doublet; t, triplet; q, quartet; m, multiplet).

Compound	Assignment	δ (ppm)	Mult.	J (Hz) / remarks
Ethanol	CH_3 / CH_2	1.18 / 3.65	t / q	7.1; ^{13}C satellites at ±0.5·^{1}J(CH), ^{1}J ≈ 125 Hz
Methanol (trace)	CH_3	3.36	s	—

Compound	Assignment	δ (ppm)	Mult.	J (Hz) / remarks
1-Propanol	CH_3 / CH_2 / CH_2OH	0.89 / 1.55 / 3.56	t / m / t	7.4 / — / 6.7
Isobutanol	$(CH_3)_2$ / CH / CH_2OH	0.89 / 1.74 / 3.35	d / m / d	6.7 / — / 6.6
Isoamyl alcohol	$(CH_3)_2$ / CH_2 / CH / CH_2OH	0.90 / 1.42 / 1.66 / 3.61	d / m / m / t	6.6 / — / — / 6.9
2-Methyl-1-butanol	CH_3 (×2)	0.88–0.92	t + d	≈7; overlapped with isoamyl
2,3-Butanediol	CH_3 (both diastereomers)	1.13–1.15	d	6.2; diastereomer pair
Glycerol	CH_2 / CH_2' / CH	3.56 / 3.65 / 3.78	dd / dd / m	11.7, 6.5 / 11.7, 4.3 / —
2-Phenylethanol	$ArCH_2$ / OCH_2 / ArH	2.85 / 3.85 / 7.26–7.38	t / t / m	6.6
Tyrosol	$ArCH_2$ / OCH_2 / H3,5 / H2,6	2.78 / 3.78 / 6.83 / 7.16	t / t / d / d	6.5 / — / 8.5 / 8.5
Ethyl acetate	OCH_2CH_3 / $C(O)CH_3$ / OCH_2	1.25 / 2.05 / 4.13	t / s / q	7.1; acetyl s overlaps acetate
Acetaldehyde (free)	CH_3 / CHO	2.23 / 9.67	d / q	2.9
Acetaldehyde hydrate	CH_3 / CH	1.31 / 5.24	d / q	5.3; hydrate dominates in beer
Acetoin	$CHCH_3$ / $C(O)CH_3$ / CH	1.37 / 2.22 / 4.42	d / s / q	7.1
Diacetyl	CH_3	2.33	s	Sensory threshold below routine ^1H LOD

Compiled and harmonized from the quantitative beer assignment literature.5–7,20,21 The dominant hydration equilibrium of acetaldehyde in aqueous ethanol means the hydrate doublet at δ 1.31, not the free aldehyde, is the practical quantitation handle.

Table 3. ^1H assignments: organic acids at beer pH (shifts quoted as ranges across pH 3.9–4.6; pK_a values listed to indicate shift sensitivity).

Acid	Assignment	δ range (ppm)	Mult.	J (Hz)	pK_a / remarks
Acetic	CH_3	2.03–2.10	s	—	4.76; overlaps ethyl acetate acetyl
L-Lactic	CH_3 / CH	1.36–1.41 / 4.15–4.35	d / q	6.9	3.86; 3–12 g/L in sour styles
Succinic	CH_2 (×2)	2.53–2.66	s	—	4.21, 5.64
Citric	CH_2 (AB)	2.68–2.92	d + d	15.7	3.13, 4.76, 6.40; strongly pH-mobile
L-Malic	CH_2 (ABX) / CH	2.52–2.90 / 4.32–4.48	dd / dd	16.5, 8.2 / 4.6	3.46, 5.10
Pyruvic	CH_3	2.36–2.41	s	—	2.49; partial hydrate equilibrium
Formic	CH	8.30–8.46	s	—	3.75; clean low-field singlet
Fumaric (trace)	=CH	6.55–6.62	s	—	3.03, 4.44

Assignments and pH behavior per the dedicated organic acid quantification studies.7,16,20 Alignment by icoshift17 or acquisition at standardized pH6,30 is required before bin-based multivariate analysis of this region.

Table 4. ^1H assignments: amino acids and nitrogenous compounds in beer.

Compound	Assignment	δ (ppm)	Mult.	J (Hz) / remarks
L-Proline	γ-CH_2 / β-CH / β-CH′ / δ-CH_2 / α-CH	1.98–2.10 / 2.06 / 2.33 / 3.30–3.45 / 4.13	m / m / m / m / dd	Dominant free amino acid in beer (Section 4.2)
L-Alanine	CH_3	1.48	d	7.3

Compound	Assignment	δ (ppm)	Mult.	J (Hz) / remarks
GABA	β-CH_2 / α-CH_2 / γ-CH_2	1.90 / 2.29–2.38 / 3.01	quint / t / t	7.4 / 7.3 / 7.5
L-Valine	CH_3 / CH_3'	0.99 / 1.04	d / d	7.0
L-Leucine	$(CH_3)_2$	0.95–0.97	d + d	6.2
L-Isoleucine	δ-CH_3 / γ′-CH_3	0.94 / 1.01	t / d	7.4 / 7.0
L-Threonine	CH_3 / β-CH	1.33 / 4.25	d / m	6.6; beneath ethanol ^{13}C satellite
Glutamine / glutamate	β,γ-CH_2	2.05–2.50	m	Overlapped; HSQC-assisted
L-Phenylalanine	H2,6 / H4 / H3,5	7.32 / 7.37 / 7.42	m	—
L-Tyrosine	H3,5 / H2,6	6.90 / 7.19	d / d	8.5
L-Histidine	H5 / H2	7.28–7.35 / 8.55–8.65	s / s	Imidazolium; strongly pH-dependent
L-Tryptophan (trace)	H7 / H4 / H2,5,6	7.54 / 7.73 / 7.20–7.32	d / d / m	8.0
Choline	$N(CH_3)_3$	3.20	s	—
Betaine	$N(CH_3)_3$ / CH_2	3.26 / 3.90	s / s	—

Under anaerobic fermentation, proline assimilation is blocked because the Put1 proline oxidase step requires molecular oxygen; proline consequently survives fermentation as the dominant free amino acid, typically at 150–700 mg/L, and its multiplet manifold is a defining feature of the beer mid-field region.6,7,21

Table 5. ^1H assignments: olefinic, aromatic, heteroaromatic, and aldehydic markers.

Compound	Assignment	δ (ppm)	Mult.	J (Hz) / remarks
Uridine	H5 / H1′ / H6	5.90 / 5.92 / 7.87	d / d / d	8.1 / 4.6 / 8.1; hopping-regime marker38
Adenosine / inosine	H1′ / H2 / H8	6.05–6.11 / 8.22–8.28 / 8.32–8.38	d / s / s	≈6 (H1′)
Iso-α-acids	olefinic envelope	5.0–6.1	m	Micromolar; see Section 719,31–33
4-Vinylguaiacol	$=CH_2$ (Z) / $=CH_2$ (E) / CH= / OCH_3	5.10 / 5.63 / 6.67 / 3.89	d / d / dd / s	10.9 / 17.6 / 17.6, 10.9; wheat beers41
5-HMF	CH_2OH / H4 / H3 / CHO	4.70 / 6.68 / 7.53 / 9.44	s / d / d / s	3.5; heat-load and aging marker35
2-Furaldehyde	H4 / H3 / H5 / CHO	6.74 / 7.55 / 7.94 / 9.49	dd / d / m / s	3.6, 1.7; staling marker35
Acetaldehyde	CHO	9.67	q	2.9
Formate	CH	8.30–8.46	s	Cross-referenced from Table 3

The near-empty aldehydic window above δ 9.4 permits trace carbonyl quantitation with extended acquisition despite the µM–low-mg/L concentration regime; vicinal-diketone flavor thresholds (diacetyl ≈ 0.1 mg/L) remain below routine one-dimensional ^1H detection limits and are more honestly addressed by headspace GC.

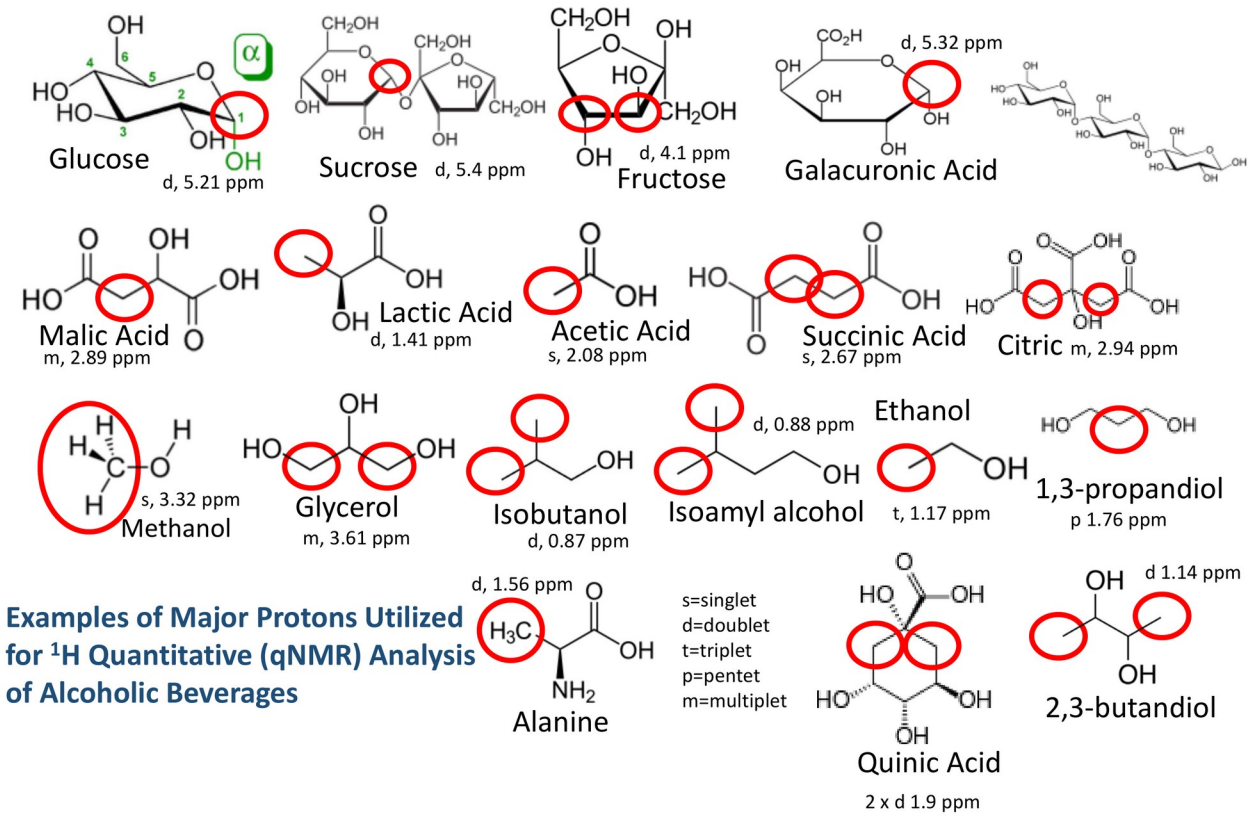

Figure 7. Representative resonances used in targeted ¹H qNMR of alcoholic beverages. Chemical shifts are approximate and matrix-dependent; the source label 'Galacuronic' should be read as galacturonic acid. Source: Process NMR Associates, author-supplied 2018 presentation (Ref. 67, p. 15).

5. Residual Dextrins, Starch Fragments, and Glucans: A Deep NMR View

Residual carbohydrates are not an undifferentiated remainder. They include glucose, maltose, maltotriose and higher linear maltooligosaccharides, branched α-limit dextrins, cereal mixed-linkage β-glucans, arabinoxylan fragments, and other minor saccharides.65 Together these components retain information about raw material, starch gelatinization, enzyme access, mash time-temperature-pH history, fermentation, adjunct use, exogenous enzymes, and post-package change. Quantitative ¹H NMR can measure resolved sugars, reducing-end pools, calibrated linkage envelopes, and reproducible fingerprints; high-resolution ¹H-¹³C methods can add individual lower-DP reporters and local branch motifs. One unfractionated spectrum does not, however, reconstruct the complete sequence, branch topology, or molecular-weight distribution of every high-DP dextrin.

Four evidence levels are kept explicit in this section. **Established** findings come from the validated primary literature. **PNA observations** are visible in the author-supplied poster and presentations but do not always include raw data, replication, or external validation. **Inferences** are chemically reasoned interpretations rather than proven causal relationships. **Proposed** quantities and experiments define the next analytical program and must be validated before routine reporting.

5.1 The carbohydrate system carried from grain to beer

5.1.1 Starch architecture and the origin of residual dextrins

Established. Cereal starch is composed principally of amylose and amylopectin. Amylose is dominated by α-(1→4)-linked glucopyranosyl residues; amylopectin contains α-(1→4) chains joined through α-(1→6) branch points. One of

the NMR studies used the useful order-of-magnitude statement that about 5% of amylopectin glucopyranosyl residues participate in α-(1→6) bonds. 54,56–57

During starch hydrolysis, enzymes cleave accessible α-(1→4) bonds much more readily than bonds near branch points, and debranching activity is required to remove α-(1→6) constraints efficiently. Consequently, short linear maltooligosaccharides and branched remnants accumulate. In the NMR literature used here, the trimmed branched products remaining after amylolysis are called **α-limit dextrins**. Their detailed local structures report where the enzyme or enzyme mixture could and could not proceed near a branch. 54–57

The term **β-limit dextrin** must not be used interchangeably. It conventionally denotes the more highly branched residue left after exhaustive β-amylase action. The 2025 automated beer NMR study used a commercial β-limit dextrin as the reference component for fitting a broad dextrin contribution and explicitly reported the result as glucose equivalents. That fitted component is therefore a practical model of the dextrin envelope, not proof that the sample contains one defined β-limit dextrin species. 21

5.1.2 What happens during mashing and fermentation

Established. Endo-cleavage creates new chain ends and a changing distribution of longer maltodextrins; exo-acting enzymes produce smaller carbohydrates from accessible chain ends. Enzymatic access is restricted in the immediate vicinity of α-(1→6) branches, which enriches branch-containing remnants as hydrolysis proceeds. Time-resolved NMR of amylopectin amylolysis, although conducted with salivary α-amylase rather than brewing enzymes, directly demonstrated the sequential appearance of large fragments, G8/G7, smaller maltooligosaccharides, maltose, glucose, and several α-limit dextrins. The experiment resolved pathway intermediates every 150 seconds. 57

PNA observation. The author-provided educational slide depicts α-(1→4) cleavage producing maltose and glucose while a branch region persists. The subsequent overlay of cooled wort and finished beer shows large losses of maltose and reducing-sugar signals during fermentation, while a smaller α-(1→6)-branch envelope remains visible. This is an effective visual illustration of selective fermentation of lower-DP sugars and persistence of branched material, but the figure should be captioned as a representative PNA example rather than a universal kinetic result. 68, pp. 19-20

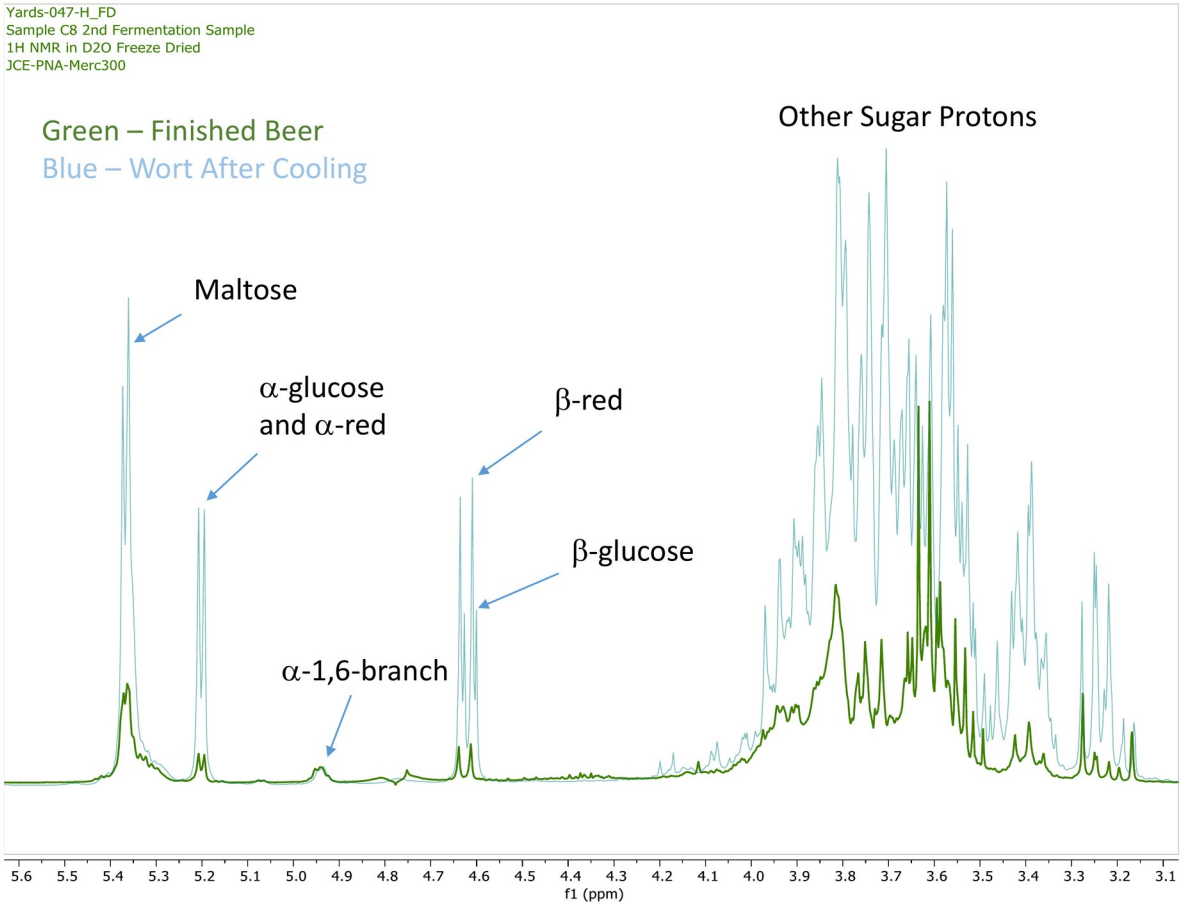

Figure 8. Cooled wort (blue) and finished beer (green) carbohydrate spectra. Depletion of maltose and reducing-sugar signals and persistence of a complex branch-containing envelope make fermentation selectivity directly visible. Scaling and matched-sample metadata must be specified before quantitative interpretation. Source: Process NMR Associates, author-supplied 2022 presentation (Ref. 68, p. 20).

Inference. The finished-beer dextrin pattern is an integrated outcome of at least four stages:

substrate architecture inherited from the grain and adjuncts;

gelatinization, solubilization, and enzyme exposure during mashing;

production of fermentable sugars and limit dextrins by the active enzyme system;

selective uptake and metabolism of the fermentable fraction by the fermentation organisms.

Consequently, a final beer fingerprint can be highly diagnostic of process history while remaining non-unique with respect to cause. A controlled longitudinal design is needed to separate malt, mash, enzyme, yeast, and post-fermentation effects.

5.1.3 Residual dextrin versus non-starch polysaccharides

Beer contains more than starch fragments. Cereal mixed-linkage β-glucan and arabinoxylan fragments also contribute signals, macromolecular baselines, viscosity, and apparent molecular-size distributions. A high-resolution ^{1}H study of non-fractionated beer assigned more than 50 carbohydrate moieties, including cleavage-site motifs from starch, β-glucan, and arabinoxylan. DOSY supplied independent size information and indicated especially high-molecular-weight arabinoxylan fragments in finished beer. 63

This distinction matters analytically. The PNA poster identifies an operational 4.9-5.5 ppm α-glucan region and a 4.4-4.75 ppm β-glucan/carbohydrate region. The latter overlaps the residual water region under many beer NMR conditions and therefore requires particularly careful water-suppression validation. 66

5.1.4 What non-fractionated beer reveals: cleavage motifs and hydrodynamic size

The principal advance of Petersen et al. is a change in the analytical unit of observation. Rather than first separating beer carbohydrate classes, the authors examined the combined carbohydrate mixture in six beers of different styles and used high-resolution ^{1}H H1-H2 reporter groups to assign more than 50 carbohydrate moieties. The resolved set included more than 20 small carbohydrates represented by more than 38 isomeric forms, together with local motifs at cleavage sites in starch, mixed-linkage β-glucan, and arabinoxylan. Differences among the beers showed that the extent and specificity of enzymatic polysaccharide cleavage varied with product and process. 63

Composition axis. Resolved small sugars and maltooligosaccharides describe what remains after mashing and fermentation; where standards and response validation are available, selected molecules can be reported as true concentrations.

Structural axis. Starch-, β-glucan-, and arabinoxylan-cleavage reporters describe local linkage or end-group environments. They reveal enzyme selectivity but do not, by themselves, reconstruct the complete sequence or topology of the parent polymer.

Mobility axis. DOSY supplies an orthogonal apparent-size descriptor. In the published beers it particularly supported high-molecular-weight arabinoxylan assignments, showing why a slow-diffusing carbohydrate signal must not automatically be labeled a higher-DP dextrin. 63

The analytical consequence is substantial. Two beers can have the same total residual-carbohydrate or broad α-glucan result and still differ in lower-DP species, branch-adjacent environments, non-starch polysaccharide cleavage patterns, and diffusion behavior. Dextrin character should therefore be reported as a linked set of composition, linkage, end-group, motif, and mobility variables rather than as one total-dextrin number.

The term non-fractionated must also be read correctly. It means that preparative chromatographic separation of carbohydrate classes was not required before the NMR measurement; it does not guarantee zero sample preparation, native colloidal state, or quantitative recovery of every polymer. Nor does observation or assignment make every reporter an absolute qNMR signal. The Petersen paper establishes exceptional structural observability and comparative profiling. Absolute concentration still requires analyte- or class-specific response validation, adequate relaxation, suppression-recovery testing, and a defined NMR-visible fraction. The paper's organoleptic and prebiotic implications are hypotheses; no direct sensory calibration was performed. 63

A companion optimized HSQC study provides the quantitative bridge for a defined subset. At 800 MHz with a cryoprobe, lyophilized beer redissolved in D_2O, and a 15-minute narrow-window ^{1}H-^{13}C HSQC experiment, G1-G8, isomaltose, and panose calibrations agreed with HPAEC-PAD at $R^2 > 0.99$ and slope 1.01 and with HILIC-UPLC fluorescence at $R^2 > 0.99$ and slope 1.02; independent reporter sites agreed at $R^2 = 0.996$, and the reported LOQ was on the order of 10 µg/mL. Those performance figures belong to that method and hardware configuration. 54

Instrument-transfer implication. The same study showed that 1D ^{1}H and DQF-COSY remained too overlapped for individual maltooligosaccharide identification and quantitation even at 800 MHz; decisive separation came from the ^{13}C dimension of the optimized HSQC. At 300 MHz proton frequency, a 0.01 ppm separation in the ^{13}C dimension corresponds to only about 0.75 Hz at 75 MHz, below the approximately 3 Hz glucan linewidths reported in the high-field work. Narrow sweep widths improve digital sampling but cannot manufacture physical resolution. A 300 MHz PNA method can defensibly emphasize aggregate linkage, reducing-end, enzyme-difference, diffusion-class, and multivariate fingerprint variables; individual G1-G8 or branch isomers should be reported only when matrix-matched standards demonstrate actual resolution, recovery, and precision. 54

5.2 Anomeric configuration and linkage-specific NMR reporters

5.2.1 Why the anomeric region is the preferred structural window

Established. The bulk ring-proton region of carbohydrates, approximately 3.1-4.2 ppm in typical beer spectra, contains intense and highly overlapping multiplets. In contrast, the anomeric H1 protons of many pyranoses occur between approximately 4.4 and 5.5 ppm. Pairing H1 with C1 in HSQC creates a much larger dispersion because the

^{13}C chemical-shift scale is roughly 20 times wider than the corresponding ^{1}H scale. Natural-abundance ^{13}C also avoids the extensive homonuclear carbon splitting that would otherwise complicate the indirect dimension. 53–57

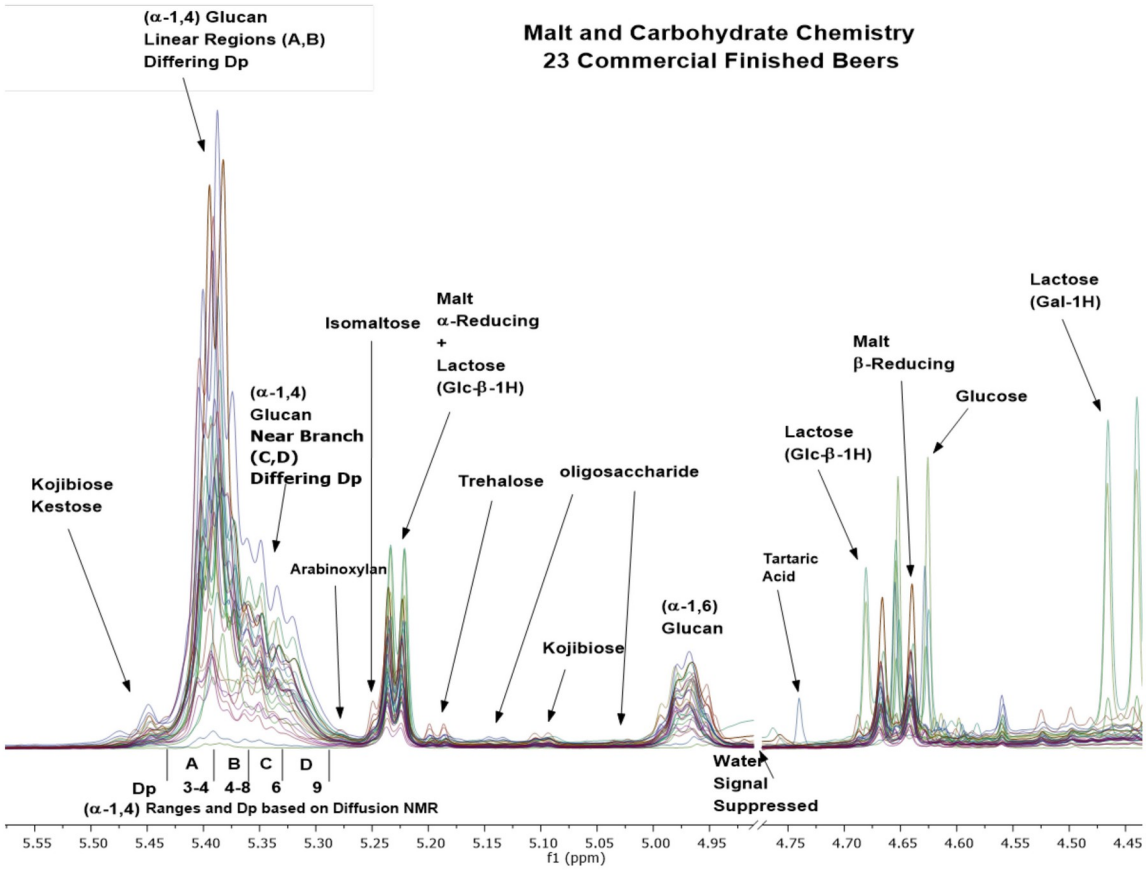

Figure 9. Anomeric-region superposition from 23 commercial beers, revealing substantial diversity in malt, maltooligosaccharide, reducing-end, branch-associated, glucose, lactose, and β-linked carbohydrate signals. DP labels are operational/model-based until calibrated with standards and 2D experiments. Source: Process NMR Associates, author-supplied 2022 presentation (Ref. 68, p. 21).

The anomeric signal identifies three different chemical situations:

a glycosidically fixed α-anomeric center, such as the donor residue in an α-(1→4) or α-(1→6) bond;

a glycosidically fixed β-anomeric center, such as cereal β-glucan or cellobiose-like linkages;

a free reducing end, which exists as an equilibrium of α and β anomers and therefore gives two reducing-end reporters.

For a reducing linear maltooligosaccharide, all glycosidically bound donor residues remain α, whereas the single reducing-end residue mutarotates between α and β forms. Time-resolved amylopectin hydrolysis resolved both forms for G1-G4. The retaining α-amylase used in that study initially produced predominantly α-maltotetraose; mutarotation occurred more slowly than its initial production. 57

5.2.2 Reference chemical shifts relevant to beer dextrins

The following values are **reference-condition values**, not universal peak positions. Most are from a consistently referenced D_2O library at 310 K; the branched-model work was also performed in D_2O at 310 K with acetone referencing. Beer pH, ionic strength, ethanol, temperature, referencing, and suppression conditions must be standardized before using sub-0.01 ppm matching criteria. 53,56

Reporter or structure	Representative $\delta^{1}H$ / $\delta^{13}C$ (ppm)	Structural meaning and caution
α-D-glucose reducing anomer	5.230 / 92.990	Free glucose α form; overlaps other α reducing-end signals

Reporter or structure	Representative $\delta^{1}H$ / $\delta^{13}C$ (ppm)	Structural meaning and caution
		in ^{1}H.
β-D-glucose reducing anomer	4.642 / 96.806	Free glucose β form; close to the water-suppression region in aqueous beer.
Amylopectin internal α-glucan envelope	5.395-5.406 / 100.470-100.635; principal value 5.401 / 100.520	Polymeric/internal α-(1→4) environment; a second reported amylopectin reporter was 5.392 / 100.686.
Maltose glycosidic H1/C1 reporter(s)	5.392-5.393 / 100.512-100.590	These are fixed glycosidic reporter sites, not the free reducing-end resonances.
Maltotriose fixed α-(1→4) sites	about 5.390 / 100.359, 100.438, 100.683	Site-to-site C1 differences provide DP information in high-resolution HSQC.
Maltotetraose fixed α-(1→4) reporter	5.380 / 100.532	A reporter peak, not a complete residue-by-residue assignment.
Maltopentaose through maltooctaose reporters	$\delta^{1}H$ about 5.387-5.399; $\delta^{13}C$ about 100.467-100.533	The values converge as the local internal environments become similar; at least one diagnostic peak can still identify G5-G8 under optimized conditions.
Isomaltose α-(1→6) reporters	4.954-4.961 / 98.847-98.886	Illustrates the separation of α-(1→6) from α-(1→4) in H1/C1 space.
Isomaltotriose α-(1→6) reporters	4.967-4.972 / 98.640-98.818	Multiple local α-(1→6) environments.
Panose branch reporter	4.961 / 98.985	α-(1→6) branch reporter; α-(1→4) reporters also occur at 5.392-5.393 / 100.614-100.702.
6^{3}-α-D-glucosyl-maltotriose	branch: 4.959 / 98.970; α-(1→4): 5.378-5.391 / 100.339-100.798	Defined singly branched limit-dextrin standard.
6^{3}-α-D-maltosyl-maltotriose	branch: 4.958 / 98.834; α-(1→4): 5.363-5.380 / 100.750-100.964	Defined branched reference.
6^{3}-α-D-maltosyl-maltotetraose	branch: 4.976 / 99.479; α-(1→4): 5.335-5.350 / 100.812-100.911	Shows substantial local-structure dependence near the branch.
Nigerose, α-(1→3) disaccharide	5.350 / 99.916 and 5.363 / 99.980	Not an α-(1→6) dextrin; reported at higher levels in the ale class in one study.
Mixed-linkage β-glucan library signals	4.537-4.780 / 103.215-103.434	β-linked cereal glucan region; direct ^{1}H work is vulnerable to water suppression.
Cellobiose β-(1→4) glycosidic reporters	4.514-4.516 / 103.404-103.442	Useful comparator for β-(1→4) environments.
α-(1→6)-substituted acceptor C6	typically about 66.25-68.20 ppm, versus about 61 ppm when unsubstituted	The downfield C6 substitution shift is independent evidence of an O6 linkage; a full HSQC/HMBC window is required because a C1-only HSQC does not observe it.

5.2.3 What branch-point chemical shifts actually report

Chemical synthesis and complete NMR assignment of branched α-dextrin standards from isomaltose through a doubly branched decasaccharide established that C1 and C6 shifts around α-(1→6) bonds depend strongly on the immediate branch environment. Addition of residues toward the non-reducing end had a particularly strong effect. Substitution at O6 also altered hydroxymethyl conformer populations, and the $^{13}C6$ shift correlated with the H5-H6R three-bond coupling and the population of the gauche-trans C5-C6 rotamer. 56

This has two analytical consequences:

A branch cross-peak is more than a simple binary marker for “branch present”; its position can classify the local motif around the branch.

The same local motif may occur in many larger molecules. A cross-peak assignment to a motif is not equivalent to assignment of the complete parent dextrin.

The optimized beer HSQC work distinguished at least 12 α-(1→6)-attached branch-point types and assigned eight using available standards. Reference-compound availability, rather than nominal spectral resolution alone, remained the limiting factor for many branched fragments. 54

5.3 Degree of polymerization, branching, and what can be quantified

5.3.1 Molecularly specific DP assignments

Established. Three levels of DP information have been demonstrated:

High-field non-fractionated ^{1}H and H1-H2 correlation profiling: more than 50 local carbohydrate moieties can be assigned under optimized high-resolution conditions, but a routine 300 MHz 1D spectrum generally supports only broad or partially resolved lower-/higher-DP and branch-adjacent operational bins. Extensive overlap prevents complete molecular speciation. 5,55,63,66-68

Targeted narrow-window HSQC: at least one diagnostic H1/C1 reporter for linear G1-G8 and multiple branched species can be resolved under high-field, high-resolution conditions. 54

LC-NMR/MS after chromatographic separation: dextrins through DP 9 were identified in 1-2 hours with degassing as the only initial treatment. α-(1→6) branching was readily indicated within a fraction, but high-DP linear versus branched forms still could not always be assigned unambiguously. 18

The apparent tension between reports that identify G1-G8 and the statement that chemically distinct carbohydrates are generally resolved only to approximately DP 4-5 is resolved by distinguishing **diagnostic reporter detection** from **complete molecular assignment**. A single end-adjacent C1 shift can remain DP-sensitive through G8, while the many internal residues in longer chains converge to nearly indistinguishable local environments. 54–55

5.3.2 Apparent number-average DP from linkage and reducing-end counts

Proposed, chemically derived metric. If all α-glycosidic anomeric protons and both reducing-end anomers are quantitatively observed, a number-average DP can be estimated from the fact that a connected reducing oligosaccharide with DP = n contains n - 1 glycosidic bonds and one reducing end. After response correction:

where terms are experimentally determined response factors under the selected pulse sequence.

Related operational metrics are:

and

These equations are analytically attractive but have not been validated here for whole beer. The principal failure modes are incomplete observation of β reducing ends near water, overlap of free glucose and α reducing ends, inclusion of non-starch α-glucans, differential relaxation or HSQC transfer, broad/invisible high-DP material, and the possibility of non-reducing cyclic material. They yield number-average and motif-average quantities, not a molecular-weight distribution or a unique topology.

5.3.3 Branch fraction is not branch topology

An integrated α-(1→6)/total α-linkage ratio can estimate the fraction of observed glycosidic bonds that are branches. It cannot reveal whether those branches occur one per molecule or are concentrated in a smaller population of multiply branched molecules. Neither can it determine branch spacing, A/B/C chain architecture, or the order in which local branch motifs occur. Those questions require fractionation, multiple standards, and potentially LC-NMR/MS, SEC/AF4 with molar-mass detection, or advanced multidimensional methods.

5.3.4 Reporting concentration: molecular species versus glucose equivalents

For a resolved analyte such as maltose, qNMR can report true molar and mass concentration when signal stoichiometry, purity of the standard, recovery, and relaxation are controlled. For a heterogeneous dextrin envelope, concentration is necessarily model-dependent unless every species is assigned. Appropriate labels include:

“total observed α-glucan anomeric proton equivalents”;

“apparent dextrin concentration as glucose equivalents”;

“apparent dextrin concentration relative to [named dextrin standard]”;

“molar concentration of the assigned G3/G4/… reporter” for individually calibrated species.

The 2025 MagMet-B supporting data illustrate this distinction. A commercial β-limit dextrin reference was used, and the reported dextrin values were explicitly marked “as glucose equivalents.” Across the 11 listed beers, manual and automated estimates were approximately 14.9-36.2 g/L. These results demonstrate that an abundant broad dextrin contribution can be modeled reproducibly; they do not establish the molecular identity or DP distribution of that entire mass. 21

5.3.5 A defensible dextrin-character vector

The combined non-fractionated-beer, optimized-HSQC, and branched-model literature supports a structured reporting panel. It does not support collapsing every result into one nominal dextrin concentration. The following variables should be kept separate because they answer different chemical questions. 54,56,63

Total observed α-glucan equivalents. Absolute q^{1}H response for a validated starch-derived envelope, reported in glucose equivalents or relative to a named dextrin standard and corrected for resolved free sugars and other α-glucans.

Resolved lower-DP species. Molecular concentrations for only those G1-G8, isomaltose, panose, or related species that pass standard-addition identity, recovery, precision, and orthogonal confirmation criteria on the instrument used.

Linkage balance. An operational α-(1→6)/α-(1→4) index and the α-(1→6) fraction of observed α-glycosidic sites. These describe linkage-site abundance, not the percentage of molecules that are branched.

Reducing ends and apparent number-average DP. The summed α/β reducing-end pool and the Section 5.3.2 linkage-to-end calculation, after free sugars, cyclic material, water-suppression bias, and mutarotation equilibrium are controlled.

Branch-neighborhood or pruning score. Calibrated high-resolution bins for simpler versus more substituted α-(1→6) environments. This can track how closely α-(1→4) chains were removed around resistant branch points; exact topology requires additional evidence.

Non-starch polysaccharide scores. Separate β-glucan and arabinoxylan cleavage-motif responses so that their signals and physical effects are not misassigned to the dextrin pool.

Diffusion-size descriptors. Family-specific apparent diffusion coefficients where resolved, plus the fraction of signal in validated fast, intermediate, and slow mobility bins. These are hydrodynamic classes, not an exact DP or molecular-weight distribution.

Enzyme-accessibility indices. Signal loss and glucose release after α-amylase, debranching enzyme, and exhaustive amyloglucosidase treatment, providing a practical way to make 300 MHz regional integrals more chemically specific.

Full dextrin-region fingerprint. Aligned spectral points, defined bins, or fitted components retained for batch, process, style, enzyme-use, and anomaly models. A fingerprint supports validated classification but is not a concentration unless separately calibrated.

This panel intentionally mixes absolute concentrations with operational structural and physical indices. Every reported variable must carry its units, calibration basis, evidence level, and uncertainty or repeatability statement. The language should never imply that a motif, regional integral, or diffusion class uniquely identifies a complete dextrin molecule.

5.4 Process information encoded in residual dextrins

5.4.1 Ale, lager, and producer effects

Established. Optimized HSQC spectra showed visibly different branch-region fingerprints among ale, lager, and pilsner samples. One study found substantial branched DP 2-5 fragments in a lager, while longer fragments with DP greater than 5 predominated in an ale around $\delta^{13}C$ 99.8 ppm. A larger 45-beer study similarly found higher complex limit-dextrin features in ales and shorter limit dextrins in lagers. 54–55

The larger study used OPLS-DA on ^{13}C projections from the anomeric region to separate ale and lager samples (R^2 = 0.67, Q^2 = 0.60). Most discriminatory features were associated with α-(1→6) linkages; nigerose was also elevated in the ale class. However, the classes differed not only in fermentation organism and temperature but also in producers, raw materials, and production practices. The observed relationship is therefore a validated class association, not a single-factor yeast mechanism. 55

5.4.2 Mash control versus fermentation variability

Established. Replicate commercial products from one producer showed smaller batch variation in the α-(1→6) limit-dextrin region than in the small linear maltooligosaccharide region. The authors interpreted the branch-region consistency as evidence of a well-controlled starch-cleavage/mashing process, while the greater variability in small oligomers could reflect the longer, biologically mediated fermentation stage. 55

PNA observation. The Bell's Brewing presentation compares two laboratory mashes, a standard mash, and a turbid mash for a New England IPA. The turbid mash has a distinctly lower DP 3-4 operational bin, a much larger DP 5-8 bin, changed reducing-end distributions, and a lower plotted total-carbohydrate value than the other three conditions. The graph is a strong white-paper example of how NMR reveals that two samples with superficially similar "total carbohydrate" can have materially different chain-length distributions. No error bars or replicate design are included on the slide, so causal and uncertainty statements should be reserved for the follow-up dataset. 67, p. 32

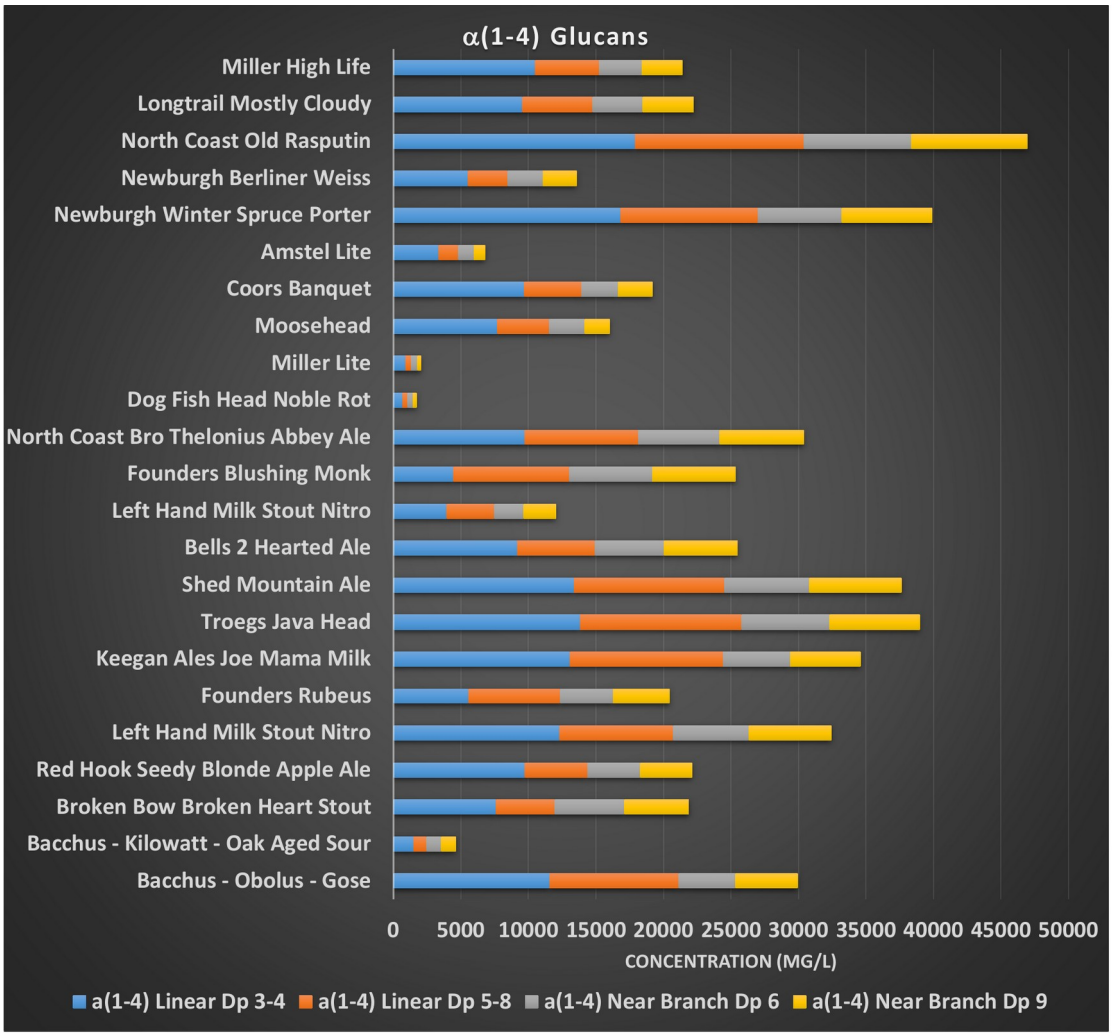

Figure 10. Residual α-(1→4) glucan distributions across the 23-beer survey, grouped into operational linear and branch-adjacent DP classes. The panel demonstrates between-product variability; it does not establish unique molecular DP distributions and does not include raw-data uncertainty. Source: Process NMR Associates, author-supplied WBC poster (Ref. 66, p. 1).

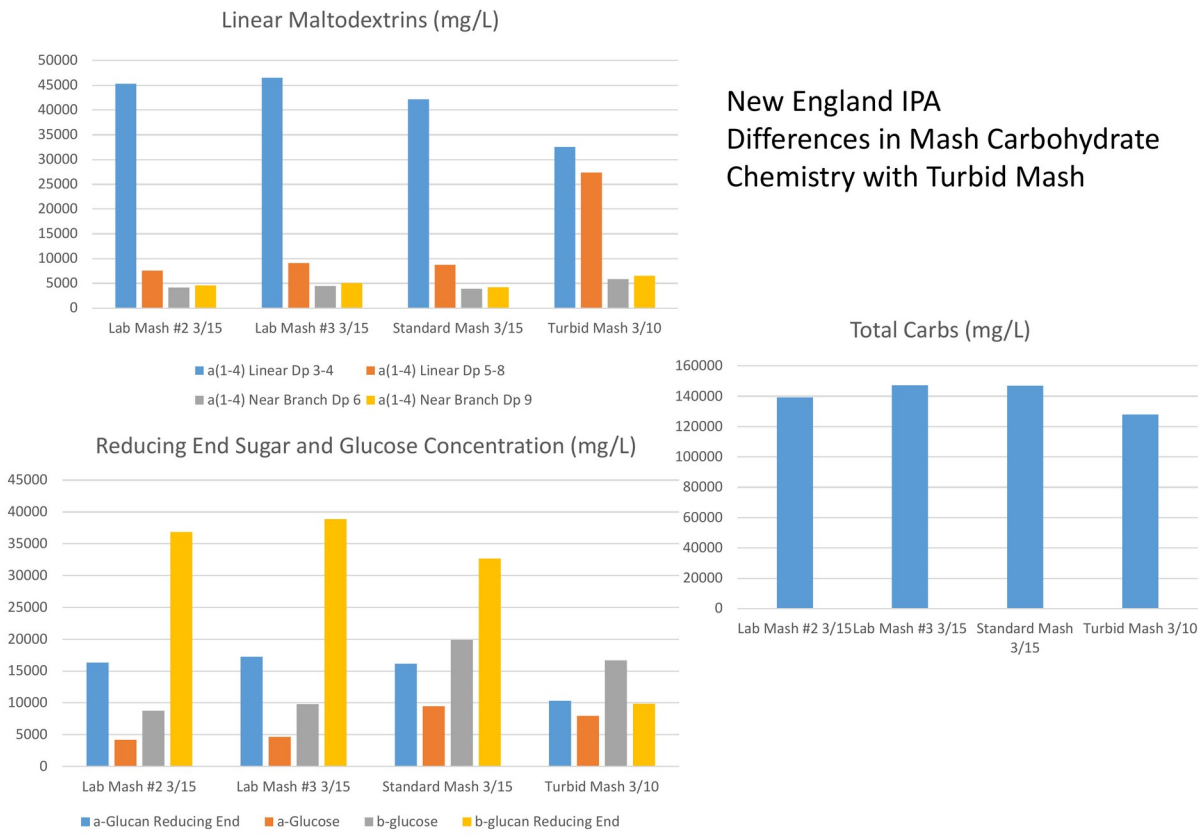

Figure 11. Laboratory, standard, and turbid mash comparison using operational linear-maltodextrin, reducing-end, glucose, and total-carbohydrate variables. The turbid mash redistributes the measured carbohydrate pattern. The presentation does not provide replicate statistics or error bars, so this is an illustrative PNA case study. Source: Process NMR Associates, author-supplied 2018 presentation (Ref. 67, p. 32).

5.4.3 Fermentation and attenuation

PNA observation. The wort-versus-finished-beer overlay shows strong depletion of maltose, α/β reducing-end signals, and much of the bulk ring-proton envelope, with a persistent α-(1→6) region. This directly motivates a time-course study of selective substrate consumption. 68, p. 20

Established. In the 45-beer HSQC study, residual starch-fragment features predicted labeled ABV over a restricted conventional range with $R^2 = 0.67$, $Q^2 = 0.62$, and RMSECV = 0.53% ABV. Adding high- and low-alcohol products reduced R^2 from 0.67 to 0.45 and Q^2 from 0.62 to 0.15 because processes such as high-gravity production or alcohol removal/addition decouple final ABV from ordinary residual starch utilization. 55

Inference. A dextrin fingerprint is therefore most defensible as a marker of process state within a defined production family. It should not be used as a universal stand-alone predictor of attenuation, original gravity, or ABV without a product-class model and external validation.

5.4.4 Adjuncts, non-alcoholic beer, and specialty processes

PNA observation. The WBC poster states that rice and other carbohydrate sources alter dextrin character and that residual dextrin fingerprints can distinguish process variations. The Bell's turbid-mash data provide one concrete example. 66–67

Established. Direct ^{1}H NMR comparisons of regular and non-alcoholic lagers showed a more intense 3-4 ppm carbohydrate region in alcohol-free products. This is consistent with different fermentation/dealcoholization strategies, but the region is highly overlapped and does not by itself identify which carbohydrate classes are responsible. 59

Proposed. Non-alcoholic beer should be a dedicated validation cohort. Limited fermentation, arrested fermentation, special maltose-negative yeasts, membrane or thermal dealcoholization, and dilution may produce similar ABV values but different glucose/maltose/maltotriose/dextrin fingerprints. A paired process-history design can test whether NMR distinguishes these pathways.

5.5 What each NMR experiment can and cannot deliver

Experiment	Defensible deliverables	Principal limitations in beer
Quantitative 1D ^{1}H, direct beer	Glucose, maltose and other resolved sugars; reducing-end pools; operational α-(1→4), α-(1→6), and β-glucan regions; total fingerprint; comparison through a process time course	Severe carbohydrate overlap; water and ethanol suppression; broad macromolecular baseline; cannot uniquely assign high-DP structures
Quantitative 1D ^{1}H, freeze-dried/redissolved nonvolatile residue	Higher concentration of nonvolatile carbohydrates; cleaner comparison without ethanol; useful for low-intensity anomeric signals	Volatile chemistry is lost; recovery, dry-mass water, reconstitution volume, pH, and solubility must be validated
Full-range ^{1}H-^{13}C HSQC	H/C correlation, α versus β linkage classes, substituted C4/C6 evidence, reference matching, carbohydrate-versus-noncarbohydrate separation	Conventional wide-window HSQC may have insufficient ^{13}C resolution at short experiment times; not intrinsically quantitative
Narrow-window H1/C1 HSQC	High-resolution G1-G8 reporter peaks, α-(1→4)/α-(1→6) motifs, branch-point fingerprint, quantitative calibration in a homologous series	Aliasing outside the selected window; needs a scout spectrum; high-field performance is not portable without validation; longer structures share local motifs
HSQC-TOCSY / ^{1}H-^{1}H TOCSY	Extends an anomeric reporter through the residue spin system; supports identification in overlap	Transfer efficiency and crowding vary; not a routine absolute qNMR experiment
HMBC	Long-range H1-to-C4 or H1-to-C6 correlations can confirm (1→4) or (1→6) connectivity	Lower sensitivity, long experiment time, variable long-range couplings, poor quantitative reliability
DQF-COSY	H1-H2 coupling and anomeric spin-system information	Published beer/glucan examples show very poor ^{1}H dispersion even at 800 MHz; best used as supporting rather than primary separation 54
DOSY / diffusion-filtered NMR	Orthogonal hydrodynamic information; directly demonstrated in six non-fractionated beers; separates small sugars from slower glucan/arabinoxylan pools operationally and supported especially high-molecular-weight arabinoxylan assignments. Suitable outputs are apparent diffusion coefficients and validated mobility-class fractions. 63	Diffusion depends on size, shape, branching, viscosity, temperature, association, and exchange. Overlap and multiexponential decay can mix polymer families; a slow component is not automatically a dextrin, and exact molar mass is unreliable without matrix-matched standards or SEC/AF4 fractions.
CPMG relaxation editing	Attenuates broad macromolecular signals and improves fitting of low-molecular-weight metabolites	Differential T_2 weighting makes the spectrum semi-quantitative; bound/exchanging analytes may be lost. It is especially inappropriate if the broad dextrin pool is itself the target 21,37
Inversion-recovery/T_1 measurements	Establishes quantitative recycle delays; can selectively null an interference in method development	Adds method-development time; T_1 values change with matrix and field
T_2 distribution / low-field relaxometry	Rapid bulk mobility/solids/viscosity-related process fingerprint; potential PAT variable	Chemically non-specific; must be calibrated against high-resolution composition and physical reference measurements
LC-NMR/MS	Adds chromatographic DP/fraction separation to NMR linkage evidence; demonstrated through DP 9	Time, solvent/interface complexity, and remaining coelution of structural isomers; high-DP topology can remain ambiguous 18

5.5.1 Why 2D HSQC is not automatically quantitative

HSQC cross-peak volume is affected by one-bond ^1JCH, INEPT delay matching, pulse excitation profile, T_1/T_2 relaxation, repetition time, and processing. The optimized glucan study reduced those response differences by using homologous anomeric reporters and an INEPT setting near 170 Hz. With individual calibration curves, its G1-G8, isomaltose, and panose results agreed with chromatographic methods at $R^2 > 0.99$ and slopes of 1.01-1.02, while independent reporter sites from the same molecules agreed at $R^2 = 0.996$. The approximate 10 µg/mL LOQ in 15 minutes was achieved at 800 MHz with a cryoprobe and a lyophilized/reconstituted sample. This success does not make arbitrary HSQC peaks universally quantitative and cannot be transferred to 300 MHz without instrument- and matrix-specific calibration, recovery, precision, and LOQ studies. 54

5.5.2 Why water suppression can erase the chemistry of interest

The β reducing-end and β-glucan region lies close to HOD in typical D_2O beer samples. One metabolomics study found its saturation profile unreliable across approximately 5.10-4.55 ppm and excluded resonances in that region from quantitation. The same work noted that CPMG was only semi-quantitative and that 3 kDa ultrafiltration improved small-metabolite fitting by physically removing oligosaccharides/dextrins and macromolecules. Those choices were appropriate for small-metabolite profiling but would discard or distort the residual-dextrin target. 37

Required implication: water-suppression validation must be performed with glucose, maltose, isomaltose, panose, β-glucan, and dextrin standards in a beer-like matrix. A suppression scheme should not be adopted merely because the water peak looks visually small.

5.5.3 Broad baselines are chemical information, not always nuisance

The MagMet-B supporting information shows that broad underlying peaks can inflate fitted concentrations of narrow metabolites if the broad component is ignored. Their solution was to fit/subtract the broad contribution before fitting small metabolites. 21

For a dextrin project, the analysis must retain both outputs:

the modeled broad macromolecular/dextrin envelope;

the narrow metabolite spectrum after that envelope is accounted for.

Blind baseline subtraction can remove precisely the chain-length and mobility information of interest.

5.5.4 What solution-state NMR does not see completely

Only dissolved and sufficiently mobile molecules produce sharp, quantitatively observable solution-state signals. Insoluble starch, large colloids, aggregates, or strongly protein/polyphenol-associated carbohydrates may be broadened beyond detection or attenuated by preparation and pulse-sequence choices. A solution NMR result should therefore be called the **NMR-visible dissolved/mobile carbohydrate fraction** unless a mass balance demonstrates complete recovery. Solid-state NMR, hot-solvent extraction, enzymatic digestion, or analysis of isolated solids may be needed for the missing fraction.

5.5.5 Non-fractionated does not mean universally quantitative

Four evidence levels should be named explicitly when reporting the carbohydrate region. The Petersen study strongly expands the first two levels and supplies comparative structural and mobility evidence; the companion HSQC work validates absolute quantitation only for a defined subset under its stated conditions. 54,63

Detected. A reproducible signal or diffusion component is present above the method's detection threshold.

Assigned. Chemical shifts, correlations, standards, enzyme response, or diffusion behavior support a molecular species, linkage class, or local motif assignment.

Comparatively measured. A defined integral, cross-peak volume, motif score, or diffusion-class fraction is repeatable across samples and suitable for a validated relative or multivariate comparison.

Absolutely quantified. Concentration is traceable to a named reference or calibration model with demonstrated relaxation adequacy, matrix recovery, selectivity, linearity, precision, LOQ, and uncertainty.

This vocabulary prevents two common errors: converting a local cleavage-site signal into the concentration of an assumed complete polymer and converting a diffusion coefficient into molecular weight without a matrix-matched hydrodynamic model.

5.6 Practical Applications and Capability Boundaries

Residual-carbohydrate analysis is useful for attenuation studies, low-carbohydrate and enzyme-assisted products, arrested fermentation, non-alcoholic beer, mash optimization, adjunct comparison, and chemical monitoring of *Saccharomyces cerevisiae* var. *diastaticus* activity. In a longitudinal contamination or challenge experiment, dextrin loss, transient glucose formation, and increasing ethanol could provide a direct chemical record of extracellular glucoamylase action. The expected trajectory is mechanistically plausible and should be tested under controlled inoculation, time-course, and microbiological confirmation rather than described as an organism-specific diagnostic from one endpoint spectrum.29

The solution-state method observes the dissolved, mobile, NMR-visible fraction. Insoluble starch, large aggregates, and strongly protein- or polyphenol-associated carbohydrate may broaden beyond quantitative detection. CPMG filtering and ultrafiltration can improve small-metabolite analysis but can suppress or remove the dextrin target; DOSY adds hydrodynamic information but does not deliver an exact molar-mass distribution without matrix-matched standards and orthogonal sizing. Consequently, the defensible hierarchy is: species-specific concentration for resolved, calibrated molecules; operational linkage or DP bins for reproducible but composite regions; local branch-motif assignments from validated 2D correlations; and SEC/AF4 or chromatographic fractionation where molecular-weight distribution or complete topology is required.

Sensory interpretation also requires restraint. Dextrin concentration alone is not a universal proxy for body or palate fullness. Any model linking NMR-derived carbohydrate features to sweetness, viscosity, fullness, filtration, foam, or haze should control ethanol, carbonation, protein, β-glucan, pH, and other correlated contributors and should be validated prospectively with sensory and physical reference measurements.

6. Quantitative ^{1}H NMR of Beer Constituents

The quantitative performance of beer ^{1}H NMR is by now thoroughly documented. The Carlsberg validation demonstrated that organic and amino acids could be quantified from a single spectrum with accuracy and precision competitive with the enzymatic and chromatographic reference methods then in routine use,7 pH-related complications in the acid region have been dissected and solved by both integration- and regression-based routes,16,20 flow-injection screening with multivariate calibration demonstrated hundred-samples-per-day throughput on production beers two decades ago,30 and current automated lineshape-fitting platforms quantify on the order of fifty to eighty constituents per spectrum with median errors against expert manual profiling below ten percent.21 Regulatory-grade automated PULCON quantification of ingredients and additives in beer and beer-based mixed beverages has been validated at the level required for legal compliance testing.15 Table 9 collects indicative concentration ranges for the constituents most commonly reported, together with the spectral windows in which each is quantified; the ranges are deliberately broad, since style, original gravity, yeast strain, and process each move individual entries severalfold.

Table 9. Indicative concentration ranges of NMR-quantifiable beer constituents (conventional lager and ale styles) and their quantitation windows.

Analyte	Indicative range	Quantitation window (δ, ppm)	Comment
Ethanol	30–50 g/L (3.8–6.3% v/v)	1.18 (t)	Sour and non-alcoholic styles outside range
Total residual carbohydrate	15–35 g/L	3.1–4.0 + 4.4–5.5	Mass-balance from ring + anomeric regions
Dextrins (DP ≥ 4)	10–30 g/L	5.34–5.44 (envelope)	Section 5; near zero in brut / light styles

Analyte	Indicative range	Quantitation window (δ, ppm)	Comment
Maltose	0.3–3 g/L	5.41 (d, resolved edge)	Elevated in NA and arrested fermentations
Maltotriose	0.3–2.5 g/L	5.38–5.42	Strain-dependent residual
Glucose	< 0.1–0.5 g/L	3.25 (dd, H2β)	H2 used to avoid anomeric overlap
Glycerol	1.2–2.5 g/L	3.56 / 3.78	Fermentation by-product
L-Lactic acid	40–250 mg/L (3–12 g/L sour)	1.36–1.41 (d)	Style-defining in sours
Acetic acid	30–200 mg/L	2.03–2.10 (s)	Elevated values flag spoilage / mixed culture
Succinic acid	30–120 mg/L	2.53–2.66 (s)	—
Citric acid	80–250 mg/L	2.68–2.92 (AB)	—
L-Malic acid	30–150 mg/L	2.52–2.90 (ABX)	—
Pyruvic acid	20–120 mg/L	2.36–2.41 (s)	—
Formic acid	5–40 mg/L	8.30–8.46 (s)	Clean low-field singlet
L-Proline	150–700 mg/L	2.00–2.10 / 4.13	Dominant amino acid
L-Alanine	20–100 mg/L	1.48 (d)	—
GABA	30–150 mg/L	3.01 (t)	—
Valine / leucine / isoleucine	10–60 mg/L each	0.94–1.04	J-res or fitting at ≤ 400 MHz
2-Phenylethanol	8–45 mg/L	2.85 (t)	Rose-like fermentation aromatic
Tyrosol	5–40 mg/L	6.83 / 7.16 (d)	—
Isoamyl alcohol	30–100 mg/L	0.90 (d)	Principal fusel
Ethyl acetate	10–40 mg/L	4.13 (q)	Quartet window clear of acetate
Acetaldehyde (total)	2–15 mg/L	1.31 (hydrate d) / 9.67	Hydrate is the practical handle
Uridine	5–30 mg/L	5.90–5.92 (d)	Hopping-regime marker
Iso-α-acids	10–100 mg/L	5.0–6.1	Section 7; enrichment-assisted

Ranges compiled and harmonized from the validated quantitative beer NMR studies.6,7,15,20,21 Values are indicative for orientation; certificate-grade reporting requires matrix-matched validation on the instrument and suppression scheme actually deployed.

6.1 Alcohol content and the volatile fermentation profile

Ethanol is the easiest major analyte in beer and one of the most useful. The methyl triplet near δ 1.18 and methylene quartet near δ 3.65 provide two independent handles, although the quartet lies in the carbohydrate/glycerol region and the triplet must be evaluated with its ^{13}C satellites. Once ethanol mass concentration is obtained, alcohol by volume follows from the density of absolute ethanol at the reporting temperature and the volume basis of the sample. This conversion is not the same as estimating alcohol from original and final gravity; it measures the ethanol present in the submitted package.

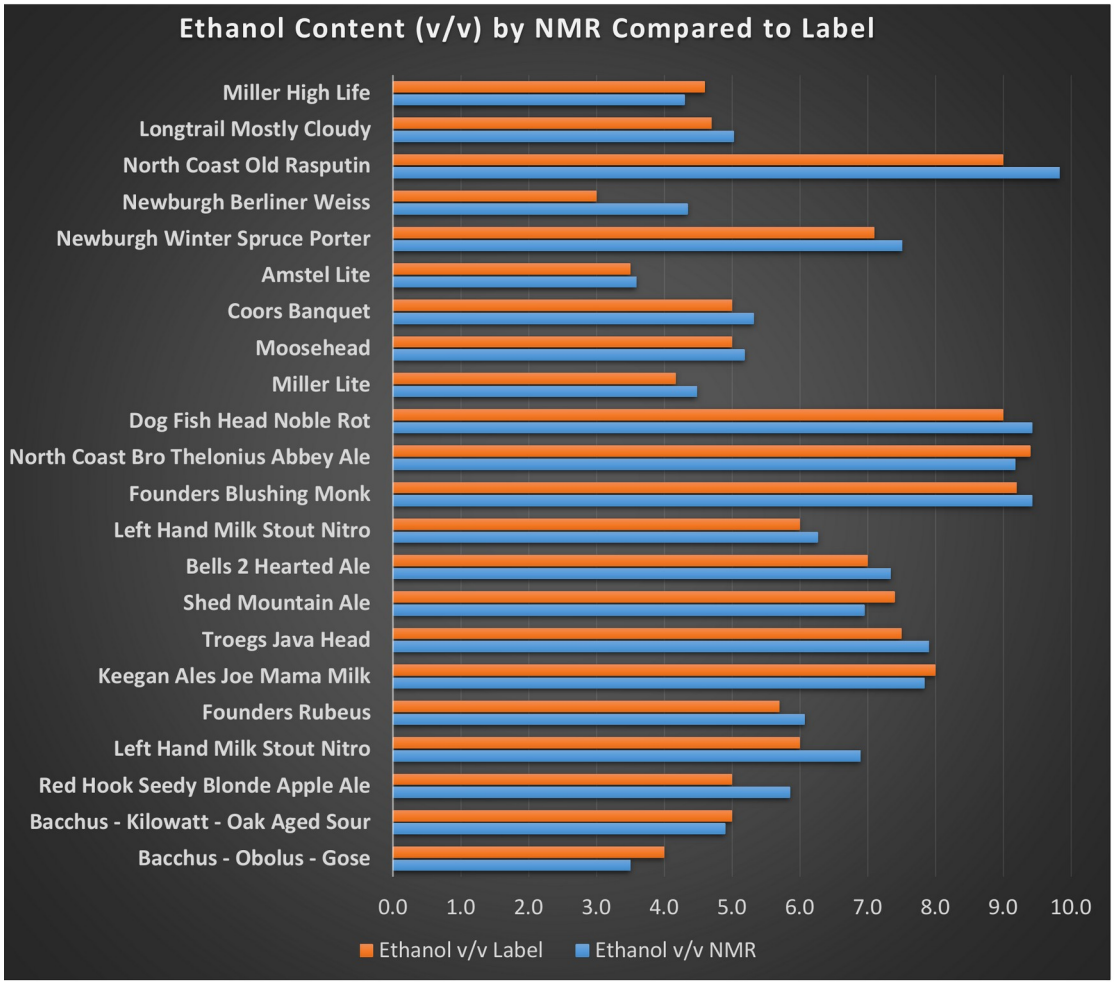

Figure 12. Label-declared and ^{1}H qNMR-derived alcohol by volume for the 23-beer survey. General agreement supports the analytical concept, but the source panel does not supply regression statistics, replicate precision, or uncertainty intervals. Product names are comparative examples and remain third-party trademarks. Source: Process NMR Associates, author-supplied WBC poster (Ref. 66, p. 1).

The neighboring fusel-alcohol region contains 1-propanol, isobutanol, 2-methyl-1-butanol, and 3-methyl-1-butanol. Their methyl patterns are partly overlapped, but the full spin systems can be confirmed by COSY/TOCSY and quantified by resolved terminal or hydroxymethylene signals, targeted deconvolution, or a validated multivariate regression. These compounds report yeast amino-acid catabolism, carbon flux, aeration, temperature, pitching, and strain behavior. A single concentration is rarely diagnostic on its own; the pattern among higher alcohols, amino-acid residues, glycerol, acetate, succinate, and ethanol is much more informative.

Methanol is usually low in conventional all-malt beer. A resolved singlet near δ 3.35 can be measured when present, but the method must distinguish it from neighboring carbohydrate signals and confirm that suppression has not created a false baseline feature. Ethyl acetate contributes a useful quartet near δ 4.1 and methyl triplet near δ 1.25; other flavor-active esters frequently occur below routine whole-beer ^{1}H qNMR sensitivity or are obscured. Acetaldehyde can be approached through its aldehydic proton near δ 9.6 and its hydrated form, with pH- and equilibrium-dependent response. The analytical panel should therefore specify whether it reports free acetaldehyde, hydrate, or an empirically validated total estimate.

An important operating rule follows from the physics: every volatile analyte must be measured on the direct aliquot. Freeze-dried spectra can establish the nonvolatile chemical context but cannot be used to prove absence or quantify recovery of the volatile fraction.

6.2 Organic acids as a map of yeast, bacteria, raw materials, and storage

Beer organic-acid chemistry is unusually well suited to NMR because several acids carry isolated singlets, doublets, or AB/ABX systems. Lactate, acetate, succinate, citrate, malate, pyruvate, formate, and in some specialty products propionate and 3-hydroxypropionate can be measured in one experiment. Their chemical shifts are pH sensitive because the beer pH range straddles relevant acid dissociation equilibria. That sensitivity is both a complication and an information source: fixed-pH buffered spectra improve intersample quantitation and alignment, while native-pH spectra preserve a chemically meaningful equilibrium fingerprint.

The pattern has direct process interpretation. Lactate can reflect intentional lactic souring, mixed-culture fermentation, or contamination. Acetate is formed by yeast and bacteria but becomes a spoilage or stress indicator when it rises outside the product's established operating envelope. Succinate is linked to yeast central metabolism and responds to strain and fermentation conditions. Malate can originate from fruit adjuncts or raw materials and may be consumed or transformed by microorganisms. Citrate may enter through formulation and can participate in bacterial metabolism. Propionate, 1,3-propanediol, and 3-hydroxypropionate can signal unusual bacterial pathways or glycerol utilization, particularly in mixed and wild fermentations. The defensible interpretation is multivariate and time-aware: the acid vector is read together with alcohols, residual sugars, glycerol, amino acids, and metadata.

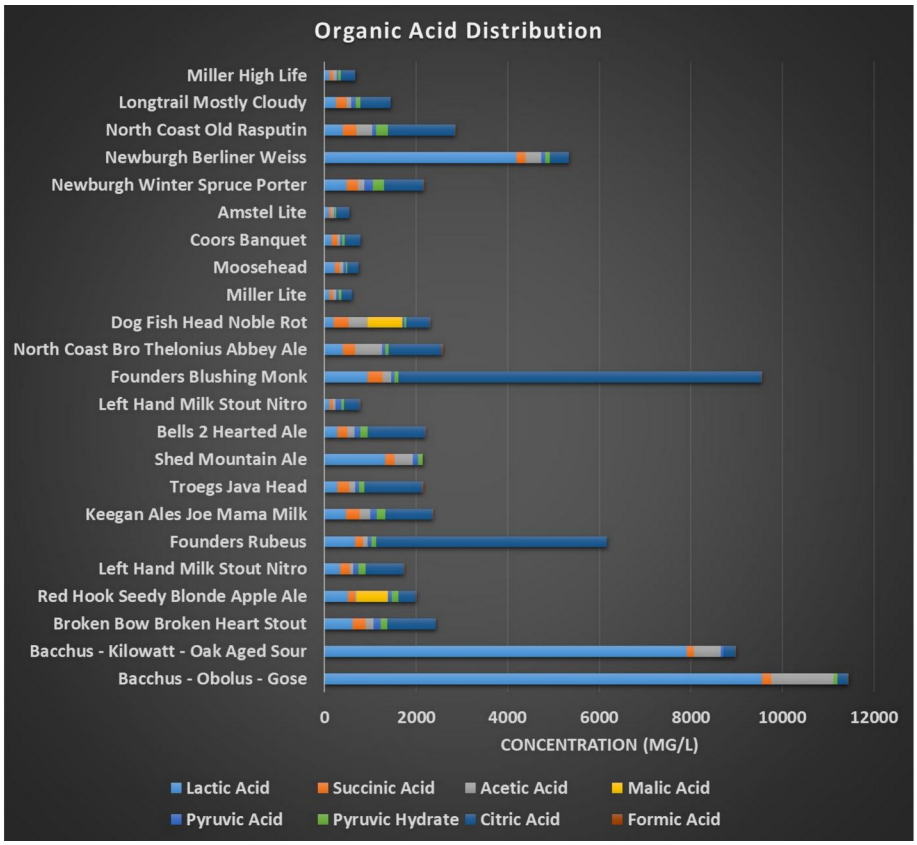

Figure 13. Organic-acid distributions across 23 commercial beers, demonstrating style- and process-dependent chemical diversity. The chart is exploratory and lacks raw data and uncertainty bars; it should not be used as a brand-ranking dataset. Source: Process NMR Associates, author-supplied 2018 presentation (Ref. 67, p. 22).

The author-supplied sour-mash study is a good example of process NMR used experimentally rather than as a pass/fail test. Mash held over a temperature series was analyzed for lactic, acetic, and succinic acids, ethanol, and γ-aminobutyric acid. The resulting concentration curves address whether the conventional approximately 120 °F set point represents a distinct metabolic optimum or merely a practical operating tradition. The study design also illustrates a key requirement for future work: temperature treatments require biological replication and time matching, because endpoint composition confounds the effect of temperature with the growth phase and initial microbiota.

6.3 Amino acids, nitrogen metabolism, and the boundary of “FAN by NMR”

Beer retains a chemically informative subset of wort amino acids after fermentation. Proline is often dominant because standard brewing yeast uses it poorly under anaerobic conditions. Alanine, valine, leucine, isoleucine, phenylalanine, tyrosine, histidine, tryptophan, glutamate/glutamine-derived signals, and γ-aminobutyric acid may also be accessible depending on field strength and concentration. The Carlsberg validation showed that a combination of direct integration and PLS regression can quantify several organic and amino acids down to approximately 10 mg/L and can recover information from partly overlapped signals when an independent test set is used.7

These measurements should not automatically be labeled “free amino nitrogen.” The classical FAN assays respond to a broader operationally defined pool, including ammonia, small peptides, and compounds with assay-specific reactivity. A sum of NMR-quantified free amino acids is chemically explicit and often more informative, but it is not interchangeable with an ASBC/EBC FAN number until a matrix- and method-specific comparison demonstrates equivalence. The strongest implementation reports the amino-acid panel by identity, a separately defined NMR-visible amino nitrogen sum, and the relationship to the reference FAN method.

Yeast nutritional and stress behavior is encoded in the joint pattern. Consumption of branched-chain amino acids is linked through the Ehrlich pathway to higher alcohol formation. Residual amino acids can expose under-attenuation, nutrient imbalance, strain differences, or process timing. Histidine and aromatic amino-acid signals populate relatively clean low-field windows, while branched-chain methyls occupy the congested high-field region. The comparison of pure amino-acid standards with product spectra in the supplied presentations demonstrates how the assignment library supports targeted measurements before those variables are carried into chemometric models.

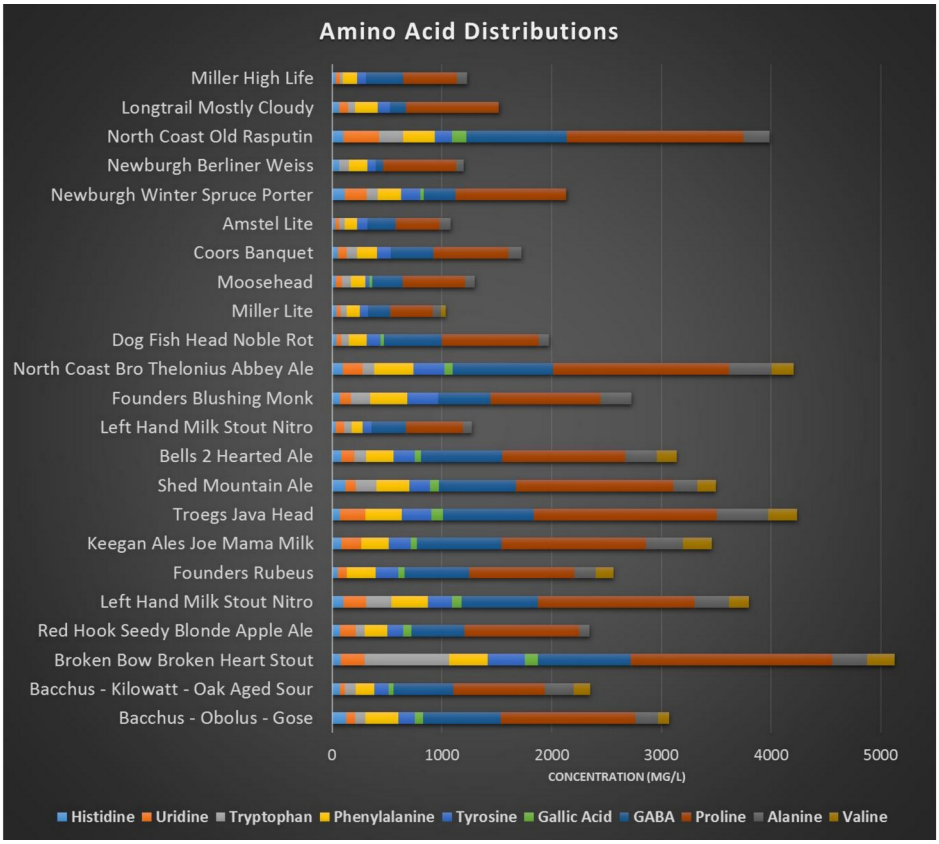

Figure 14. Selected free amino acids and related metabolites across 23 commercial beers. Uridine and gallic acid are included in the source panel but are not amino acids; the figure is therefore interpreted as a broader nitrogenous/aromatic metabolite pattern. No raw-data uncertainty was supplied. Source: Process NMR Associates, author-supplied 2018 presentation (Ref. 67, p. 24).

6.4 Nucleosides, purines, and hopping-dependent yeast metabolism

Uridine, adenosine, inosine, hypoxanthine, adenine-related species, and nicotinamide cofactors contribute well-dispersed aromatic or anomeric resonances. Their concentrations are lower than those of carbohydrates and acids, but

their low-field signals can be relatively uncluttered. Spevacek, Benson, Bamforth, and Slupsky followed 76 metabolites through five brewing stages and showed that late versus dry hopping altered the purine metabolome, including significant differences in adenine, adenosine, and 2′-deoxyadenosine after fermentation.38 That result is strategically important: hopping is not only the addition and extraction of hop molecules; it can change yeast-associated metabolism, and the effect remains visible in the finished beer.

Nucleoside measurements can therefore serve two roles. Targeted concentrations act as mechanistic markers of yeast turnover and process history. In full-spectrum models, the collective aromatic pattern can improve discrimination of hopping regime or production conditions. Either role requires careful identification, because low-field peaks are sparse but not necessarily unique; spiking and 2D confirmation should anchor the library.

6.5 Carbohydrate mass balance, calories, and label-facing calculations

NMR distinguishes the chemically measured inputs to energy calculations rather than estimating calories from a single empirical relationship. Ethanol mass is converted using the agreed energy factor; measured sugars and residual carbohydrate are converted separately; amino acids and organic acids can be included under explicitly stated factors; and all results are placed on the declared serving volume. The 2016 commercial-beer panel showed that the resulting component-by-component calorie breakdown varied substantially among products even when nominal alcohol content was similar, because residual carbohydrate differed.

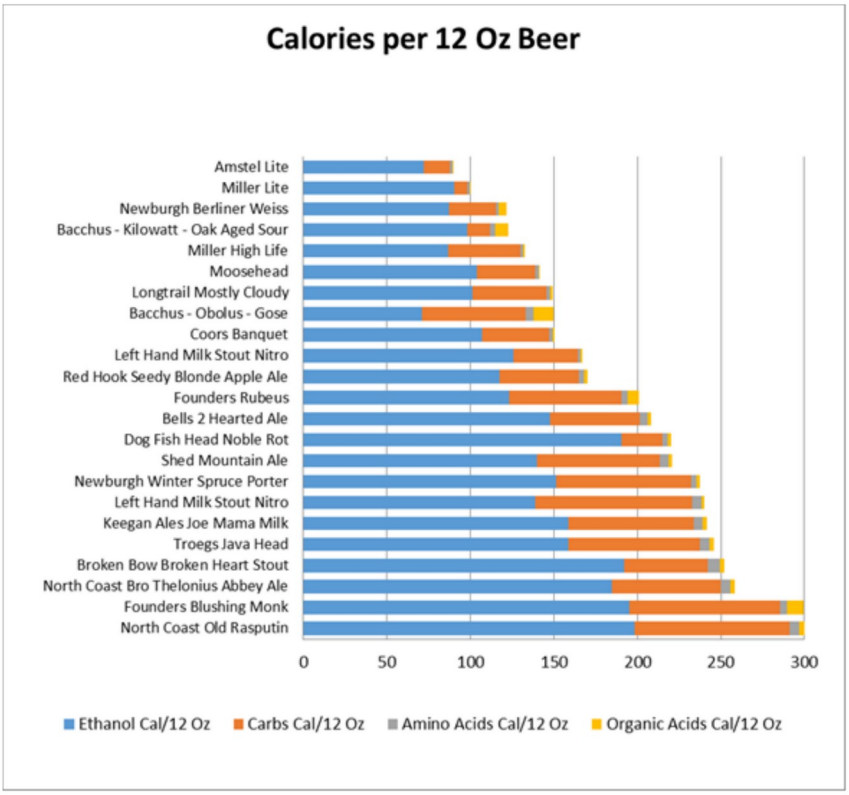

Figure 15. Calculated energy contributions from ethanol, residual carbohydrate, free amino acids, and organic acids in the 23-beer survey. These are analytical estimates, not official nutrition labels; energy factors and independent validation are required for label use. Source: Process NMR Associates, author-supplied 2018 presentation (Ref. 67, p. 25).

The approach is especially valuable for low- and non-alcoholic products, where an error of a few tenths of a percent alcohol by volume is commercially and regulatorily significant and the energy budget is dominated by residual carbohydrate rather than ethanol. In an author-supplied example, a 12 oz product labeled at 40 Calories, 8 g carbohydrate, and less than 0.5% alcohol by volume returned approximately 40.1 Calories, 7.6 g carbohydrate, and 0.47% alcohol by volume by NMR.

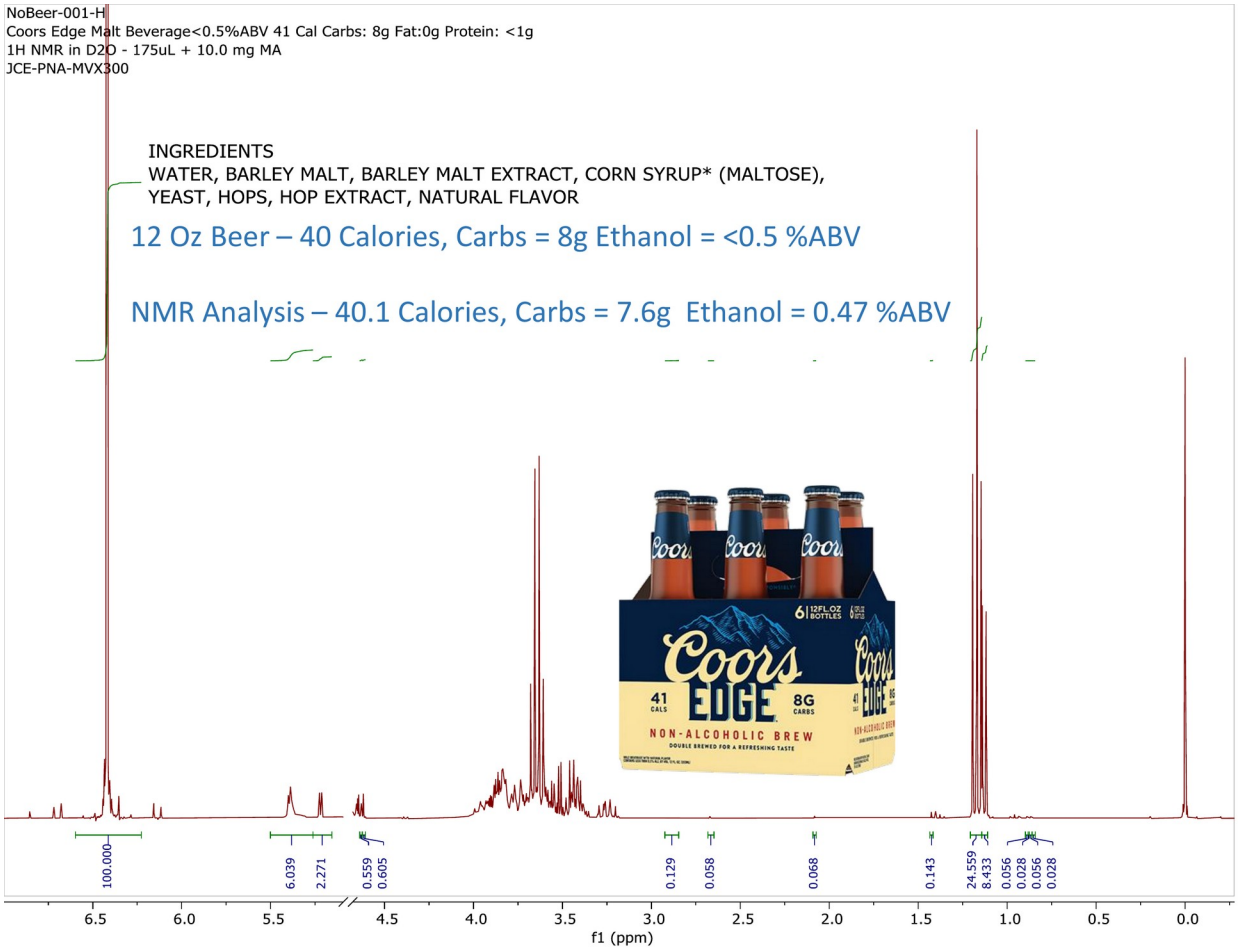

Figure 16. Single-product low-alcohol nutrition example comparing declared values with qNMR-derived alcohol, carbohydrate, and calorie estimates. The result demonstrates the integrated calculation but requires formal measurement uncertainty before a threshold decision. The product name is a third-party trademark used only for attribution. Source: Process NMR Associates, author-supplied 2022 presentation (Ref. 68, p. 43).

That result should be read as a technical demonstration, not as a universal validation claim. Under current U.S. malt-beverage regulations, a product labeled “non-alcoholic” must contain less than 0.5% alcohol by volume and no tolerance is permitted around that threshold; an “alcohol free” claim requires no alcohol.51 Any label-facing method must therefore demonstrate uncertainty small enough to support the decision at the relevant limit.

Total carbohydrate by NMR is also definition-sensitive. Direct integration of the full carbohydrate region measures proton equivalents and must be converted with an assumed or modeled residue composition. Summing individually fitted glucose, maltose, maltotriose, and dextrin components is more interpretable but can omit unresolved polysaccharide material. For nutrition work, NMR should be cross-validated against an accepted total-carbohydrate or mass-balance method and should distinguish total residual carbohydrate from total sugars.

6.6 Non-alcoholic beer and dealcoholization diagnostics

Non-alcoholic beer is not simply conventional beer minus ethanol. Arrested fermentation retains wort-like maltose, maltotriose, amino-acid, and aldehyde patterns. Restricted-yeast processes create a different metabolite balance. Thermal or vacuum dealcoholization redistributes higher alcohols, esters, and aldehydes between the distillate and residual beer, while membrane processes impose their own selectivity. NMR can compare the starting beer, volatile fraction, and residual phase in a common molecular framework. Labrado and co-workers used 1D and 2D NMR to identify n-propanol, isobutanol, 2- and 3-methylbutanol, 2-phenylethanol, ethyl acetate, isoamyl acetate, and acetaldehyde across beer distillates and residues, illustrating how flavor loss can be diagnosed mechanistically rather than only sensorially.52

The direct spectrum tests residual alcohol and volatile flavor chemistry; the lyophilized spectrum shows retained sugar, acid, amino-acid, and dextrin composition. Together they differentiate four fundamentally different routes to a low-alcohol label: dilution, arrested fermentation, selective biological fermentation, and physical alcohol removal. That distinction becomes a powerful classification target for the next-stage chemometric program.

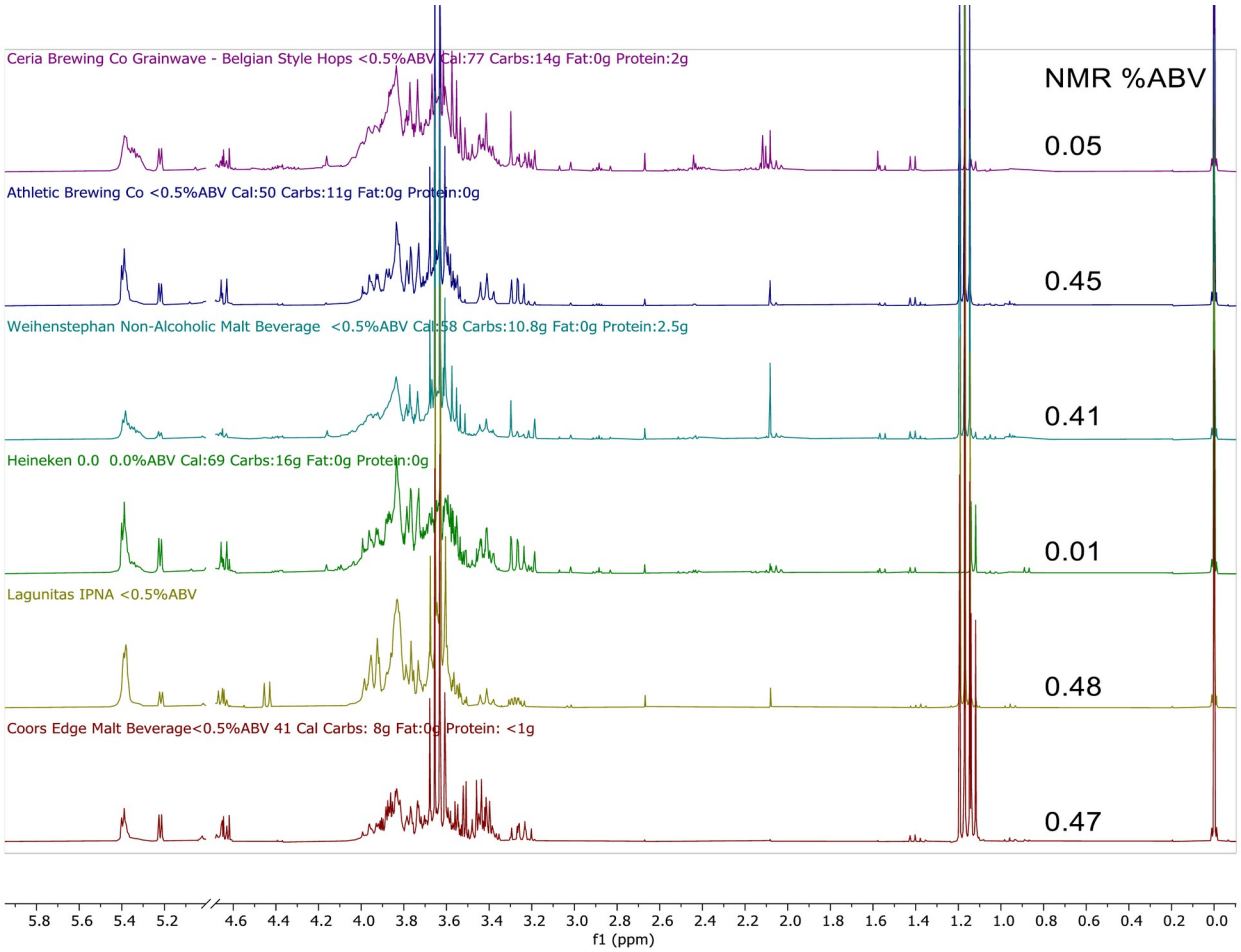

Figure 17. Stacked ^{1}H spectra and qNMR-derived residual alcohol values for six low- and non-alcoholic products. The displayed results are author presentation examples; calibration uncertainty and replicate measurements should be recovered before market-wide claims. Brand names are third-party trademarks. Source: Process NMR Associates, author-supplied 2022 presentation (Ref. 68, p. 47).

6.7 Adjuncts, specialty ingredients, and formulation markers

Specialty beers deliberately expand the observable matrix. Fruit additions introduce malate, citrate, tartrate, quinate, characteristic sugar ratios, and sometimes sorbate or benzoate. Lactose is directly visible in milk stout and persists because standard brewing yeast does not ferment it.

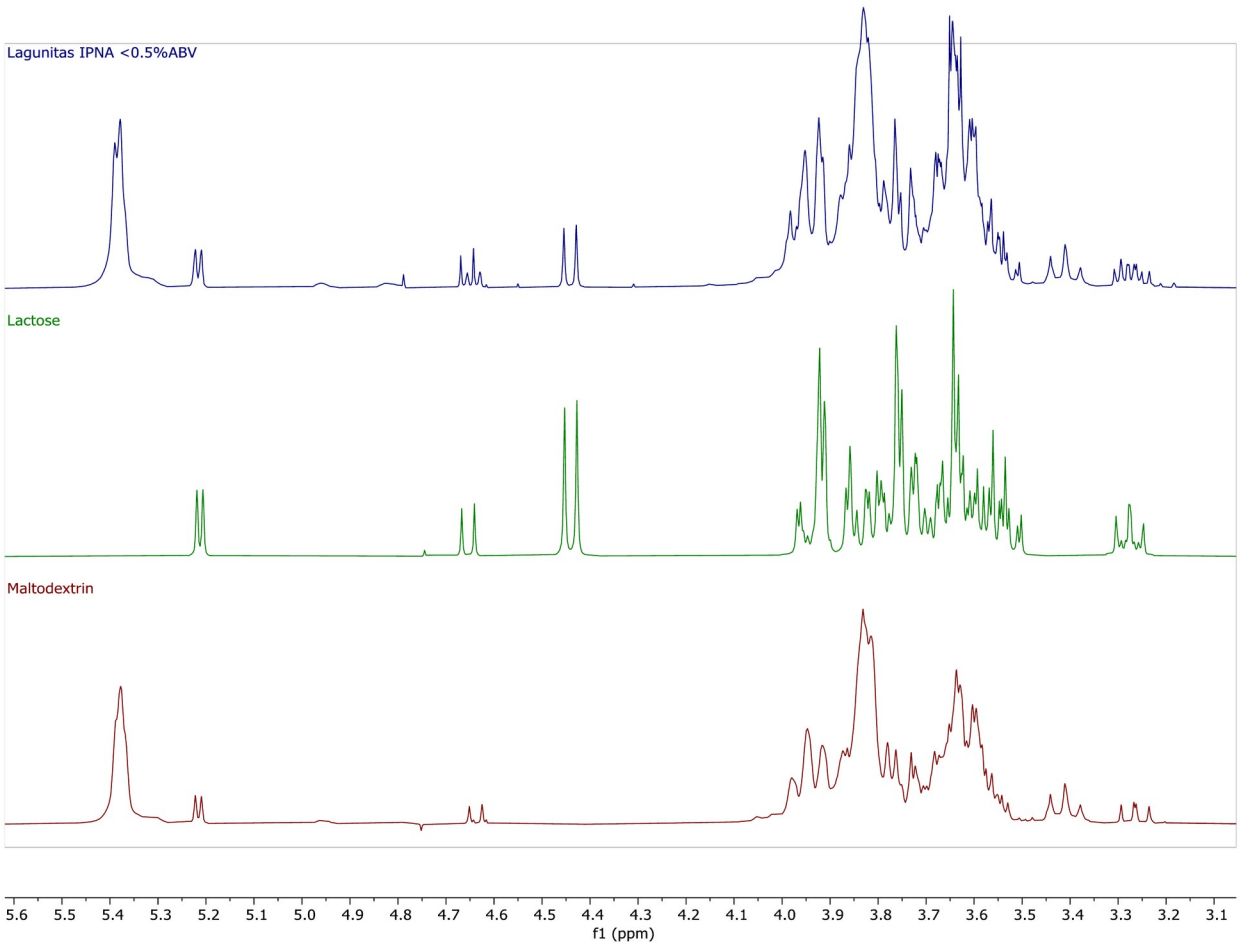

Figure 18. Comparison of a low-alcohol beer carbohydrate region with lactose and maltodextrin reference spectra. The distinct reference patterns show how declared formulation components can be tested, provided concentrations and acquisition conditions are matched. The product name is a third-party trademark. Source: Process NMR Associates, author-supplied 2022 presentation (Ref. 68, p. 48).

Coffee contributes caffeine and chlorogenic-acid-related aromatic signals; cocoa contributes theobromine and related methylxanthines; tea, spices, botanicals, and wood contact contribute phenolics and organic acids. Sweeteners such as sucrose, glucose, fructose, dextrose syrups, and non-nutritive agents can often be identified or constrained by targeted reference spectra.

The correct claim is ingredient-informed authentication, not universal ingredient identification from one peak. Many plant-derived phenolics overlap, and absence by NMR may reflect a concentration below detection. When the declared ingredient is known, targeted spiking, 2D confirmation, and extraction experiments can determine whether a marker is measurable and quantitative. When the ingredient is unknown, the full spectrum generates candidates that must be confirmed by orthogonal methods.

6.8 Hops, lipids, proteins, and colloids: observable, but method-dependent

Hop resins and essential oils are chemically rich but present at low concentrations and variable solubility. The author-supplied hop work used a modified extraction derived from the ASBC Hops-6A concept to quantify adhumulone, cohumulone, humulone, adlupulone, colupulone, lupulone, additional β-acid tautomers, and major terpenes across stored and freshly collected hop samples. This is an extracted-raw-material application, not a claim that every compound can be quantified directly in finished beer. The distinction matters because an extraction can raise analytes above the NMR detection floor and move them away from the aqueous-beer matrix.

Lipids in beer are low and partly associated with foam-active or colloidal material. NMR can observe sufficiently concentrated fatty-acid and glyceride signals in raw materials, process fractions, or enriched extracts, while direct finished-beer quantitation is generally difficult. Proteins and peptides contribute broad aliphatic and aromatic

envelopes whose intensity depends on molecular motion and T_2; solution ^1H NMR will not provide a complete protein assay without a defined calibration and sample treatment. Relaxation and diffusion experiments, however, can characterize the physical state of macromolecular and colloidal fractions and may connect to haze, filtration, and foam behavior. This is a promising research area, but it requires reference methods for particle size, protein, β-glucan, and turbidity before operational claims are made.

6.9 An analyte-to-process interpretation matrix

NMR-observable domain	Primary chemical variables	Brewing questions informed	Major confounders / orthogonal checks
Fermentable sugars	Glucose, maltose, maltotriose, sucrose where added	Conversion rate, arrested fermentation, priming, refermentation risk	Overlap; enzyme/HPLC sugar panel
Residual α-glucans	Internal α-(1→4), α-(1→6), reducing ends, diffusion distribution	Mash conversion, enzyme regime, attenuation potential, diastatic activity	β-glucan/arabinoxylan; SEC, enzymatic assays
Alcohols and polyols	Ethanol, glycerol, propanols, fusel alcohols, 2,3-butanediol	Fermentation progress, yeast metabolism, label alcohol	Volatile loss; GC-FID/headspace GC
Organic acids	Lactate, acetate, succinate, citrate, malate, pyruvate, formate	Souring, contamination, stress, adjuncts, maturation	pH shifts; ion chromatography/capillary electrophoresis
Amino acids	Proline, alanine, GABA, branched-chain and aromatic amino acids	Nutrient uptake, strain/process differences, precursor-product patterns	Not identical to FAN; HPLC amino-acid analyzer
Nucleosides/purines	Uridine, adenosine, inosine, adenine-related signals	Yeast turnover and hopping-regime effects	Low concentration; LC-MS confirmation
Carbonyl/furan markers	Acetaldehyde, 5-HMF, furfural-related signals	Thermal load, aging, dealcoholization effects	Sensory thresholds below NMR for some compounds; GC-MS/HPLC
Hop bitter chemistry	α/β acids in extracts; iso-α-acid and transformation signals	Hop quality, bittering inputs, storage/aging	Extraction recovery; HPLC-UV/MS, IBU
Specialty markers	Lactose, caffeine, theobromine, fruit acids, preservatives	Label consistency, formulation, adjunct differentiation	Ingredient variability; targeted standards and LC-MS
Physical/ macromolecular response	Broad carbohydrate/protein signals, T_1/T_2, diffusion	Colloid state, polysaccharide size, potential filtration/haze trends	Strong matrix/temperature effects; turbidity, SEC, rheology

The matrix illustrates how NMR changes the analytical conversation. Instead of asking whether one analyte passed, the brewer can ask which chemical subsystem moved, when it moved, and whether the movement is consistent with the process history.

7. Hop-Derived Bitter Acids and Beer Aging Chemistry

The bitter principles of beer — the cis- and trans-iso-α-acids produced by thermal isomerization of hop humulones during wort boiling — occupy a special position in the beer NMR story, because their chemistry during storage was solved by NMR. Present at only 10–100 mg/L (roughly 30–280 µM) and distributed over congested olefinic and aliphatic multiplets, the intact iso-α-acids sit near the practical limit of direct one-dimensional observation in whole beer, and their characterization has relied on two-dimensional methods and on enrichment of the bitter-acid fraction ahead of spectroscopy.19,31 The structural payoff was substantial. High-field NMR together with LC–MS identified the storage-induced transformation products of the bitter principles — the tri- and tetracyclic degradation products tricyclocohumol, tricyclocohumene, isotricyclocohumene, tetracyclocohumol, and epitetracyclocohumol among them — establishing the proton-catalyzed cyclization routes by which they arise;31 complementary work established that autoxidation contributes a separate degradation channel;32 and X-ray crystallography subsequently settled the absolute configurations of the cis- and trans-iso-α-acids themselves.34

The kinetics carry the practical message. Quantitative monitoring of forced and natural aging demonstrated that degradation is strongly trans-selective: the trans-iso-α-acids decay with half-lives of months at ambient temperature while their cis counterparts remain comparatively stable, so the cis/trans ratio functions as an internal chemical clock recording the time–temperature history of packaged beer, and the accumulating cyclic transformation products track the associated development of harsh, lingering bitterness.33 In parallel, untargeted NMR monitoring of whole beer through forced aging mapped the broader staling trajectory — rising 5-HMF and furan aldehydes from Maillard and sugar dehydration chemistry, shifts in the organic acid and amino acid pools, and progressive changes across the aromatic region — placing the bitter-acid clock inside a whole-spectrum aging signature accessible from a single acquisition.35 For a testing laboratory, the operational conclusion is that freshness and thermal-abuse questions are answerable by NMR at two levels of effort: whole-spectrum multivariate aging models on the untreated beer, and targeted cis/trans bitter-acid ratios where the client question warrants the additional enrichment step. Vicinal diketones, it should be stated plainly, remain outside the technique at sensory-relevant levels: diacetyl thresholds near 0.1 mg/L lie below routine ^{1}H detection limits, and headspace gas chromatography retains that assignment.

8. Multivariate Analysis and NMR Metabolomics of Beer

Because a single beer spectrum carries thousands of resolved intensities, the pairing of NMR with multivariate analysis was natural and early. The foundational studies demonstrated that principal component analysis of full-resolution or binned spectra separates ales from lagers and tracks the carbohydrate, aliphatic, and aromatic contributions to that separation;5,36 that spectra of one hundred beers from different sites and dates cluster by brewery and production period, with the discriminating power traceable to identified constituents;6 and that flow-injection NMR with PLS calibration supports routine industrial screening.30 The subsequent literature has extended the approach along every axis a brewer or regulator might care about, and Table 10 summarizes the principal studies. Style discrimination has been demonstrated across pilsner, wheat, IPA, sour, and specialty categories;16 craft versus industrial production leaves a classifiable signature;37 Trappist provenance — a legally protected designation — has been verified against imitators with NMR–chemometric models;39 brewery-of-origin classification has been reproduced on Brazilian lagers;40 hopping regime reads out through yeast purine metabolism, with late and dry hopping measurably altering nucleoside pools;38 and wheat beer substyles have been resolved through fifty quantified metabolites.41 Reviews of NMR authentication place beer alongside honey and spices among the matrices where spectral databases support routine authenticity control.42

Table 10. Principal NMR–multivariate studies of beer: design, methods, and outcomes.

Study (year)	Samples / design	Platform	Chemometrics	Principal outcome
Duarte et al. (2002)5	~50 beers; ales, lagers, alcohol-free	500 MHz ^{1}H	PCA on binned spectra	Ale / lager separation; regional assignment framework
Duarte et al. (2004)36	Same corpus; NMR + FTIR	500 MHz ^{1}H; MIR	PCA, outer-product analysis	Data fusion improves compositional interpretation
Lachenmeier et al. (2005)30	~300 commercial beers	400 MHz flow ^{1}H	PCA, PLS	Industrial-throughput QC screening
Almeida et al. (2006)6	100 beers, 2 sites, multiple dates	500 MHz ^{1}H	PCA, PLS-DA	Site and date discrimination; constituent-level drivers
Khatib et al. (2006)19	Commercial beers	2D J-resolved projections	PCA	Congestion relief improves classification
Rodrigues et al. (2011)35	Forced + natural aging series	500 MHz ^{1}H	PCA, PLS	Whole-spectrum aging trajectory mapped
Spevacek et al. (2016)38	Hopping-regime trial	600 MHz ^{1}H	Targeted profiling, MVA	Late / dry hopping alters purine metabolome
Mannina et al. (2016)39	Trappist vs non-Trappist	600 MHz ^{1}H	PCA, LDA-class models	Protected-designation verification

Study (year)	Samples / design	Platform	Chemometrics	Principal outcome
da Silva et al. (2019)40	Brazilian lagers, multiple breweries	600 MHz ^{1}H	PCA, HCA, PLS-DA	Brewery-of-origin classification
Palmioli et al. (2020)37	17 craft + 14 industrial	600 MHz cryoprobe	Untargeted + targeted OPLS-DA	Craft vs industrial signature
Kaufmann et al. (2022)16	Multi-style German market set	400 MHz ^{1}H	Consecutive PCA; shift-based quantification	Style resolution; organic-acid drivers; anomaly detection
Chorbadzhiev et al. (2025)41	Wheat beer substyles	600 MHz ^{1}H	PCA, OPLS-DA, 50 metabolites	Weizenbock / Hefeweizen / Witbier resolved

Platform and method entries are summarized at the level reported in the cited publications; sample counts are approximate where the source reports ranges across sub-experiments.

A statistical caution belongs in any honest account of this literature. Beer classification studies routinely model tens of samples against thousands of spectral variables, a regime in which supervised methods will separate almost any labeling if permitted to. Findings deserve weight in proportion to their validation: cross-validation is the minimum, permutation testing and genuinely held-out or later-vintage test sets are the credible standard, and classification accuracies quoted without them — particularly from OPLS-DA, whose apparent class separation is notoriously flattering — should be read as hypotheses rather than results. The stronger studies in Table 10 meet this bar with cross-validated and permutation-tested models;37,41 the practical implication for a commercial laboratory is that authentication opinions should rest on models validated against samples the model never saw, with the discriminating variables traced back to assigned, mechanistically sensible constituents rather than to anonymous bins.

9. Multinuclear and Advanced NMR Dimensions

9.1 ^{13}C and ^{1}H-^{13}C correlation spectroscopy

The ^{13}C chemical-shift range is roughly twenty times wider than the ^{1}H range and separates carbonyl, aromatic, anomeric, oxygenated aliphatic, and hydrocarbon environments cleanly. Direct ^{13}C spectra of beer at natural abundance are sensitivity-limited, but concentrated or lyophilized samples can supply confirmation of major carbohydrates, acids, and alcohols. In most practical studies, ^{1}H-^{13}C HSQC is the more efficient route: it combines proton sensitivity with carbon dispersion and gives a two-coordinate fingerprint for each directly bonded CH pair. The optimized narrow-window HSQC methods developed for glucans can resolve starch fragments that collapse into the same one-dimensional proton envelope.53-56

HSQC peak intensities are not automatically quantitative because transfer efficiency depends on one-bond coupling, pulse calibration, relaxation, and sequence timing. The experiment is therefore best used for identification, branch-environment classification, and relative profiling unless a quantitative HSQC method has been validated. HMBC adds long-range connectivity and is particularly useful for confirming glycosidic linkage positions and aromatic substituent patterns. COSY and TOCSY remain the fastest tools for tracing proton spin systems in acids, amino acids, sugars, and higher alcohols.

Selective one-dimensional mixture-dissection methods can add another assignment layer when ordinary deconvolution fails. The SCALPEL approach, for example, uses selective excitation and coupling information to separate components of highly overlapped mixture spectra and has been demonstrated on beer-related carbohydrate mixtures.64 Such methods are best treated as targeted structure tools rather than replacements for the standardized full-spectrum experiment used for quantitative databases.

9.2 ^{2}H NMR and site-specific isotope fractionation

A different authentication axis is available from deuterium. Site-specific natural isotope fractionation NMR (SNIF-NMR) uses quantitative ^{2}H NMR of isolated ethanol to measure the site-specific deuterium abundance at the methyl and methylene positions. Those ratios reflect water, botanical precursor, and fermentation fractionation and can help

distinguish carbon derived from C_3 cereals from C_4 cane or maize sources.43-45 The technique is substantially more demanding than routine ^{1}H profiling: ethanol must be recovered quantitatively, the spectrum requires specialized acquisition and standards, and the interpretation requires an appropriate database. It is not a shortcut for generic beer provenance. It is a targeted isotope-ratio method for a defined authenticity question.

9.3 ^{23}Na, ^{31}P, and other nuclei

Sodium-23 is 100% naturally abundant and readily observed. In beer, ^{23}Na NMR can provide a rapid total sodium response with minimal sample preparation if the method is calibrated against matrix-matched standards and accounts for ionic strength and linewidth. The World Brewing Congress poster identified sodium as a future labeling target. This is technically plausible, but a released method should be validated against ICP-OES, ICP-MS, or ion chromatography across the relevant range and should demonstrate that relaxation and probe tuning do not introduce matrix-dependent response.

Phosphorus-31 can observe inorganic phosphate and sufficiently concentrated phosphorylated metabolites without the water/ethanol interference that dominates ^{1}H. The beer matrix is not rich in high-concentration organophosphates, so ^{31}P is more likely to support process or raw-material studies than a broad finished-beer panel. Carbon-13 can in principle observe carbonate/bicarbonate and carbonyl pools; oxygen-17 and other low-sensitivity nuclei are research tools rather than routine brewery assays. Multinuclear NMR should be deployed when the target chemistry justifies a separate acquisition, not merely because the nucleus is observable.

9.4 DOSY, diffusion editing, and relaxation

Diffusion measurements convert molecular mobility into an additional separation dimension. Free sugars, small maltooligosaccharides, larger dextrins, β-glucans, arabinoxylans, and protein/colloid-associated material can diffuse at different rates even when proton shifts overlap. The non-fractionated six-beer study demonstrated that this is direct beer evidence rather than an analogy: DOSY supplied independent size information and particularly supported the presence of high-molecular-weight arabinoxylan fragments. 63 DOSY can display the mobility distribution explicitly, while a diffusion-edited 1D experiment suppresses fast-diffusing species and emphasizes larger material. Practical reportable variables include family-specific apparent diffusion coefficients where peaks are assigned, the fraction of signal in validated fast/intermediate/slow bins, and a diffusion-weighted spectral fingerprint. The measured coefficient is not a universal molecular-weight value: temperature, viscosity, molecular shape, branching, aggregation, and matrix interactions all matter. Branching can make a molecule more compact and faster-diffusing than a linear molecule of the same mass, biasing an uncalibrated diffusion-to-DP conversion downward. Size interpretation therefore requires temperature control, viscosity normalization, and calibration with linear and branched maltodextrins, β-glucan, arabinoxylan, or SEC/AF4 fractions.

T_1 and T_2 measurements provide complementary physical information. T_1 controls quantitative repetition time. T_2 and CPMG filtering distinguish narrow mobile signals from broad macromolecular or exchange-broadened components. Low-field time-domain NMR can follow total proton pools and relaxation changes rapidly, potentially supporting fermentation, solids, or colloid monitoring even when high-resolution assignments are unavailable. These measurements are process-sensitive, but their selectivity is empirical and must be anchored to reference chemistry.

10. From a Spectrum to Pattern Recognition and Process Understanding

10.1 Two linked data products: targeted chemistry and the full fingerprint

Every spectrum should be retained in two analytically distinct forms. The targeted table contains identified compounds, structural ratios, uncertainty, and QC flags. It supports mass balance, labeling, mechanism, and human interpretation. The full-spectrum matrix preserves the peaks that have not yet been assigned and captures coordinated changes too distributed for one-analyte rules. It supports PCA, HCA, PLS regression, supervised classification, anomaly detection, UMAP, t-SNE, and future machine-learning methods.

Neither representation is sufficient by itself. Targeted chemistry can miss unknown markers and subtle line-shape information. Untargeted models can separate batches for irrelevant reasons and are difficult to defend if loadings cannot be assigned. The strongest program uses the targeted matrix to explain the full-spectrum models and uses full-spectrum anomalies to direct new assignment work.

10.2 Process trajectories rather than static product clusters

Beer production is a sequence. Malt extraction, mash rests, conversion, lautering, boiling, whirlpool, cooling, pitching, primary fermentation, conditioning, filtration, packaging, and aging each move a different subset of spectral variables. A batch therefore traces a trajectory through chemical space. Plotting that path is more informative than comparing isolated endpoints: the point at which a batch diverges indicates which process operation requires investigation.

The attached presentations already contain the building blocks for this approach. Wort-to-beer overlays show disappearance of maltose and changes in the reducing-end and branch regions. Sour-mash temperature experiments show acid trajectories. Standard and turbid mash extracts differ in linear and near-branch maltodextrin groups. Commercial beer panels show wide diversity in organic acids, α-(1→4) glucans, amino acids, ethanol, and calorie allocation. The next stage is to put all of these observations into a common sample-by-variable matrix with complete process metadata.

10.3 Preprocessing must be subordinate to chemistry

Phase, baseline, chemical-shift alignment, exclusion of suppression regions, intensity normalization, centering, and scaling can each change a model. The preprocessing record is therefore part of the method, not an analyst preference. For qNMR-derived concentration matrices, no constant-sum normalization should be applied when absolute concentration carries the scientific signal; mean centering and Pareto scaling are usually appropriate starting points because they reduce domination by ethanol and total carbohydrate without giving trace noise the same weight as major metabolites. For full spectra, an internal or external quantitative reference, probabilistic or total-area normalization only where scientifically justified, and a carefully documented alignment method are required.

Derivative spectra and aggressive baseline correction can improve classification but damage quantitative interpretability. Binning improves robustness to peak movement but sacrifices structural resolution, especially in the dextrin anomeric region. A practical compromise is a hybrid variable set: aligned full-resolution windows for discrete markers, chemically defined integrals for known analytes, and coarser bins only in unresolved envelopes.

10.4 Validation strategy for chemometric and machine-learning models

Random cross-validation alone is inadequate when replicate bottles, production lots, acquisition days, or brewery sources are correlated. Samples from the same lot can leak nearly identical spectral information into training and test folds, producing an accuracy that will not survive a new production campaign. Grouped validation should hold out entire lots, batches, breweries, acquisition periods, or vintages according to the intended claim. A final locked external test set should be acquired after model development whenever the result will support authentication, troubleshooting, or litigation.

Unsupervised analysis should precede supervised modeling. PCA and HCA expose outliers, drift, duplicate structure, and the main chemical axes without using class labels. Supervised PLS-DA, SVM, random forest, KNN, or neural methods should then be benchmarked against simple baselines and assessed by balanced accuracy, sensitivity, specificity, class-wise precision/recall, calibration, permutation tests, and applicability-domain diagnostics. UMAP and t-SNE are excellent visualization tools but do not by themselves establish class separability or predictive performance. Every model should return chemical drivers, not only a class label.

10.5 Metadata is an analytical measurement

A beer spectral library without metadata becomes a collection of pretty fingerprints. At minimum, each sample should carry manufacturer, product, style, package, declared alcohol and nutrition, lot, packaging date, acquisition date, storage history, raw materials where known, mash program, gravity/extract values, yeast and bacteria, hopping

schedule, temperature profile, processing interventions, filtration/pasteurization status, and sensory or conventional-laboratory results. Process samples additionally require exact stage, elapsed time, temperature, vessel, and sampling/quench method.

Metadata also defines nuisance variables. Tube, operator, instrument, probe, pulse program, receiver gain, temperature, shimming, water suppression, reference lot, and processing software must be stored so that drift can be separated from product variation. The database should retain original FIDs, processed spectra, targeted results, metadata, model-ready matrices, model objects, and QC reports under version control.

11. High-Field, Benchtop, and Process NMR Deployment

11.1 The two-tier architecture

High-field NMR provides the resolution needed for structural assignment, dextrin branch chemistry, complex-mixture deconvolution, and discovery of minor markers. Benchtop instruments trade resolution and sensitivity for lower capital cost, simpler siting, and faster access. The roles are complementary. A high-field laboratory establishes reference assignments and validated concentrations; an at-line or benchtop system performs high-frequency measurements of ethanol, gross carbohydrate conversion, glycerol, and other robust composite variables; transfer models are checked periodically against the high-field anchor.

At low field, overlapping multiplets are a fact of life. Direct integration gives way to constrained line-shape fitting, Bayesian analysis, or chemometric prediction. Those methods can be accurate, but they are calibration models and must be maintained as raw materials, products, temperature, and instrument response change. A model trained on conventional lager fermentation should not be assumed to quantify a fruit sour, milk stout, or high-adjunct hard beverage.

11.2 At-line fermentation monitoring

The most immediate process application is a repeatable, rapidly degassed sample measured near the fermenter. The core trajectories are declining glucose/maltose/maltotriose, increasing ethanol and glycerol, movement in organic acids, amino-acid consumption, and stabilization of the dextrin envelope. Alarm logic can be based on deviation from a historical multivariate trajectory rather than a single gravity limit. A stalled fermentation, bacterial acidification, or diastatic dextrin loss should then appear as a chemically interpretable divergence.

True online flow introduces additional challenges: bubbles, pressure, temperature, sanitation, residence-time distribution, flow-dependent shimming, and representative sampling. These are engineering problems, not reasons to abandon the concept. A staged implementation should begin off-line, move to at-line automation, then use a bypass flow cell only after the sampling and cleaning system has been proven.

11.3 Method transfer and lifecycle control

A deployed model requires system suitability, transfer samples spanning the calibration space, bias checks against the reference platform, drift monitoring, and a defined retraining trigger. Instrument replacement, probe service, software changes, or a new product family can all move the response. The model lifecycle should be governed like an analytical method: versioned, locked for reporting, challenged with controls, and revalidated when the intended-use domain changes.

12. Validation Framework for a Brewery qNMR Method

12.1 Intended use comes first

A method cannot be validated “for beer” in the abstract. Ethanol label verification at 0.5% and 5% alcohol by volume, organic-acid profiling of sour beer, residual-dextrin structural analysis, and untargeted anomaly detection are different

intended uses with different performance requirements. Each analyte or model must have a reportable range, sample classes, decision rule, and reference method.

12.2 Core validation characteristics

Characteristic	Beer-qNMR implementation
Selectivity/specificity	Pure standards, matrix spikes, 2D confirmation, alternate resonances, suppression-artifact checks, and interference challenges
Linearity and response	Gravimetric multilevel mixtures and standard additions covering the reportable range; receiver-linearity challenge across major/minor signal ratios
Trueness	Comparison with traceable gravimetric materials and independent reference methods such as GC-FID for ethanol/volatiles, HPLC/CE for sugars/acids, and ICP for sodium
Precision	Repeat acquisition, repeat preparation, analyst, day, instrument, and lot components; separate within-run from intermediate precision
Recovery	Spikes before degassing, after degassing, and before/after lyophilization as appropriate; recovery of volatile and nonvolatile classes evaluated separately
LOD/LOQ	Signal- and decision-specific estimates verified in beer matrix, not derived only from baseline noise in D_2O
Robustness	pH, temperature, D_2O fraction, suppression power/frequency, relaxation delay, line broadening, phase/baseline choices, and tube filling height
Stability	Autosampler residence, sealed-tube storage, microbial activity, oxidation, and repeated freeze/thaw where relevant
Measurement uncertainty	Standard purity/mass, sample volume or mass, integral/model fit, recovery, repeatability, conversion factors, and reference-method bias

12.3 System suitability and ongoing QC

A daily system-suitability mixture should challenge chemical shift, linewidth, quantitative response, water suppression, and the dynamic range relevant to beer. A pooled beer QC can monitor the entire workflow. Replicate control charts should track ethanol, a representative acid, an amino acid, a sugar, the α-(1→4) dextrin envelope, the α-(1→6) branch integral, reference response, linewidth, and key model scores. Control limits must distinguish analytical drift from real instability of the pooled material.

For untargeted models, score-distance and residual-distance charts provide additional system checks. A spectrum outside the applicability domain should be reported as unclassified or requiring review, not forced into the nearest known class.

12.4 Reporting language

Reports should separate measured fact from interpretation. “Lactate = 2.8 g/L” is a measured result with uncertainty. “Consistent with a sour-beer profile” is an interpretation against a database. “Evidence of bacterial contamination” is a stronger causal opinion requiring process history, microbiology, and exclusion of intentional acidification. The same hierarchy applies to authenticity, adjunct use, storage damage, and fermentation fault conclusions.

13. Process NMR Associates Beer Studies: Evidence Already Demonstrated

13.1 The 23-commercial-beer World Brewing Congress panel

The 2016 poster presented 23 commercial finished beers spanning mainstream lagers, light beer, IPA, stout, Abbey-style beer, fruit beer, milk stout, sour beer, and gose. Each sample was evaluated by ^1H qNMR on a 300 MHz instrument using direct and/or lyophilized preparations. The figures show that product diversity is not a single alcohol

gradient. Organic-acid distributions, α-(1→4) maltodextrin groupings, amino-acid patterns, and the calorie allocation among ethanol, carbohydrate, amino acids, and organic acids vary independently.

This is exactly the kind of dataset from which a beer chemical-space map can be built, but it also illustrates the limitations of early exploratory panels. Products are single market samples rather than replicated manufacturing lots, styles and brands are confounded, and storage histories are not controlled. The figures should therefore be used as demonstrations of observable chemical diversity and analytical capability, not as population estimates or brand rankings.

13.2 Wort-to-beer and mash-extract comparisons

The presentation overlay of cooled wort and finished beer makes fermentation visible without a numerical model. Maltose and other fermentable carbohydrate signals decline; branch and reducing-end regions change; non-fermentable features persist. A second case compares laboratory, standard, and turbid mash extracts using grouped integrals assigned to shorter and longer linear α-(1→4) maltodextrins and near-branch environments. These figures demonstrate that mash procedure changes the residual carbohydrate distribution before yeast is introduced.

The immediate next experiment is replication with time-resolved mash sampling, reference enzyme assays, and SEC/HPAEC-PAD. That design will test which one-dimensional integrals are truly proportional to specific DP/branch groups and which are composite spectral features. It will also establish how temperature, pH, grist, water chemistry, and enzyme additions shift the trajectory.

13.3 Sour-mash temperature series

The sour-mash experiment quantified acid and fermentation products across temperature. Its strategic value is not limited to identifying an optimum. It shows how qNMR can follow several competing microbial pathways in the same samples: desirable lactate, contaminating acetate, succinate, ethanol, and γ-aminobutyric acid.

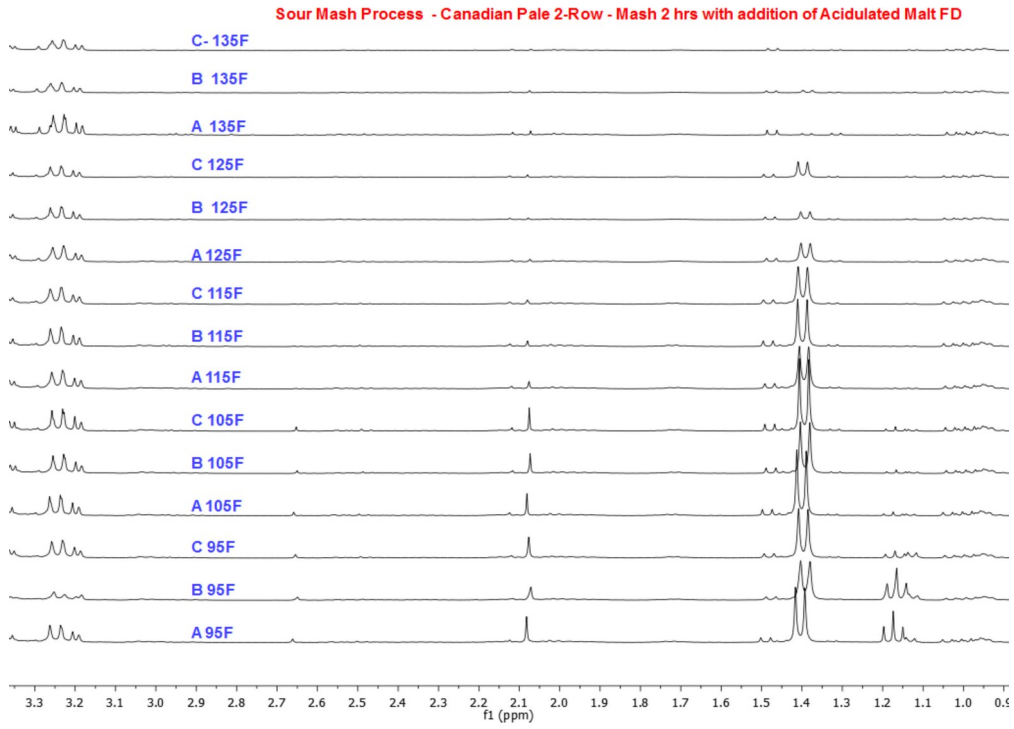

Figure 19. Replicate sour-mash spectra collected across 95-135 °F treatments, revealing temperature-dependent metabolite patterns. The source does not provide complete elapsed-time or microbiological metadata; temperature association is shown, but organism-specific causation is not claimed. Source: Process NMR Associates, author-supplied 2022 presentation (Ref. 68, p. 37).

Absolute Metabolite Proportions

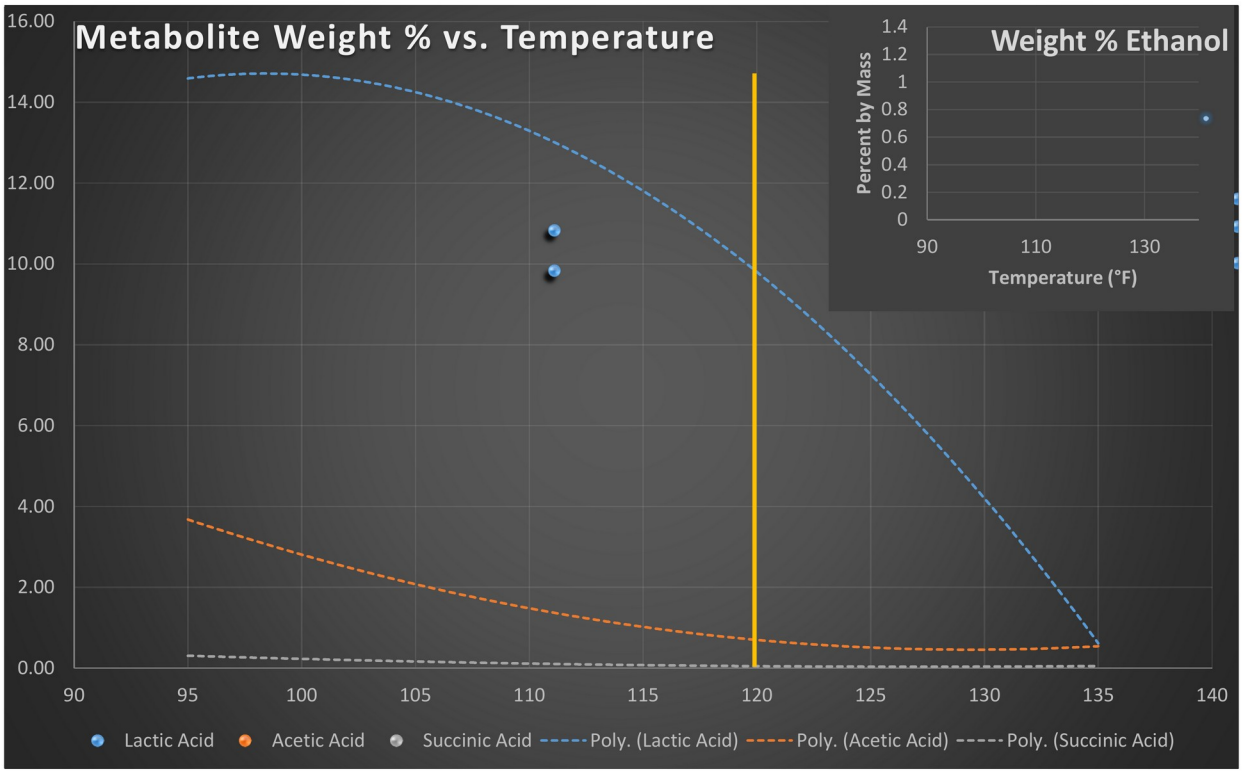

Figure 20. Measured lactic-, acetic-, and succinic-acid proportions across the sour-mash temperature series, with an ethanol inset. Polynomial curves are descriptive visual fits, not kinetic or mechanistic models; raw values and uncertainty should be recovered for formal optimization. Source: Process NMR Associates, author-supplied 2022 presentation (Ref. 68, p. 38).

A mature version should combine ^{1}H qNMR with microbial enumeration or sequencing so that the chemical outcome can be connected to the organisms responsible.

13.4 Near-beer label check

The low-alcohol example demonstrates why qNMR is attractive for label-facing analysis: ethanol, carbohydrate, and energy inputs are obtained from the same tube, and the product sits close to a legally consequential alcohol threshold. The example also sets a validation challenge. A result of 0.47% alcohol by volume requires an uncertainty statement and a method capable of distinguishing 0.47% from 0.50% for the intended decision. That precision target should drive replicate preparation, temperature control, reference-material selection, and comparison with an official alcohol method.

13.5 Hop raw-material profiling

The modified extraction data show simultaneous quantitation of α-acids, β-acids, tautomeric material, and selected terpenes in hop samples with different storage histories and moisture contents.

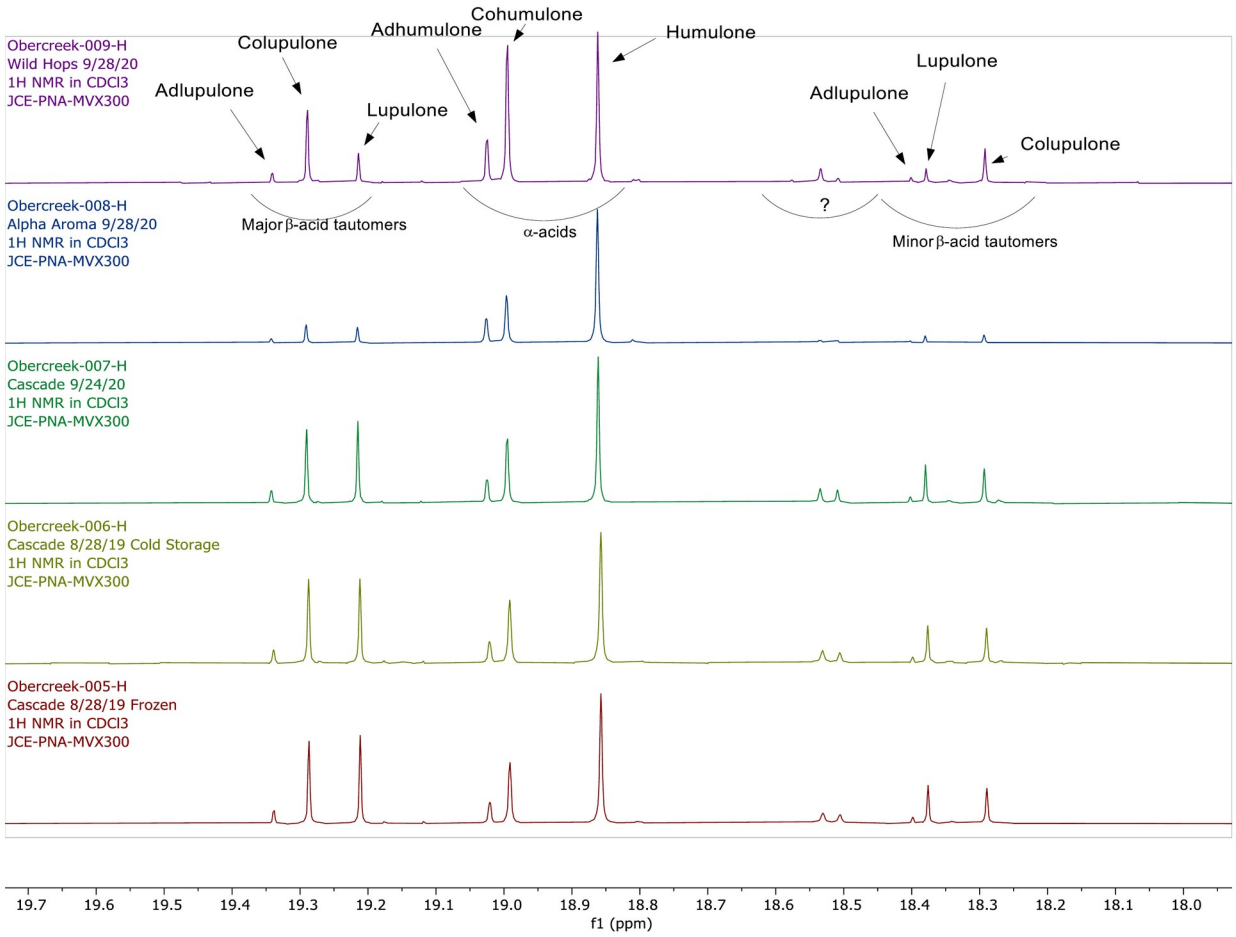

Figure 21. Highly dispersed chelated/enolic proton region used for targeted identification of hop α-acids, β-acids, and β-acid tautomers in $CDCl_3$ extracts. This is a hop-extract method, not a direct finished-beer measurement. Source: Process NMR Associates, author-supplied 2022 presentation (Ref. 68, p. 53).

This is a valuable bridge between raw-material QC and finished-beer chemistry. Future work should pair extracted-hop NMR with HPLC bitter-acid analysis, GC terpene analysis, moisture, cultivar, harvest date, storage temperature, and brewing trials to determine which raw-material spectral variables predict finished-beer bitter and aroma outcomes.

14. Research Program for Residual Dextrins and Beer Chemical Space

14.1 Dextrins are the priority development axis

Residual dextrins represent the strongest opportunity for a distinctive PNA method because they are abundant, structurally rich, process-dependent, and poorly represented by routine finished-beer sugar panels. The immediate objective should not be a single total-dextrin number. It should be a validated structural panel containing total α-glucan proton equivalents, reducing-end concentration, α-(1→6) branch response, α-(1→4) backbone response, estimated apparent number-average DP, lower-/higher-DP reporter patterns, branch-neighborhood or pruning scores, and diffusion-weighted size descriptors. The non-fractionated beer evidence also requires positive β-glucan and arabinoxylan motif/mobility measurements rather than treating those families only as generic interference flags. Lactose and free sugars remain separate quantitative confounders. 63

The one-dimensional formulas in Section 5 are a first-order working model. They should be challenged with mixtures of known maltooligosaccharides and branched standards, commercial maltodextrins of known dextrose equivalent, enzymatically generated limit dextrins, size-fractionated wort/beer material, and standard-addition experiments. Optimized ^{1}H-^{13}C HSQC should determine whether branch-neighborhood peaks provide more specific markers than

the integrated ^{1}H branch envelope. SEC-MALS, HPAEC-PAD, enzymatic debranching, total β-glucan, and reducing-sugar methods should provide orthogonal structure and mass-balance checks.

14.2 Proposed staged experimental design

Analytical standards and mixtures. Acquire replicate ^{1}H, J-resolved, COSY/TOCSY, HSQC, and DOSY data for glucose, maltose through at least maltoheptaose, panose/isopanose or other branch standards, pullulan-derived standards, β-glucan, arabinoxylan, and representative maltodextrins.

Controlled mash matrix. Use a factorial design varying mash temperature, time, pH, grist, and enzyme condition. Sample throughout conversion, not only at endpoint.

Controlled fermentations. Ferment matched worts with strains differing in maltotriose utilization and with/without diastatic activity. Track sugar, dextrin, ethanol, glycerol, acids, and gravity in parallel.

Commercial diversity panel. Sample multiple lots and production dates within major styles, with replicated preparation and acquisition. Include low-/non-alcoholic, sour, wheat/oat, lactose-containing, fruit, high-gravity, and enzyme-treated products.

Stability and challenge studies. Evaluate packaged aging, temperature abuse, deliberate bacterial inoculation, and low-level diastatic contamination under controlled conditions.

Reference-method bridge. Apply conventional sugars, total carbohydrate, FAN, organic acids, volatile analysis, bitter acids, β-glucan, SEC, and microbiology to a strategically selected subset.

Preparation- and field-strength-transfer study. Measure matched direct beer, lyophilized/reconstituted beer, and any concentrated or filtered variants at 300 MHz and at the high-field reference site. Quantify recovery, line broadening, peak coalescence, and any preparation-induced change in diffusion or polymer association before claiming that non-fractionated structural assignments are portable.

Enzyme-difference validation. Apply α-amylase, pullulanase or isoamylase, and exhaustive amyloglucosidase treatments to matched aliquots. Track disappearance of α-(1→4)/α-(1→6) regions, glucose release, reducing-end formation, residual slow-diffusing material, and resistant β-glucan/arabinoxylan signals to make 300 MHz regional integrals chemically testable.

14.3 Chemometric deliverables for the next phase

The resulting data should be released internally as a traceable X matrix with spectra in rows and a second targeted-chemistry matrix sharing the same sample identifiers. Initial unsupervised analyses should include PCA, hierarchical clustering with Ward linkage, UMAP, and t-SNE for visualization, always colored by process stage, style, raw material, strain, and lot rather than only by brand. Supervised work should be limited to questions supported by adequate replication and independent holdout samples. Regression targets can include ethanol, extract, total carbohydrate, dextrin descriptors, conventional acid results, gravity, and sensory or process parameters.

Every chemometric study should archive the exact input matrix, variable axis, preprocessing, scaling, sample metadata, scores, loadings, predictions, validation folds, metrics, and model version in an Excel workbook alongside the report. That archive is not an administrative extra; it is what makes future model updates, expert review, and legal defensibility possible.

14.4 The forward-looking analytical product

The commercial endpoint is a tiered service rather than one oversized assay. A rapid direct-beer qNMR screen can report alcohol, principal acids, glycerol, higher alcohols, selected sugars, and an overall fingerprint. A full beer chemical profile can add the lyophilized nonvolatile panel, amino acids, nucleosides, nutritional calculations, and chemometric comparison. A structural dextrin module can add high-resolution anomeric analysis, HSQC, and diffusion descriptors. Troubleshooting and authentication projects can then add targeted extractions, isotope work, microbiology, chromatography, or mass spectrometry as the question requires.

This architecture keeps routine cost and turnaround under control while preserving a technically serious route for difficult process, authenticity, and litigation questions.

15. Conclusions

Proton NMR provides beer analysis with what no other single platform offers: simultaneous, calibration-light quantitation of major and minor small molecules; structural characterization of a residual-carbohydrate fraction that routine sugar panels do not resolve; an aging chemistry centered on trans-selective iso-α-acid decay; a validated multivariate authentication literature; an isotopic dimension addressing carbon-source claims; and a credible low-field pathway to fermentation monitoring. The non-fractionated beer paper materially expands the dextrin argument: more than 50 local carbohydrate moieties and diffusion-resolved starch-, β-glucan-, and arabinoxylan-related behavior demonstrate that the residual fraction is a composition-structure-mobility system, not one dextrin number. 63 The anomeric fingerprint and equations (1)-(3) therefore propose a testable route to apparent chain length, linkage balance, reducing ends, branch behavior, and glucose-equivalent mass; they are not yet a released universal method. Species-specific concentration, motif-equivalent response, integrated envelope, and diffusion class must be reported at their proper evidence levels and validated on the 300 MHz instrument against standards, enzyme treatments, and orthogonal size/composition measurements. The framework assembled here is intended to be populated with experimental spectra and case data generated at Process NMR Associates, and the final interpretive conclusions remain the province of the author.

References

1. Gil, A. M.; Rodrigues, J. Methods for the Characterization of Beer by Nuclear Magnetic Resonance Spectroscopy. In *Beer in Health and Disease Prevention*; Preedy, V. R., Ed.; Academic Press: Amsterdam, 2009; pp 935–942. DOI: 10.1016/B978-0-12-373891-2.00093-6.

2. Gil, A. M.; Duarte, I. F. High-Resolution Nuclear Magnetic Resonance Spectroscopy of Wine, Beer, and Spirits. In *Modern Magnetic Resonance*; Webb, G. A., Ed.; Springer: Dordrecht, 2006; pp 1689–1694. DOI: 10.1007/1-4020-3910-7_189.

3. Hatzakis, E. Nuclear Magnetic Resonance (NMR) Spectroscopy in Food Science: A Comprehensive Review. *Compr. Rev. Food Sci. Food Saf.* 2019, 18, 189–220. DOI: 10.1111/1541-4337.12408.

4. Anderson, H. E.; Santos, I. C.; Hildenbrand, Z. L.; Schug, K. A. A Review of the Analytical Methods Used for Beer Ingredient and Finished Product Analysis and Quality Control. *Anal. Chim. Acta* 2019, 1085, 1–20. DOI: 10.1016/j.aca.2019.07.061.

5. Duarte, I.; Barros, A.; Belton, P. S.; Righelato, R.; Spraul, M.; Humpfer, E.; Gil, A. M. High-Resolution Nuclear Magnetic Resonance Spectroscopy and Multivariate Analysis for the Characterization of Beer. *J. Agric. Food Chem.* 2002, 50, 2475–2481. DOI: 10.1021/jf011345j.

6. Almeida, C.; Duarte, I. F.; Barros, A.; Rodrigues, J.; Spraul, M.; Gil, A. M. Composition of Beer by ^{1}H NMR Spectroscopy: Effects of Brewing Site and Date of Production. *J. Agric. Food Chem.* 2006, 54, 700–706. DOI: 10.1021/jf0526947.

7. Nord, L. I.; Vaag, P.; Duus, J. Ø. Quantification of Organic and Amino Acids in Beer by ^{1}H NMR Spectroscopy. *Anal. Chem.* 2004, 76, 4790–4798. DOI: 10.1021/ac0496852.

8. Marinelli, L.; Whitney, D. Gas Liquid Chromatography of Wort and Beer Carbohydrates. II. Quantitative Determination of Wort, Beer, and Brewing Syrup Carbohydrates. *J. Inst. Brew.* 1967, 73, 35–39. DOI: 10.1002/j.2050-0416.1967.tb03015.x.

9. McKay, R. T. How the 1D-NOESY Suppresses Solvent Signal in Metabonomics NMR Spectroscopy: An Examination of the Pulse Sequence Components and Evolution. *Concepts Magn. Reson. Part A* 2011, 38A, 197–220. DOI: 10.1002/cmr.a.20223.

10. Smallcombe, S. H.; Patt, S. L.; Keifer, P. A. WET Solvent Suppression and Its Applications to LC NMR and High-Resolution NMR Spectroscopy. *J. Magn. Reson., Ser. A* 1995, 117, 295–303. DOI: 10.1006/jmra.1995.0759.

11. Hwang, T. L.; Shaka, A. J. Water Suppression That Works. Excitation Sculpting Using Arbitrary Wave-Forms and Pulsed-Field Gradients. *J. Magn. Reson., Ser. A* 1995, 112, 275–279. DOI: 10.1006/jmra.1995.1047.

12. Wider, G.; Dreier, L. Measuring Protein Concentrations by NMR Spectroscopy. *J. Am. Chem. Soc.* 2006, 128, 2571–2576. DOI: 10.1021/ja055336t.

13. Akoka, S.; Barantin, L.; Trierweiler, M. Concentration Measurement by Proton NMR Using the ERETIC Method. *Anal. Chem.* 1999, 71, 2554–2557. DOI: 10.1021/ac981422i.

14. Bharti, S. K.; Roy, R. Quantitative ^{1}H NMR Spectroscopy. *TrAC, Trends Anal. Chem.* 2012, 35, 5–26. DOI: 10.1016/j.trac.2012.02.007.

15. Milbert, S.; Laumeyer, J. T.; Müller, T. M.; Krenz, O.; Fuchs, J.; Lehmann, L.; Seifert, S. T. Quantification of Ingredients and Additives of Beer and Beer-Based Mixed Beverages by ^{1}H NMR Spectroscopy and Automated PULCON Analysis. *Anal. Chem.* 2026, 98, 12351–12361. DOI: 10.1021/acs.analchem.5c07171.

16. Kaufmann, M.; Schwarz, K. J.; Dallmann, A.; Kuballa, T.; Bergmann, M. ^{1}H NMR Spectroscopic Discrimination of Different Beer Styles Combined with a Chemical Shift-Based Quantification Approach. *Eur. Food Res. Technol.* 2022, 248, 635–645. DOI: 10.1007/s00217-021-03914-8.

17. Savorani, F.; Tomasi, G.; Engelsen, S. B. icoshift: A Versatile Tool for the Rapid Alignment of 1D NMR Spectra. *J. Magn. Reson.* 2010, 202, 190–202. DOI: 10.1016/j.jmr.2009.11.012.

18. Duarte, I. F.; Godejohann, M.; Braumann, U.; Spraul, M.; Gil, A. M. Application of NMR Spectroscopy and LC-NMR/MS to the Identification of Carbohydrates in Beer. *J. Agric. Food Chem.* 2003, 51, 4847–4852. DOI: 10.1021/jf030097j.

19. Khatib, A.; Wilson, E. G.; Kim, H. K.; Lefeber, A. W. M.; Erkelens, C.; Choi, Y. H.; Verpoorte, R. Application of Two-Dimensional J-Resolved Nuclear Magnetic Resonance Spectroscopy to Differentiation of Beer. *Anal. Chim. Acta* 2006, 559, 264–270. DOI: 10.1016/j.aca.2005.11.064.

20. Rodrigues, J. E. A.; Erny, G. L.; Barros, A. S.; Esteves, V. I.; Brandão, T.; Ferreira, A. A.; Cabrita, E.; Gil, A. M. Quantification of Organic Acids in Beer by Nuclear Magnetic Resonance (NMR)-Based Methods. *Anal. Chim. Acta* 2010, 674, 166–175. DOI: 10.1016/j.aca.2010.06.029.

21. Lee, B. L.; Shahin, F.; Selim, A.; Berjanskii, M.; Torres-Calzada, C.; Kovur, P.; Mandal, R.; Wishart, D. S. Automated Beer Analysis by NMR Spectroscopy. *ACS Food Sci. Technol.* 2025, 5, 378–388. DOI: 10.1021/acsfoodscitech.4c00896.

22. Enevoldsen, B. S.; Bathgate, G. N. Structural Analysis of Wort Dextrins by Means of β-Amylase and the Debranching Enzyme, Pullulanase. *J. Inst. Brew.* 1969, 75, 433–443. DOI: 10.1002/j.2050-0416.1969.tb06377.x.

23. Enevoldsen, B. S.; Schmidt, F. Dextrins in Brewing. *J. Inst. Brew.* 1974, 80, 520–533. DOI: 10.1002/j.2050-0416.1974.tb03643.x.

24. Gidley, M. J. Quantification of the Structural Features of Starch Polysaccharides by N.M.R. Spectroscopy. *Carbohydr. Res.* 1985, 139, 85–93. DOI: 10.1016/0008-6215(85)85074-6.

25. Nilsson, G. S.; Gorton, L.; Bergquist, K.-E.; Nilsson, U. Determination of the Degree of Branching in Normal and Amylopectin Type Potato Starch with ^{1}H-NMR Spectroscopy. *Starch/Stärke* 1996, 48, 352–357. DOI: 10.1002/star.19960481003.

26. Tizzotti, M. J.; Sweedman, M. C.; Tang, D.; Schaefer, C.; Gilbert, R. G. New ^{1}H NMR Procedure for the Characterization of Native and Modified Food-Grade Starches. *J. Agric. Food Chem.* 2011, 59, 6913–6919. DOI: 10.1021/jf201209z.

27. Dais, P.; Perlin, A. S. High-Field ^{13}C-N.M.R. Spectroscopy of β-D-Glucans, Amylopectin, and Glycogen. *Carbohydr. Res.* 1982, 100, 103–116. DOI: 10.1016/S0008-6215(00)81029-0.

28. Nilsson, M.; Duarte, I. F.; Almeida, C.; Delgadillo, I.; Goodfellow, B. J.; Gil, A. M.; Morris, G. A. High-Resolution NMR and Diffusion-Ordered Spectroscopy of Port Wine. *J. Agric. Food Chem.* 2004, 52, 3736–3743. DOI: 10.1021/jf049797u.

29. Meier-Dörnberg, T.; Kory, O. I.; Jacob, F.; Michel, M.; Hutzler, M. Saccharomyces cerevisiae Variety diastaticus Friend or Foe?—Spoilage Potential and Brewing Ability of Different Saccharomyces cerevisiae Variety diastaticus Yeast Isolates by Genetic, Phenotypic and Physiological Characterization. *FEMS Yeast Res.* 2018, 18, foy023. DOI: 10.1093/femsyr/foy023.

30. Lachenmeier, D. W.; Frank, W.; Humpfer, E.; Schäfer, H.; Keller, S.; Mörtter, M.; Spraul, M. Quality Control of Beer Using High-Resolution Nuclear Magnetic Resonance Spectroscopy and Multivariate Analysis. *Eur. Food Res. Technol.* 2005, 220, 215–221. DOI: 10.1007/s00217-004-1070-7.

31. Intelmann, D.; Kummerlöwe, G.; Haseleu, G.; Desmer, N.; Schulze, K.; Fröhlich, R.; Frank, O.; Luy, B.; Hofmann, T. Structures of Storage-Induced Transformation Products of the Beer's Bitter Principles, Revealed by Sophisticated NMR Spectroscopic and LC–MS Techniques. *Chem. – Eur. J.* 2009, 15, 13047–13058. DOI: 10.1002/chem.200902058.

32. Intelmann, D.; Hofmann, T. On the Autoxidation of Bitter-Tasting Iso-α-Acids in Beer. *J. Agric. Food Chem.* 2010, 58, 5059–5067. DOI: 10.1021/jf100083e.

33. Intelmann, D.; Haseleu, G.; Dunkel, A.; Lagemann, A.; Stephan, A.; Hofmann, T. Comprehensive Sensomics Analysis of Hop-Derived Bitter Compounds during Storage of Beer. *J. Agric. Food Chem.* 2011, 59, 1939–1953. DOI: 10.1021/jf104392y.

34. Urban, J.; Dahlberg, C. J.; Carroll, B. J.; Kaminsky, W. Absolute Configuration of Beer's Bitter Compounds. *Angew. Chem., Int. Ed.* 2013, 52, 1553–1555. DOI: 10.1002/anie.201208450.

35. Rodrigues, J. A.; Barros, A. S.; Carvalho, B.; Brandão, T.; Gil, A. M. Probing Beer Aging Chemistry by Nuclear Magnetic Resonance and Multivariate Analysis. *Anal. Chim. Acta* 2011, 702, 178–187. DOI: 10.1016/j.aca.2011.06.042.

36. Duarte, I. F.; Barros, A.; Almeida, C.; Spraul, M.; Gil, A. M. Multivariate Analysis of NMR and FTIR Data as a Potential Tool for the Quality Control of Beer. *J. Agric. Food Chem.* 2004, 52, 1031–1038. DOI: 10.1021/jf030659z.

37. Palmioli, A.; Alberici, D.; Ciaramelli, C.; Airoldi, C. Metabolomic Profiling of Beers: Combining ^{1}H NMR Spectroscopy and Chemometric Approaches to Discriminate Craft and Industrial Products. *Food Chem.* 2020, 327, 127025. DOI: 10.1016/j.foodchem.2020.127025.

38. Spevacek, A. R.; Benson, K. H.; Bamforth, C. W.; Slupsky, C. M. Beer Metabolomics: Molecular Details of the Brewing Process and the Differential Effects of Late and Dry Hopping on Yeast Purine Metabolism. *J. Inst. Brew.* 2016, 122, 21–28. DOI: 10.1002/jib.291.

39. Mannina, L.; Marini, F.; Antiochia, R.; Cesa, S.; Magrì, A.; Capitani, D.; Sobolev, A. P. Tracing the Origin of Beer Samples by NMR and Chemometrics: Trappist Beers as a Case Study. *Electrophoresis* 2016, 37, 2710–2719. DOI: 10.1002/elps.201600082.

40. da Silva, L. A.; Flumignan, D. L.; Tininis, A. G.; Pezza, H. R.; Pezza, L. Discrimination of Brazilian Lager Beer by ^{1}H NMR Spectroscopy Combined with Chemometrics. *Food Chem.* 2019, 272, 488–493. DOI: 10.1016/j.foodchem.2018.08.077.

41. Chorbadzhiev, P.; Gerginova, D.; Simova, S. Weiss or Wit: Chemical Profiling of Wheat Beers via NMR-Based Metabolomics. *Foods* 2025, 14, 1621. DOI: 10.3390/foods14091621.

42. Kuballa, T.; Brunner, T. S.; Thongpanchang, T.; Walch, S. G.; Lachenmeier, D. W. Application of NMR for Authentication of Honey, Beer and Spices. *Curr. Opin. Food Sci.* 2018, 19, 57–62. DOI: 10.1016/j.cofs.2018.01.007.

43. Martin, G. J.; Martin, M. L. Deuterium Labelling at the Natural Abundance Level as Studied by High Field Quantitative ^{2}H NMR. *Tetrahedron Lett.* 1981, 22, 3525–3528. DOI: 10.1016/S0040-4039(01)81948-1.

44. Martin, M. L.; Martin, G. J. Deuterium NMR in the Study of Site-Specific Natural Isotope Fractionation (SNIF-NMR). In *NMR Basic Principles and Progress*; Springer: Berlin, Heidelberg, 1990; pp 1–61. DOI: 10.1007/978-3-642-75932-1_1.

45. Cross, J. L.; Gallaher, T. N.; Leary, J. J.; Schreiner, S. The Application of Site-Specific Natural Isotope Fractionation-Nuclear Magnetic Resonance (SNIF-NMR) to the Analysis of Alcoholic Beverages. *Chem. Educator* 1998, 3, 1–9. DOI: 10.1007/s00897980252a.

46. Isaac-Lam, M. F. Determination of Alcohol Content in Alcoholic Beverages Using 45 MHz Benchtop NMR Spectrometer. *Int. J. Spectrosc.* 2016, 2016, 2526946. DOI: 10.1155/2016/2526946.

47. Matviychuk, Y.; Steimers, E.; von Harbou, E.; Holland, D. J. Bayesian Approach for Automated Quantitative Analysis of Benchtop NMR Data. *J. Magn. Reson.* 2020, 319, 106814. DOI: 10.1016/j.jmr.2020.106814.

48. Jenne, A.; Soong, R.; Downey, K.; Biswas, R. G.; Decker, V.; Busse, F.; Goerling, B.; Haber, A.; Simpson, M. J.; Simpson, A. J. Brewing Alcohol 101: An Undergraduate Experiment Utilizing Benchtop NMR for Quantification and Process Monitoring. *Magn. Reson. Chem.* 2024, 62, 429–438. DOI: 10.1002/mrc.5428.

49. Kreyenschulte, D.; Paciok, E.; Regestein, L.; Blümich, B.; Büchs, J. Online Monitoring of Fermentation Processes via Non-Invasive Low-Field NMR. *Biotechnol. Bioeng.* 2015, 112, 1810–1821. DOI: 10.1002/bit.25599.

50. Phuong, J.; Salgado, B.; Heiß, J.; Steimers, E.; Nickolaus, P.; Keller, L.; Fischer, U.; von Harbou, E.; Holland, D. J.; Jirasek, F. Real-Time Monitoring of Fermentation Processes in Wine Production with Benchtop ^{1}H NMR Spectroscopy. *Food Res. Int.* 2025, 203, 115741. DOI: 10.1016/j.foodres.2025.115741.

51. Electronic Code of Federal Regulations. *27 CFR § 7.65 - Alcohol content (malt beverages).* Current through August 20, 2026. https://www.ecfr.gov/current/title-27/chapter-I/subchapter-A/part-7/subpart-E/section-7.65.

52. Labrado, D.; Ferrero, S.; Caballero, I.; Alvarez, C. M.; Villafañe, F.; Blanco, C. A. Identification by NMR of Key Compounds Present in Beer Distillates and Residual Phases after Dealcoholization by Vacuum Distillation. *J. Sci. Food Agric.* 2020, 100, 3971-3978. DOI: 10.1002/jsfa.10441.

53. Petersen, B. O.; Hindsgaul, O.; Meier, S. Profiling of Carbohydrate Mixtures at Unprecedented Resolution Using High-Precision ^{1}H-^{13}C Chemical Shift Measurements and a Reference Library. *Analyst* 2014, 139, 401-406. DOI: 10.1039/C3AN01922E.

54. Bøjstrup, M.; Petersen, B. O.; Beeren, S. R.; Hindsgaul, O.; Meier, S. Fast and Accurate Quantitation of Glucans in Complex Mixtures by Optimized Heteronuclear NMR Spectroscopy. *Anal. Chem.* 2013, 85, 8802-8808. DOI: 10.1021/ac401980m.

55. Sundekilde, U. K.; Meier, S. ^{1}H-^{13}C NMR-Based Profiling of Biotechnological Starch Utilization. *Anal. Chem.* 2016, 88, 9685-9690. DOI: 10.1021/acs.analchem.6b02555.

56. Petersen, B. O.; Motawie, M. S.; Møller, B. L.; Hindsgaul, O.; Meier, S. NMR Characterization of Chemically Synthesized Branched α-Dextrin Model Compounds. *Carbohydr. Res.* 2015, 403, 149-156. DOI: 10.1016/j.carres.2014.05.011.

57. Beeren, S. R.; Petersen, B. O.; Bøjstrup, M.; Hindsgaul, O.; Meier, S. Time-Resolved in-Situ Observation of Starch Polysaccharide Degradation Pathways. *ChemBioChem* 2013, 14, 2506-2511. DOI: 10.1002/cbic.201300461.

58. Jeong, J.-H.; Cho, S.-J.; Kim, Y. High-Resolution NMR Spectroscopy for the Classification of Beer. *Bull. Korean Chem. Soc.* 2017, 38, 466-470. DOI: 10.1002/bkcs.11113.

59. Sánchez-Estébanez, C.; Ferrero, S.; Alvarez, C. M.; Blanco, C. A. Nuclear Magnetic Resonance Methodology for the Analysis of Regular and Non-Alcoholic Lager Beers. *Food Anal. Methods* 2018, 11, 11-22. DOI: 10.1007/s12161-017-0953-8.

60. Walther, A.; Ravasio, D.; Qin, F.; Wendland, J.; Meier, S. Development of Brewing Science in (and since) the Late 19th Century: Molecular Profiles of 110-130 Year Old Beers. *Food Chem.* 2015, 183, 227-234. DOI: 10.1016/j.foodchem.2015.03.051.

61. Vanderhaegen, B.; Neven, H.; Verachtert, H.; Derdelinckx, G. The Chemistry of Beer Aging - A Critical Review. *Food Chem.* 2006, 95, 357-381. DOI: 10.1016/j.foodchem.2005.01.006.

62. DiCaprio, A.; Edwards, J. C. Application of Quantitative Nuclear Magnetic Resonance Spectroscopy to Biological Acidification of Barley Mashes. *J. Inst. Brew.* 2014, 120, 207-211. DOI: 10.1002/jib.138.

63. Petersen, B. O.; Nilsson, L. M.; Bøjstrup, M.; Hindsgaul, O.; Meier, S. ^{1}H NMR Spectroscopy for Profiling Complex Carbohydrate Mixtures in Non-Fractionated Beer. *Food Chem.* 2014, 150, 65-72. DOI: 10.1016/j.foodchem.2013.10.136.

64. Dal Poggetto, G.; Castañar, L.; Adams, R. W.; Morris, G. A.; Nilsson, M. Dissect and Divide: Putting NMR Spectra of Mixtures under the Knife. *J. Am. Chem. Soc.* 2019, 141, 5766-5771. DOI: 10.1021/jacs.8b13290.

65. Li, M.; Du, J.; Zhang, K. Profiling of Carbohydrates in Commercial Beers and Their Influence on Beer Quality. *J. Sci. Food Agric.* 2020, 100, 3062-3070. DOI: 10.1002/jsfa.10337.

66. Edwards, J. C. *The Chemical Fingerprint of Beer from a Single Experiment with Minimum Sample Preparation: A Rapid Quantitative Analysis by ^{1}H NMR Spectroscopy.* World Brewing Congress poster 077, 2016. Author-supplied conference source; no DOI.

67. Edwards, J. C. *The Complex Fingerprint Analysis of Alcoholic Beverages by Quantitative NMR (qNMR).* Bell's Brewery presentation, October 12, 2018. Author-supplied presentation; no DOI.

68. Edwards, J. C. *Quantitative NMR Metabolomics - A Window into the Chemistry of Brewing and the Quality of Yeast and Bacterial Excrement.* UC Davis Master Brewers Certificate Program presentation, April 28, 2022. Author-supplied presentation; no DOI.

Summary

Quantitative ^{1}H NMR can provide a unified compositional view of beer from one direct spectrum and, where deeper nonvolatile coverage is required, a complementary lyophilized aliquot. The observable panel spans ethanol and selected volatiles; residual sugars and dextrins; glycerol; organic and amino acids; nucleosides and purines; selected carbonyl, furan, hop, adjunct, and preservative markers; and broad macromolecular behavior. ^{13}C correlation, diffusion, relaxation, ^{2}H isotope analysis, and other nuclei extend the method when the scientific question justifies additional experiments.

The most differentiated opportunity is residual dextrin chemistry. NMR can observe α-(1→4) backbone, α-(1→6) linkage, reducing-end, local cleavage-motif, and size-dependent diffusion behavior in the solution-state, NMR-visible carbohydrate mixture. Petersen et al. extend that view to more than 50 carbohydrate moieties across small sugars, starch fragments, β-glucan, and arabinoxylan and show that DOSY can add independent hydrodynamic information. 63 The practical output is a dextrin-character vector - absolute concentrations where individual compounds or total equivalents are validated, operational linkage/end-group/motif indices where resolution is composite, and calibrated mobility classes rather than assumed molecular weights. The present formulas and assignments are a rigorous working framework, but apparent DP, branching, pruning, and diffusion outputs must be validated against defined standards, enzymatic transformations, and orthogonal size/composition methods before routine certificate reporting on the 300 MHz platform.

The author-supplied studies already demonstrate the breadth of the platform: 23 commercial beers differed in organic acids, maltodextrins, amino acids, alcohol, and calorie allocation; wort-to-beer spectra made carbohydrate consumption visible; mash design changed maltodextrin distributions; sour-mash temperature changed competing acid pathways; a low-alcohol product was checked near the 0.5% threshold; and hop extracts yielded α-acid, β-acid,

tautomer, and terpene information. These results establish analytical observability and generate hypotheses. Replicated lots, controlled experiments, metadata, and formal uncertainty are the next requirement.

The recommended program retains both the targeted concentration matrix and the full spectral X matrix. PCA, HCA, UMAP, and t-SNE can map variability and diversity; regression and supervised classification can be added only with grouped lot/batch holdouts and an external test set. Process samples should be represented as chemical trajectories through brewing stages, and all model inputs, outputs, preprocessing, QC, and metadata should be archived with the report. This approach positions high-field NMR as the structural and reference anchor, with benchtop or at-line systems carrying appropriately validated high-frequency process measurements.